US008571819B2

(12) **United States Patent**
Henry

(10) **Patent No.: US 8,571,819 B2**
(45) **Date of Patent: Oct. 29, 2013**

(54) **CORIOLIS MODE PROCESSING TECHNIQUES**

(75) Inventor: **Manus P. Henry**, Oxford (GB)

(73) Assignee: **Invensys Systems, Inc.**, Foxboro, MA (US)

(*) Notice: Subject to any disclaimer, the term of this patent is extended or adjusted under 35 U.S.C. 154(b) by 0 days.

(21) Appl. No.: **13/317,495**

(22) Filed: **Oct. 19, 2011**

(65) **Prior Publication Data**

US 2013/0041598 A1 Feb. 14, 2013

Related U.S. Application Data

(63) Continuation of application No. 12/761,781, filed on Apr. 16, 2010, now Pat. No. 8,060,320, which is a continuation of application No. 11/953,773, filed on Dec. 10, 2007, now Pat. No. 7,711,501, which is a continuation of application No. 11/456,461, filed on Jul. 10, 2006, now Pat. No. 7,313,488.

(60) Provisional application No. 60/697,574, filed on Jul. 11, 2005.

(51) **Int. Cl.**
G01F 23/00 (2006.01)

(52) **U.S. Cl.**
USPC **702/54**; 702/45; 73/861.355; 73/861.356

(58) **Field of Classification Search**
USPC 702/54, 45; 73/861.355–861.356
See application file for complete search history.

(56) **References Cited**

U.S. PATENT DOCUMENTS

6,507,791 B2 * 1/2003 Henry et al. 702/45

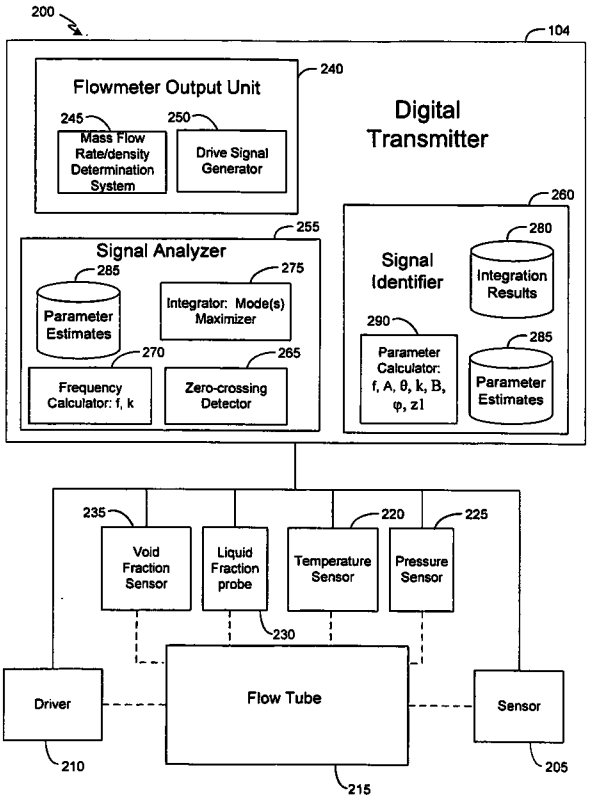
* cited by examiner

Primary Examiner — Jonathan C Teixeira Moffat
Assistant Examiner — Hien Vo
(74) *Attorney, Agent, or Firm* — Edward S. Jamolowicz, Esq.

(57) **ABSTRACT**

Flowmeters are described in which a sensor signal received from a sensor that is attached to vibratable flowtube, so as to determine properties of a fluid within the flowtube, contains a drive signal component and a Coriolis mode component. The flowmeters are operable to determine drive parameters of the drive signal component, as well as Coriolis parameters of the Coriolis mode component. By analyzing the sensor signal based on the drive signal parameters, and not on the Coriolis signal parameters, the flowmeters are able to provide stable and accurate determinations of the properties of the fluid.

14 Claims, 22 Drawing Sheets



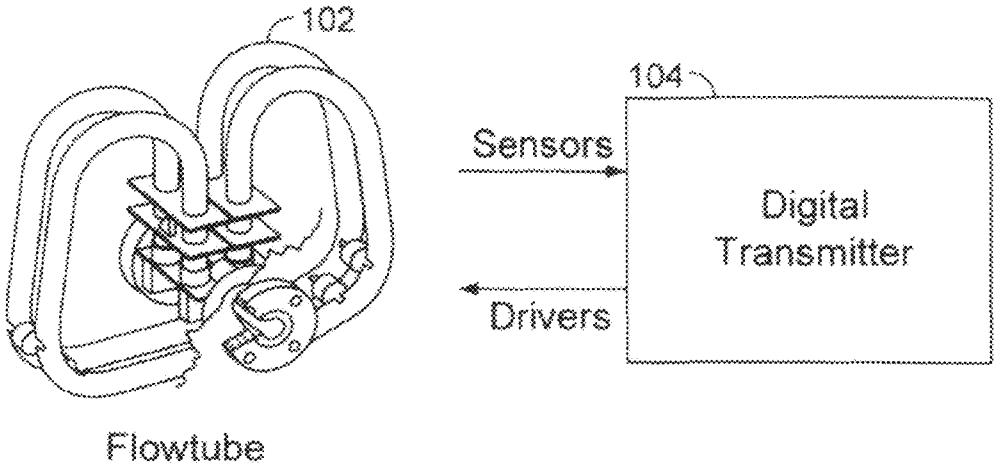

102
104
Sensors
Digital
Transmitter
Drivers
Flowtube

FIG. 1A

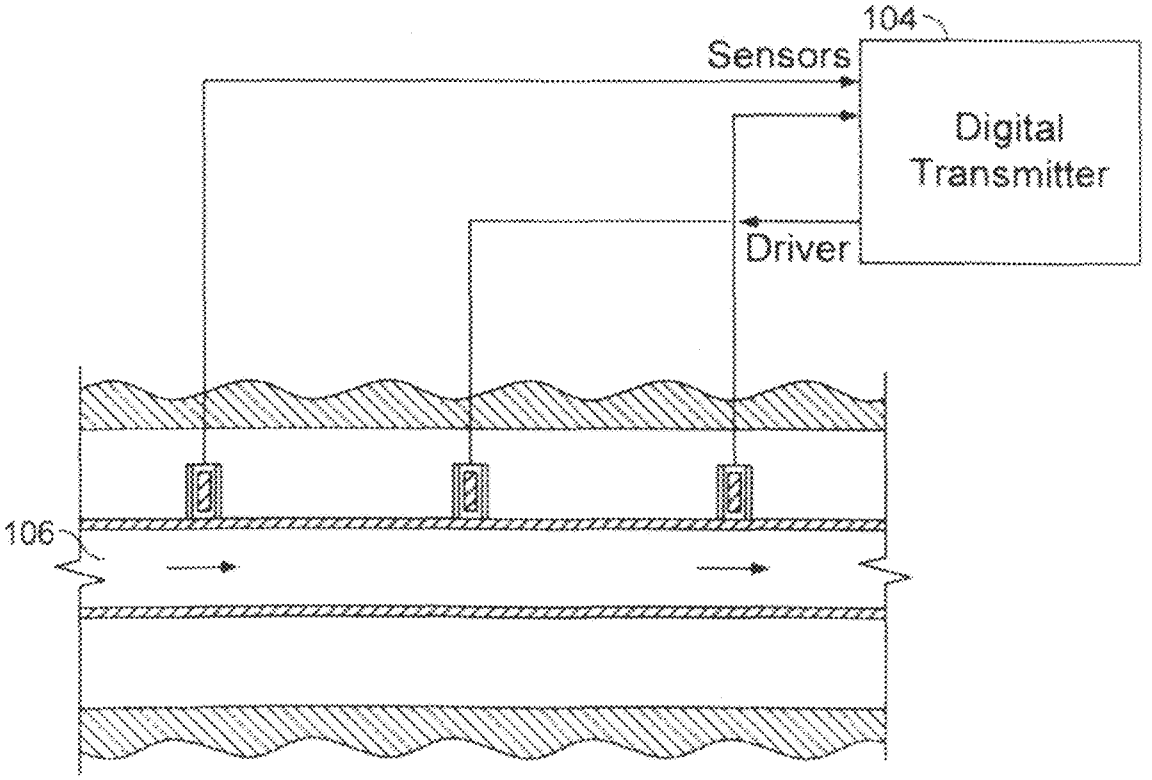

104
Sensors
Digital
Transmitter
Driver
106

FIG. 1B

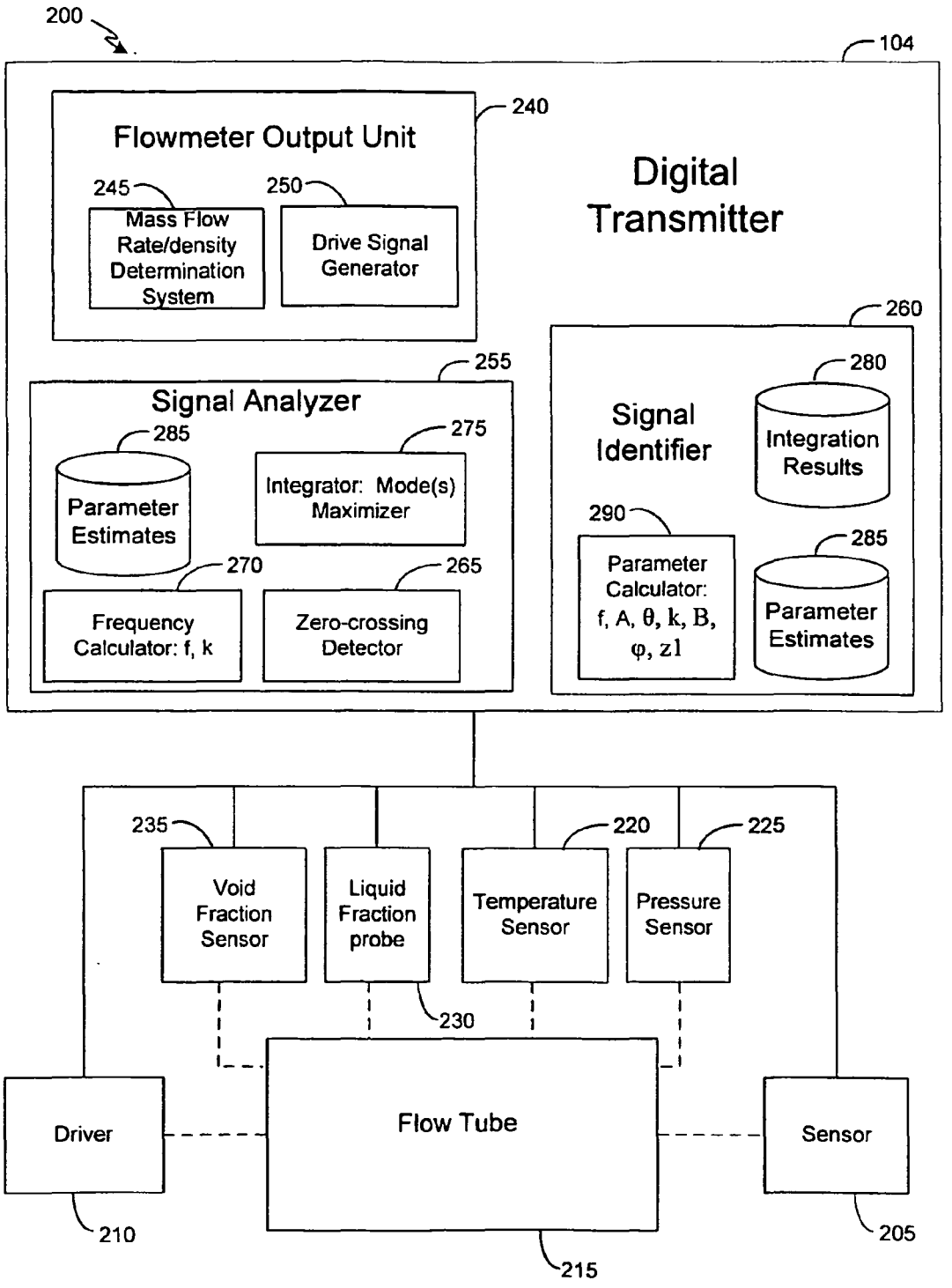

200
104
Digital Transmitter
240
Flowmeter Output Unit
245
Mass Flow Rate/density Determination System
250
Drive Signal Generator
260
Signal Identifier
280
Integration Results
290
Parameter Calculator: f, A, θ, k, B, φ, z1
285
Parameter Estimates
255
Signal Analyzer
285
Parameter Estimates
275
Integrator: Mode(s) Maximizer
270
Frequency Calculator: f, k
265
Zero-crossing Detector
235
Void Fraction Sensor
Liquid Fraction probe
220
Temperature Sensor
225
Pressure Sensor
230
Driver
Flow Tube
Sensor
210
215
205

FIG. 2

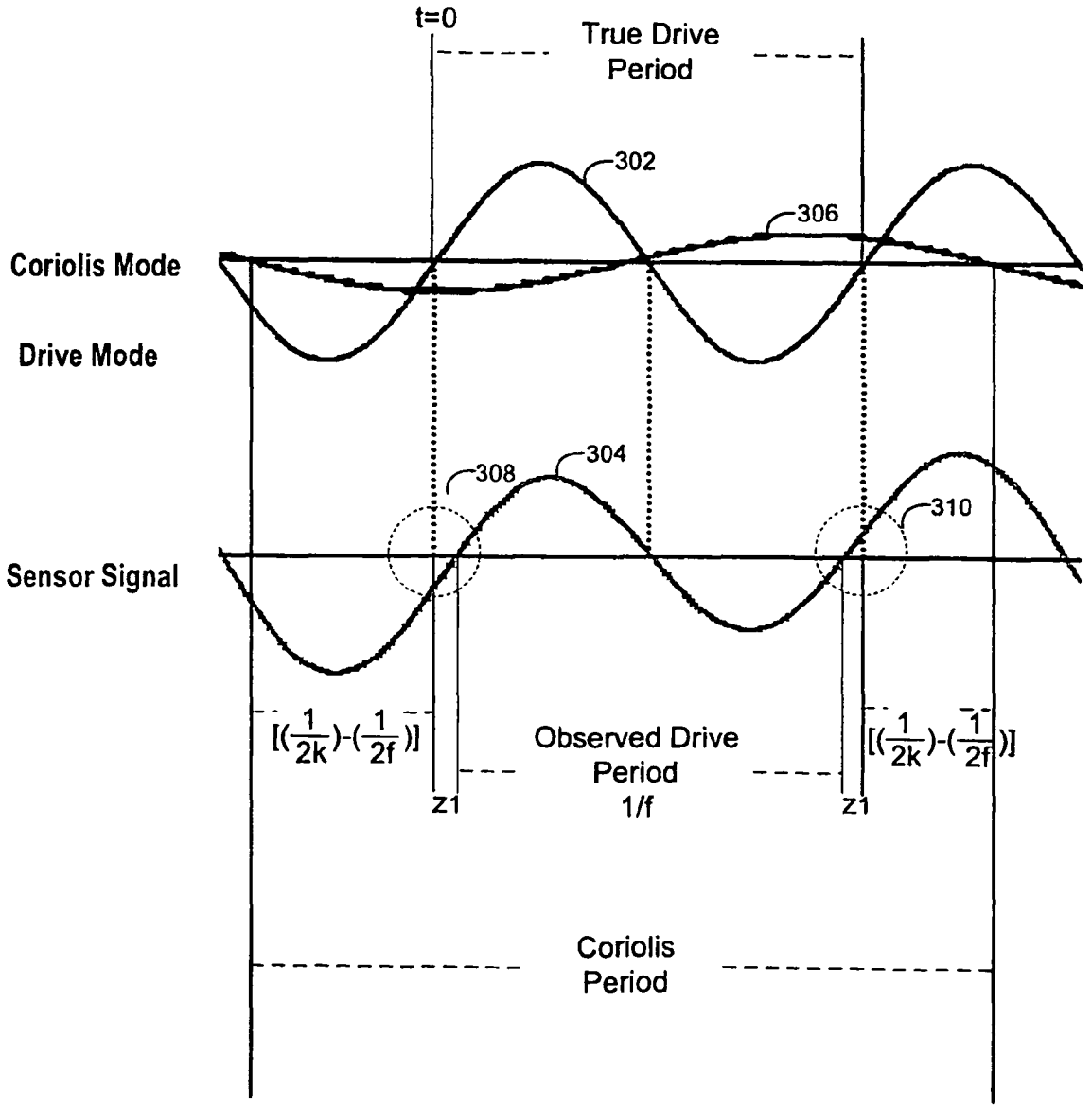

t=0
True Drive Period
302
306
Coriolis Mode
Drive Mode
308
304
310
Sensor Signal
$[(\frac{1}{2k})-(\frac{1}{2f})]$
Observed Drive Period 1/f
$[(\frac{1}{2k})-(\frac{1}{2f})]$
z1
z1
Coriolis Period

FIG. 3

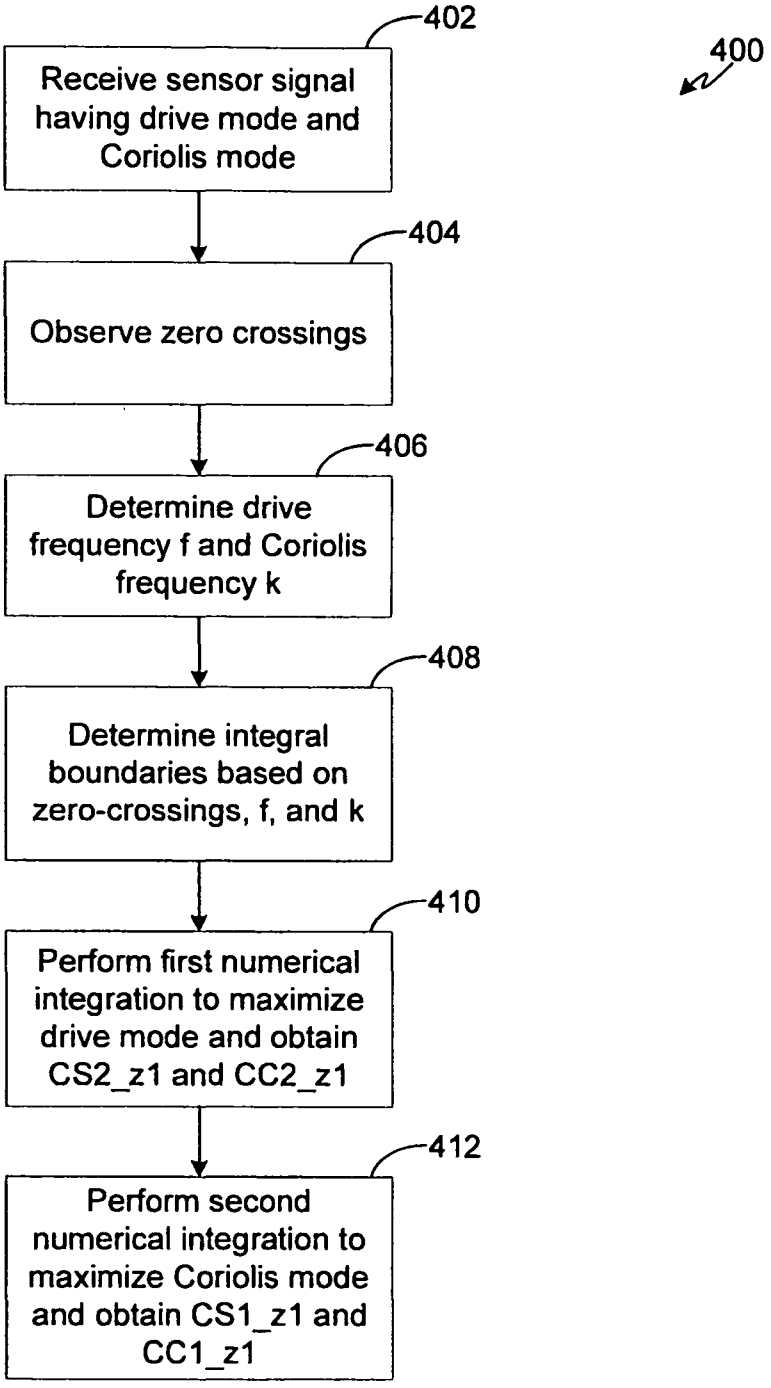

400
402
Receive sensor signal having drive mode and Coriolis mode
404
Observe zero crossings
406
Determine drive frequency f and Coriolis frequency k
408
Determine integral boundaries based on zero-crossings, f, and k
410
Perform first numerical integration to maximize drive mode and obtain CS2_z1 and CC2_z1
412
Perform second numerical integration to maximize Coriolis mode and obtain CS1_z1 and CC1_z1

FIG. 4

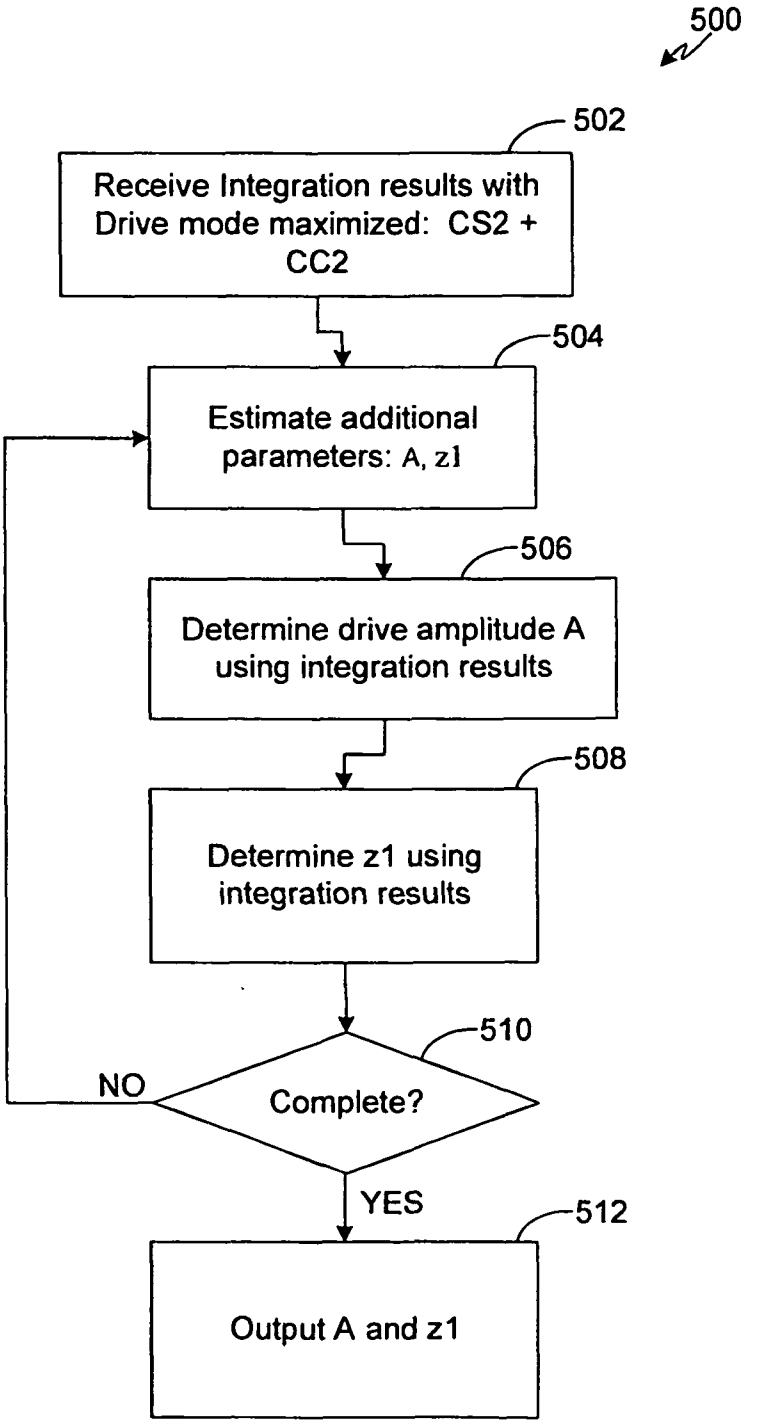

500
502
Receive Integration results with Drive mode maximized: CS2 + CC2
504
Estimate additional parameters: A, z1
506
Determine drive amplitude A using integration results
508
Determine z1 using integration results
510
Complete?
NO
YES
512
Output A and z1

FIG. 5

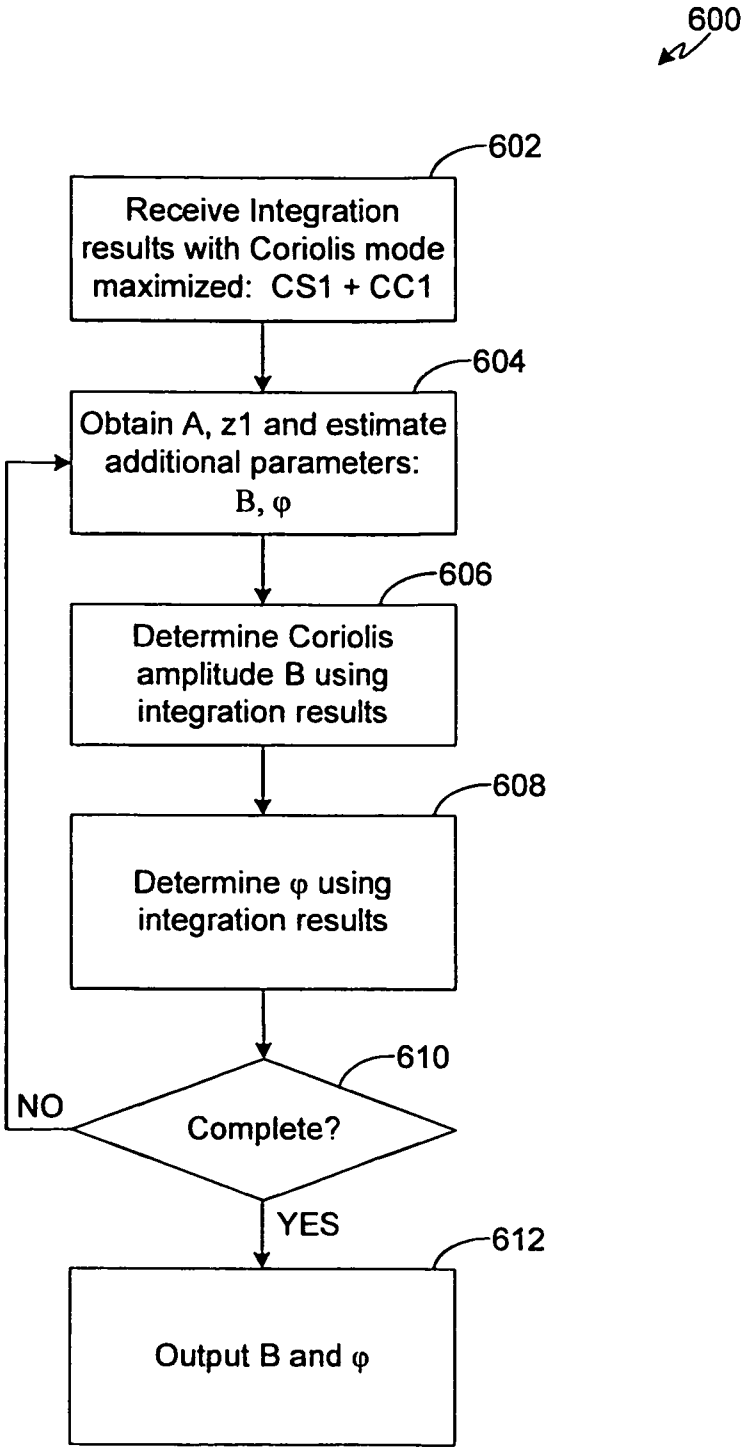

600
602
Receive Integration results with Coriolis mode maximized: CS1 + CC1
604
Obtain A, z1 and estimate additional parameters: B, φ
606
Determine Coriolis amplitude B using integration results
608
Determine φ using integration results
610
Complete?
NO
YES
612
Output B and φ

FIG. 6

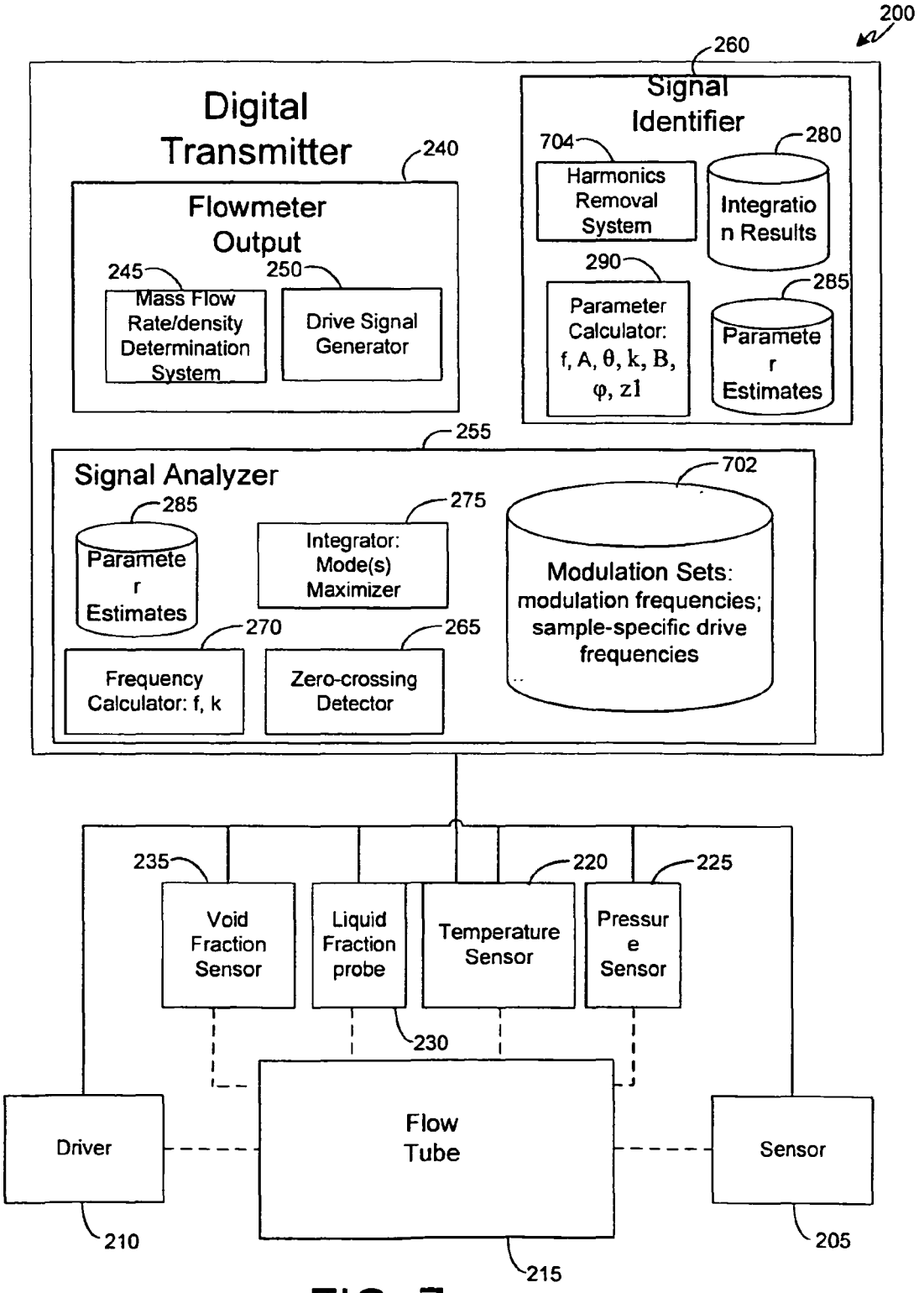

200
260
Digital Transmitter
240
Flowmeter Output
245
Mass Flow Rate/density Determination System
250
Drive Signal Generator
Signal Identifier
704
Harmonics Removal System
280
Integratio n Results
290
Parameter Calculator: f, A, θ, k, B, φ, z1
285
Paramete r Estimates
255
Signal Analyzer
285
Paramete r Estimates
275
Integrator: Mode(s) Maximizer
702
Modulation Sets: modulation frequencies; sample-specific drive frequencies
270
Frequency Calculator: f, k
265
Zero-crossing Detector
235
Void Fraction Sensor
Liquid Fraction probe
220
Temperature Sensor
225
Pressur e Sensor
230
Driver
Flow Tube
Sensor
210
215
205

FIG. 7

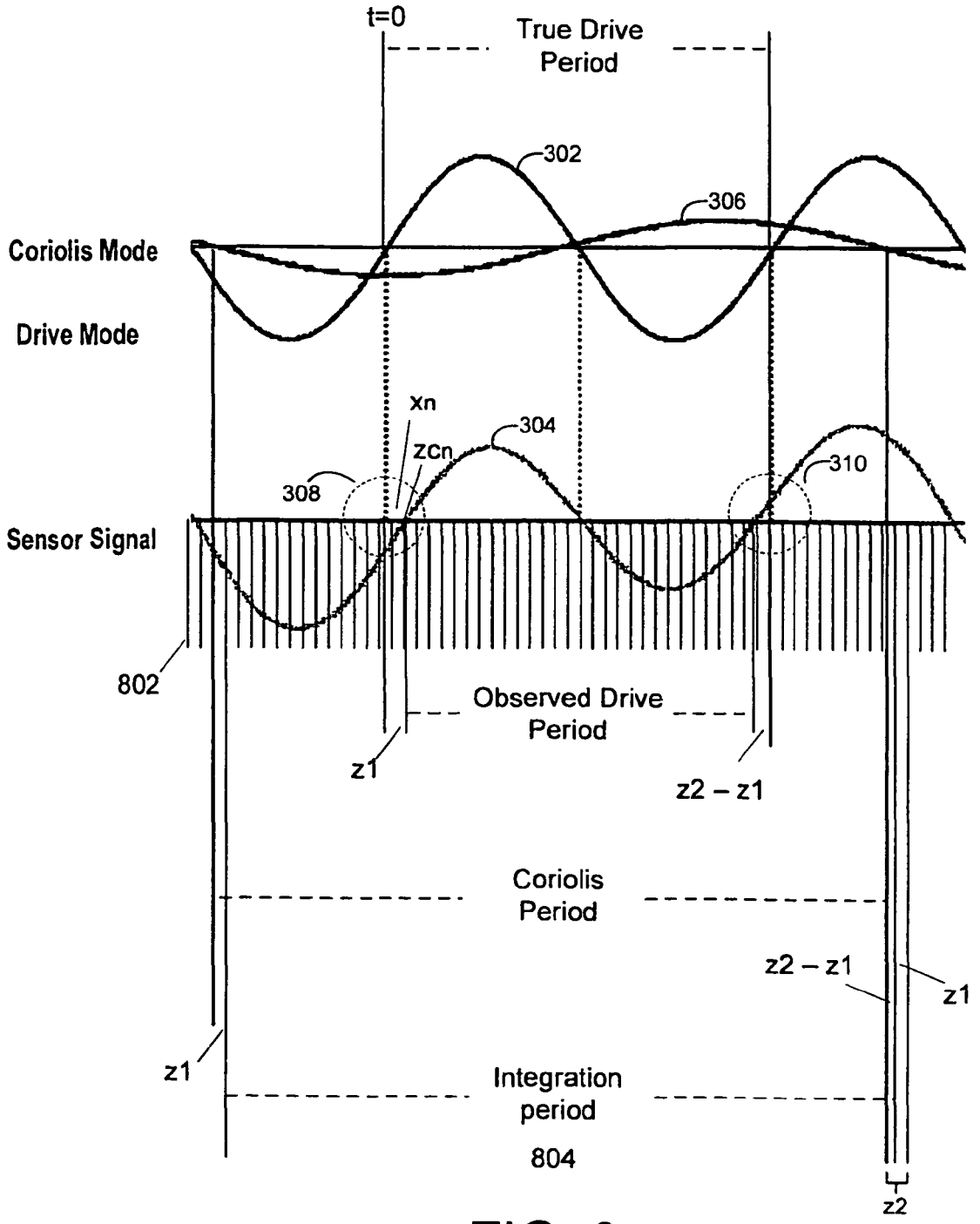

t=0
True Drive Period
302
306
Coriolis Mode
Drive Mode
xn
304
zcn
310
308
Sensor Signal
802
Observed Drive Period
z1
z2 – z1
Coriolis Period
z2 – z1
z1
z1
Integration period
804
z2

FIG. 8

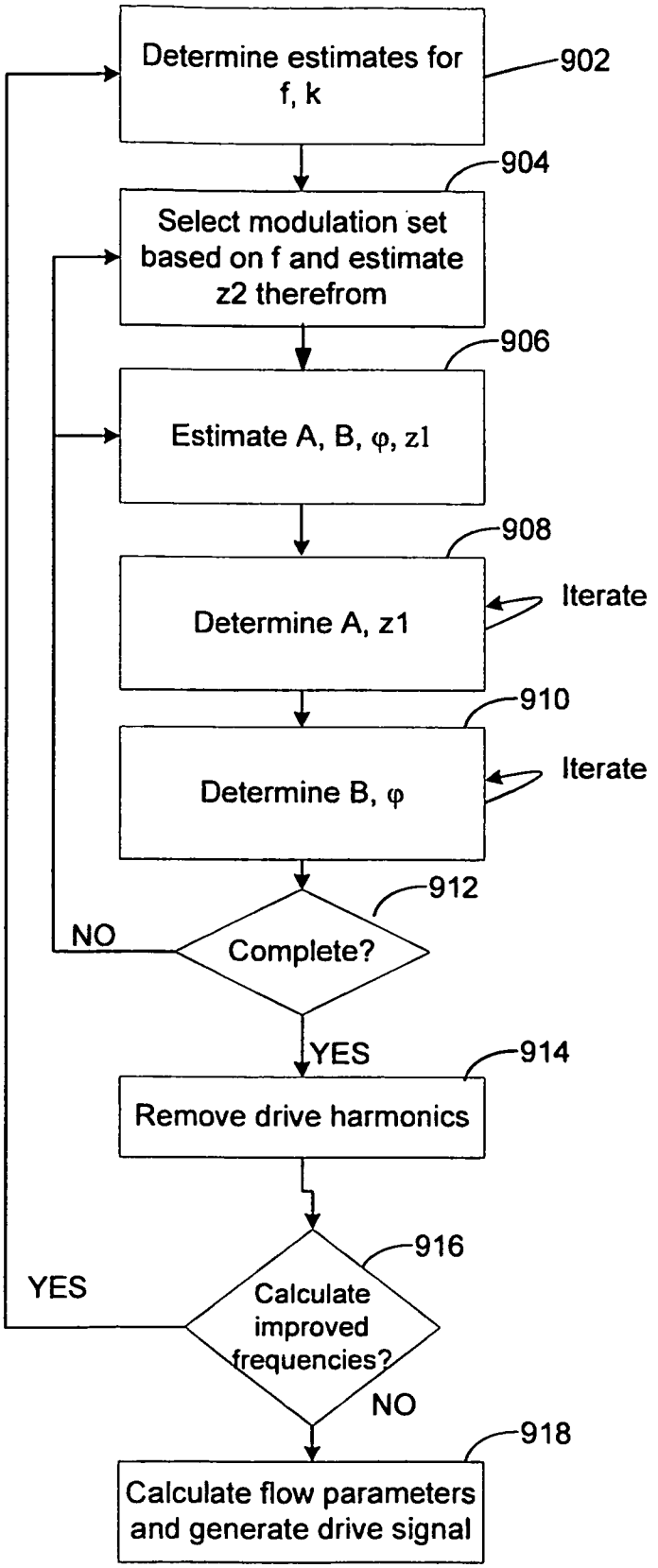

Determine estimates for f, k
902
900
904
Select modulation set based on f and estimate z2 therefrom
906
Estimate A, B, φ, z1
908
Determine A, z1
Iterate
910
Determine B, φ
Iterate
912
Complete?
NO
YES
914
Remove drive harmonics
916
Calculate improved frequencies?
YES
NO
918
Calculate flow parameters and generate drive signal

FIG. 9

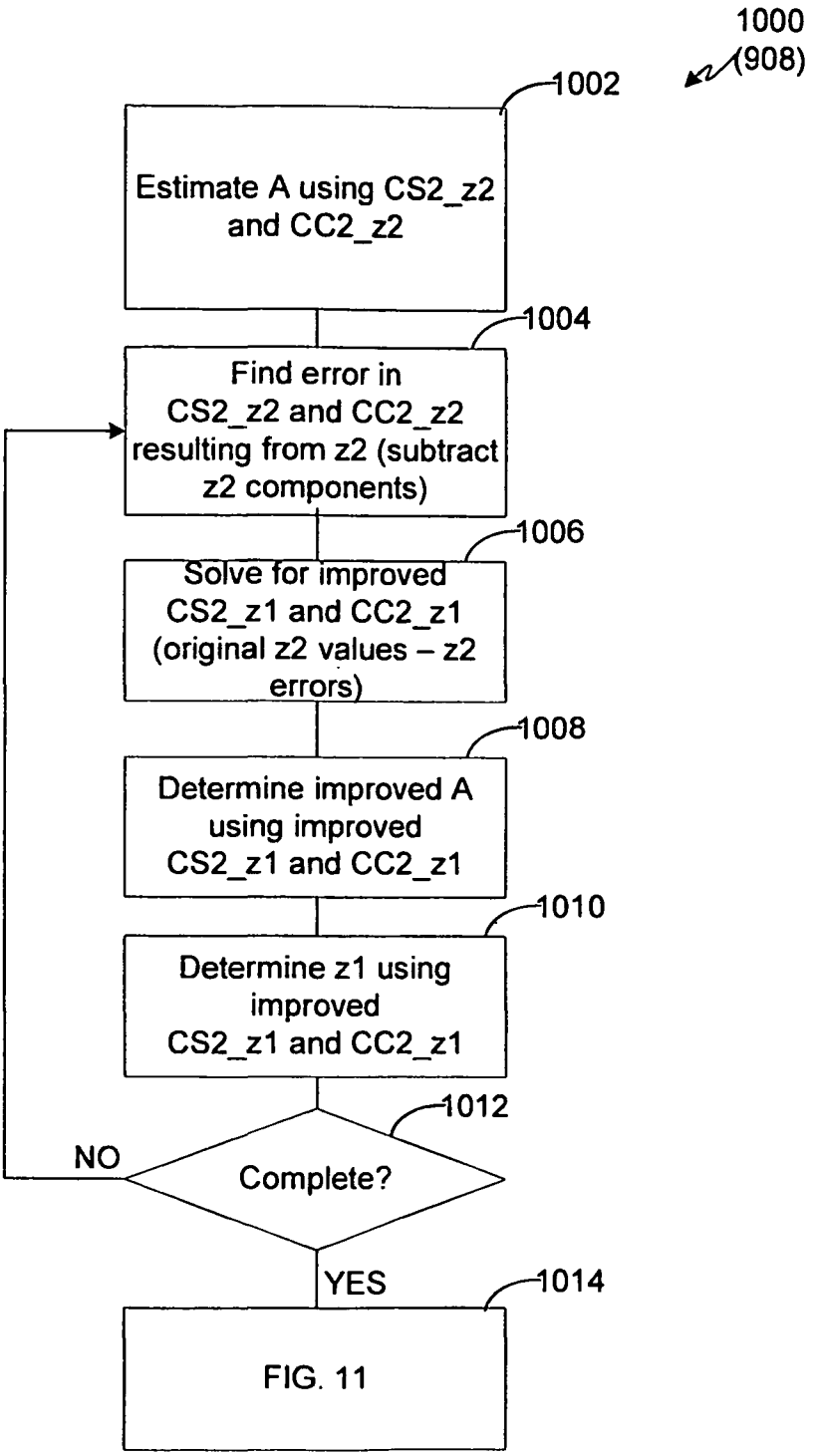

1000
(908)
1002
Estimate A using CS2_z2 and CC2_z2
1004
Find error in CS2_z2 and CC2_z2 resulting from z2 (subtract z2 components)
1006
Solve for improved CS2_z1 and CC2_z1 (original z2 values – z2 errors)
1008
Determine improved A using improved CS2_z1 and CC2_z1
1010
Determine z1 using improved CS2_z1 and CC2_z1
1012
Complete?
NO
YES
1014
FIG. 11

FIG. 10

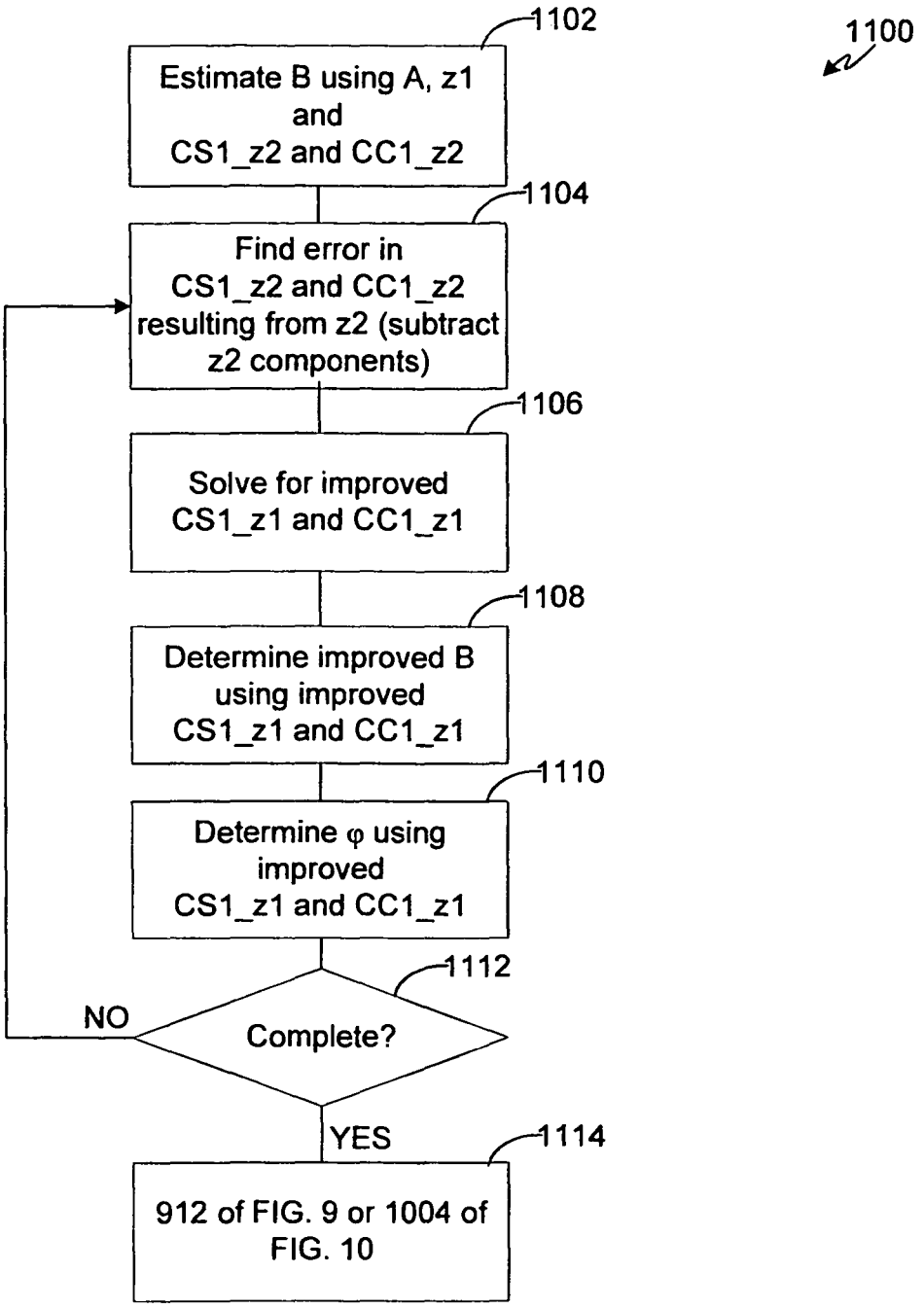

1100
1102
Estimate B using A, z1 and CS1_z2 and CC1_z2
1104
Find error in CS1_z2 and CC1_z2 resulting from z2 (subtract z2 components)
1106
Solve for improved CS1_z1 and CC1_z1
1108
Determine improved B using improved CS1_z1 and CC1_z1
1110
Determine φ using improved CS1_z1 and CC1_z1
1112
Complete?
NO
YES
1114
912 of FIG. 9 or 1004 of FIG. 10

FIG. 11

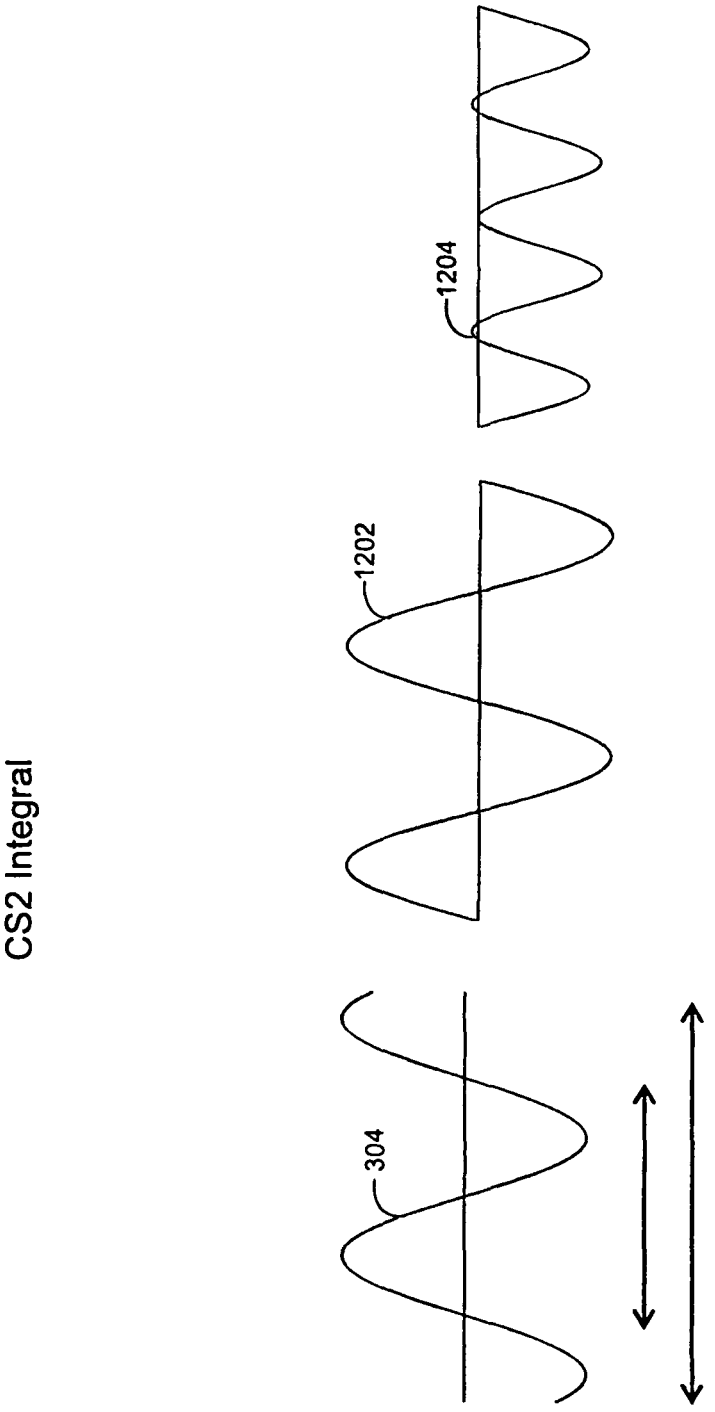


FIG. 12

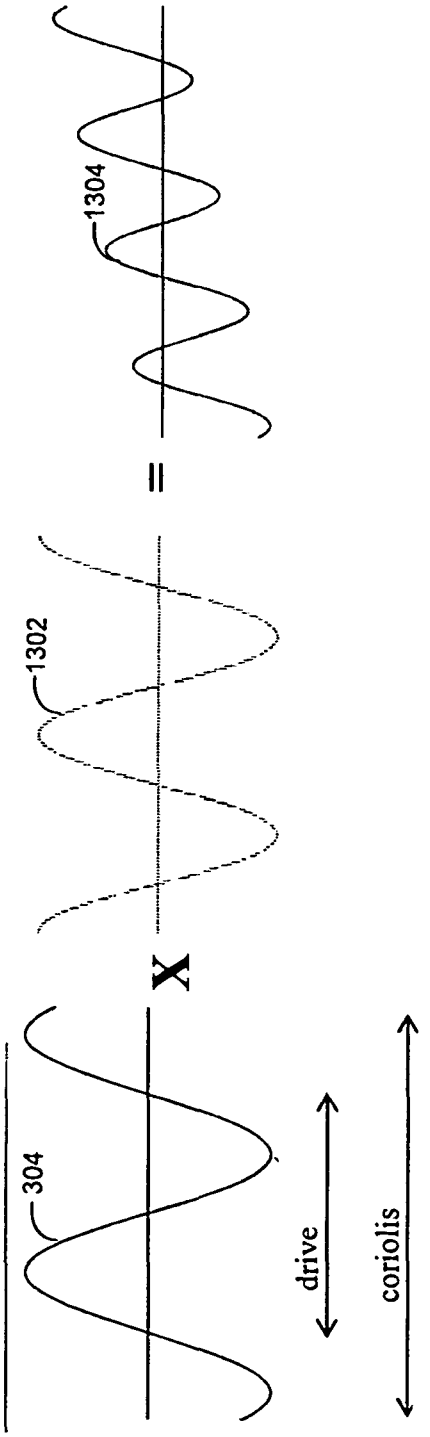


FIG. 13

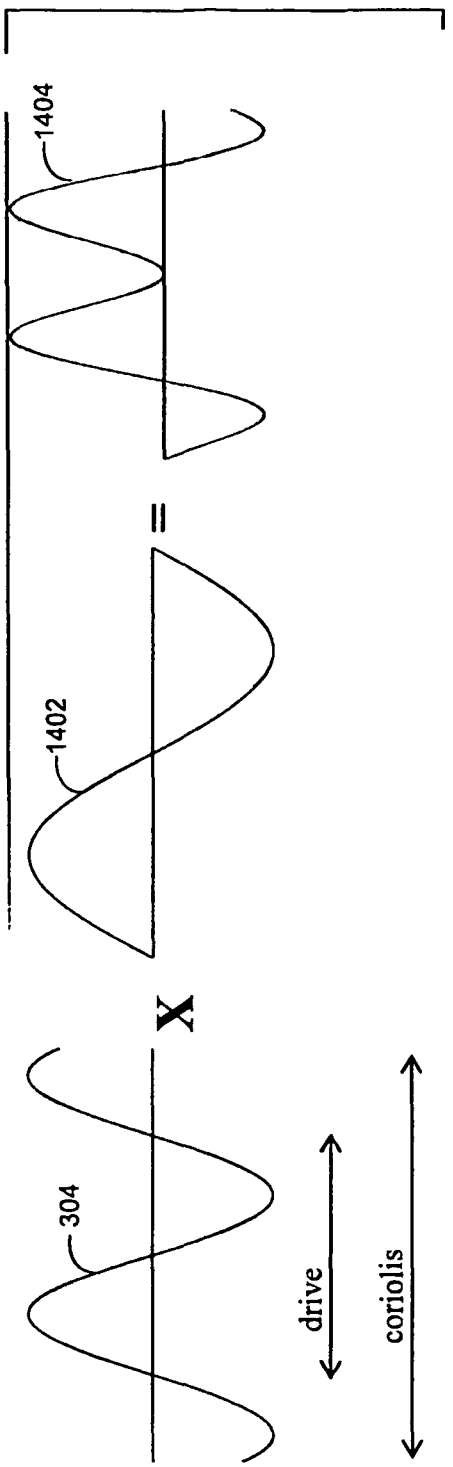


FIG. 14

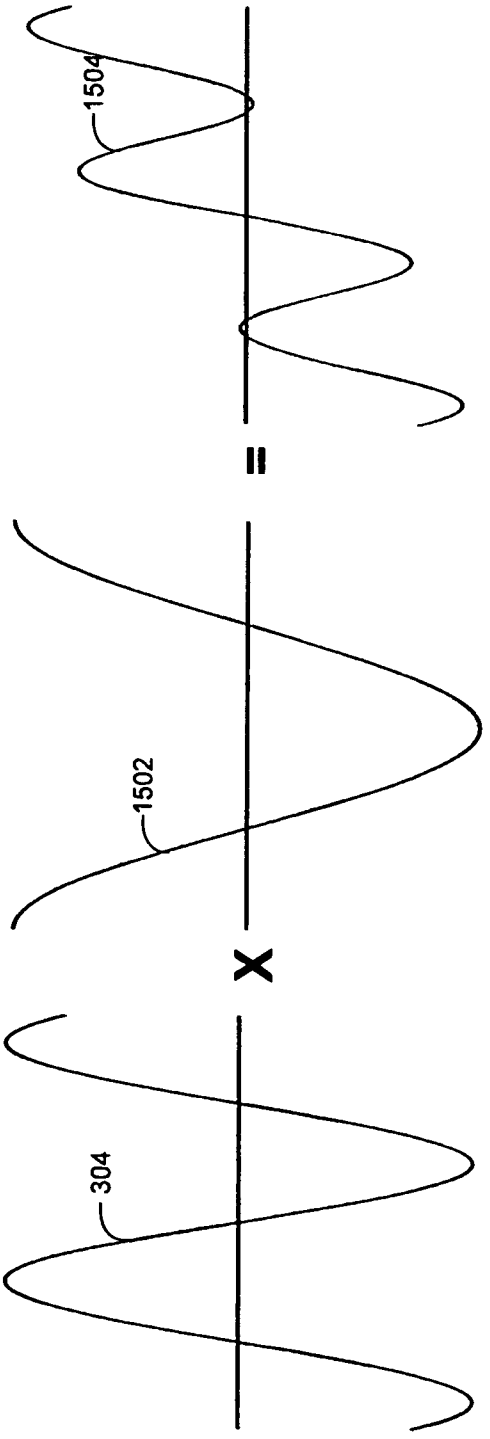


FIG. 15

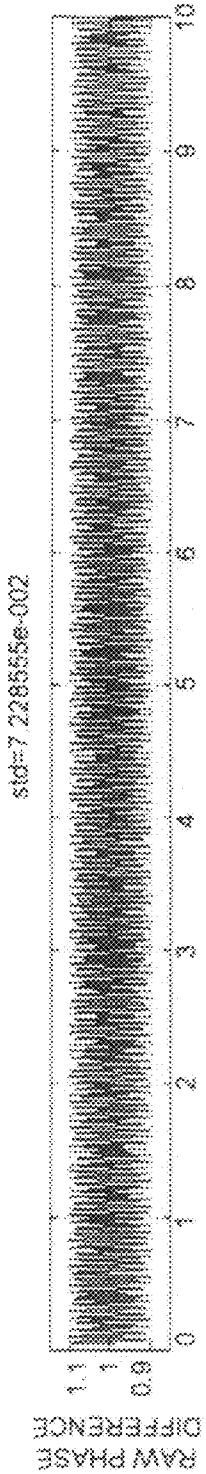


FIG. 16A

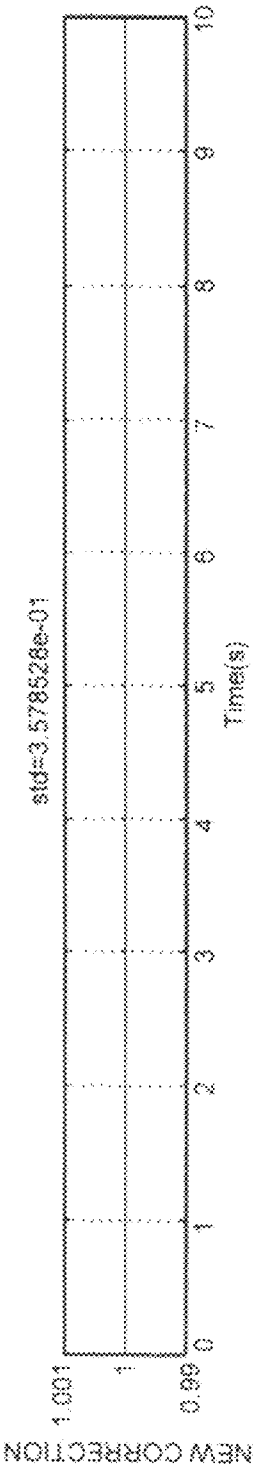


FIG. 16B

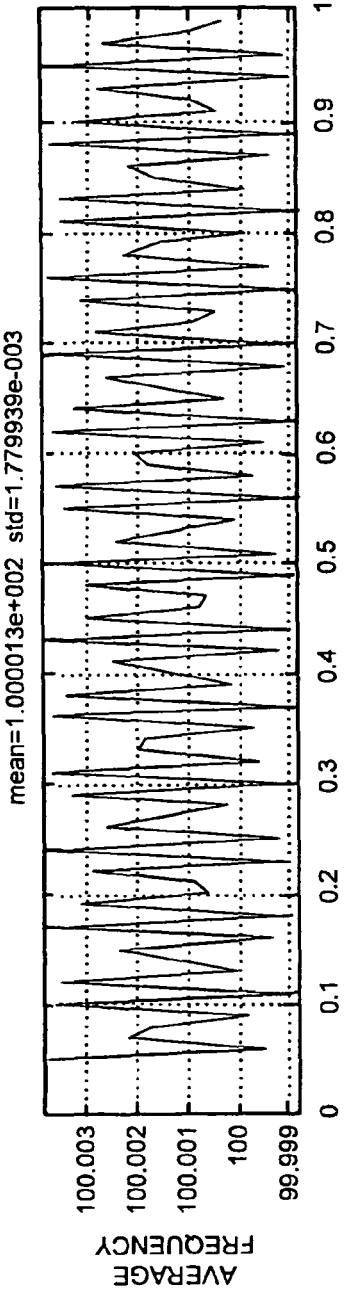


FIG. 17A

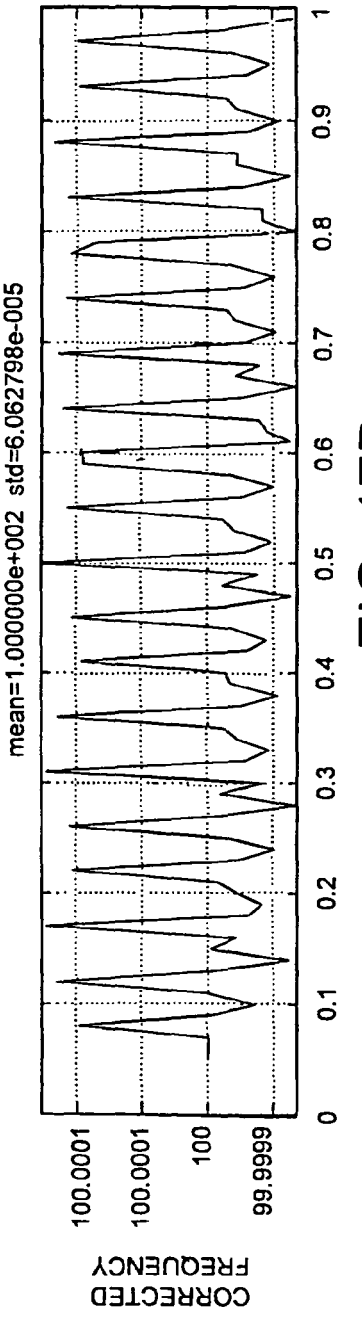


FIG. 17B

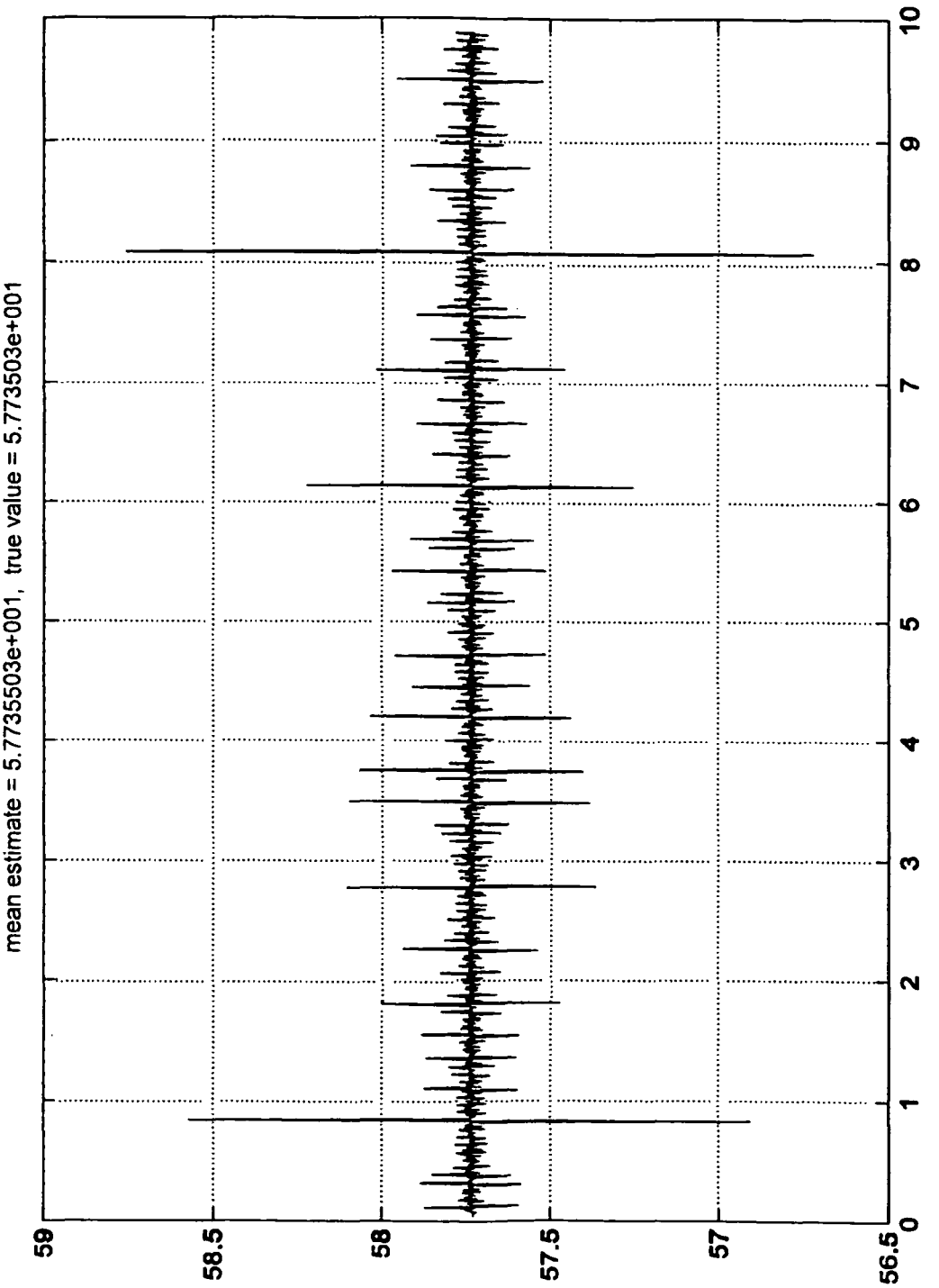

mean estimate = 5.7735503e+001, true value = 5.773503e+001
59
58.5
58
57.5
57
56.5
0
1
2
3
4
5
6
7
8
9
10

FIG. 18

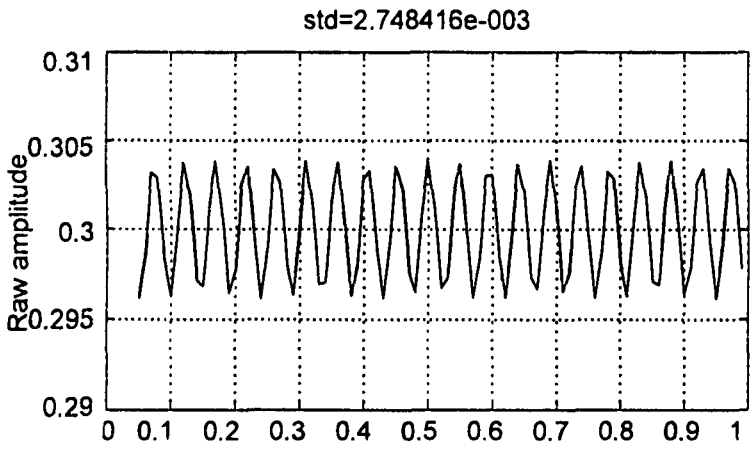


FIG. 19A

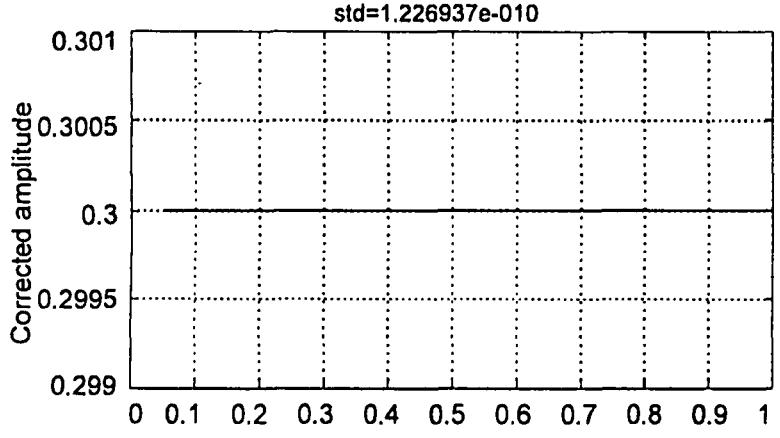


FIG. 19B

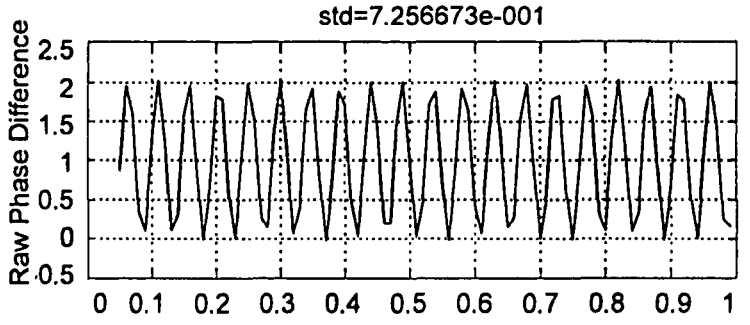


FIG. 19C

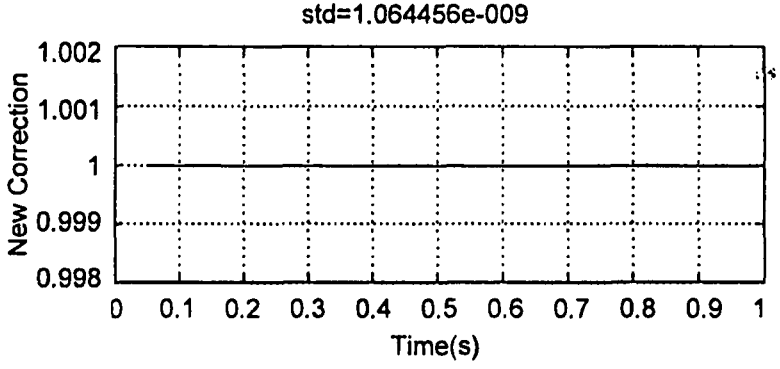


FIG. 19D

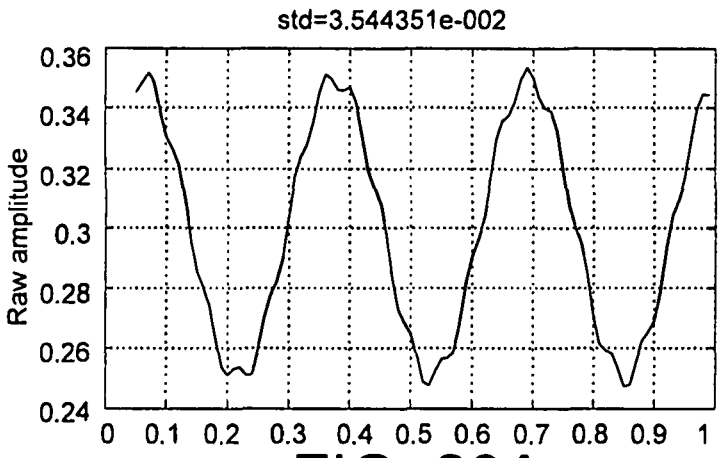


FIG. 20A

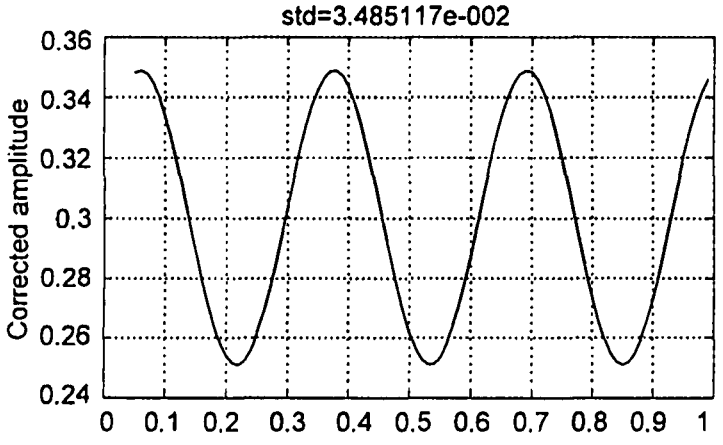


FIG. 20B

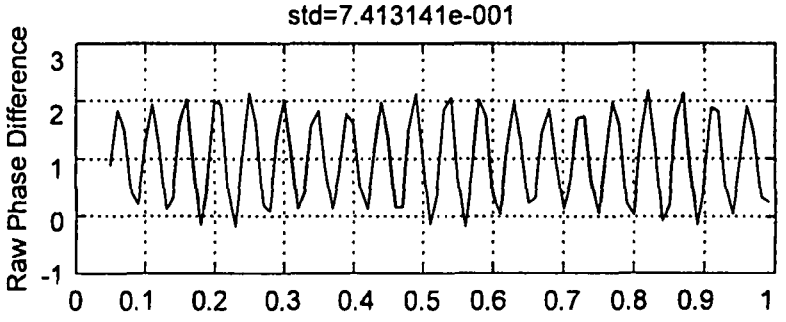


FIG. 20C

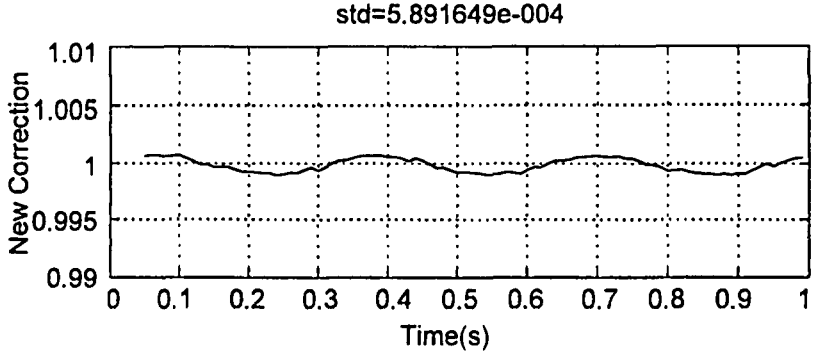


FIG. 20D

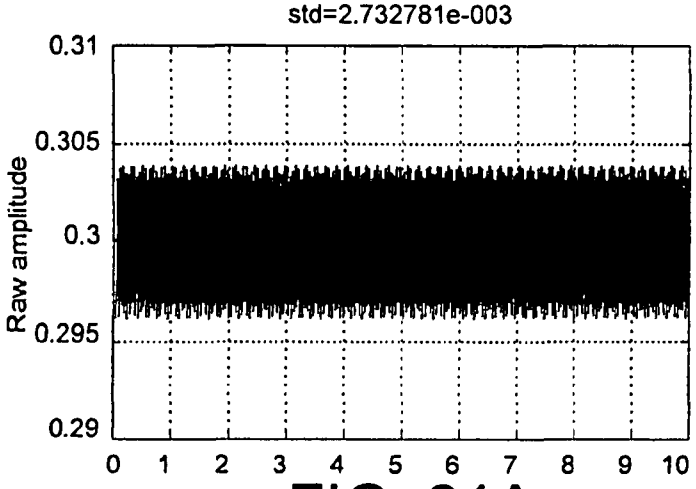


FIG. 21A

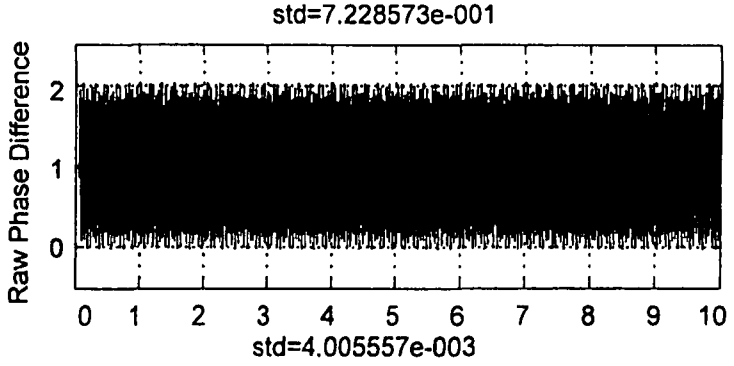


FIG. 21C

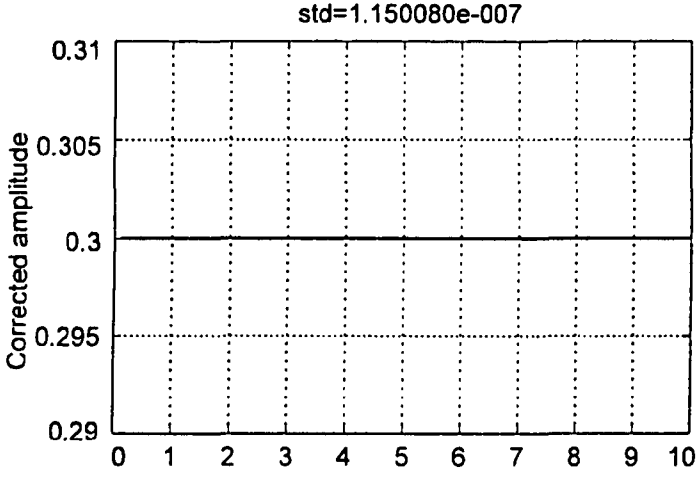


FIG. 21B

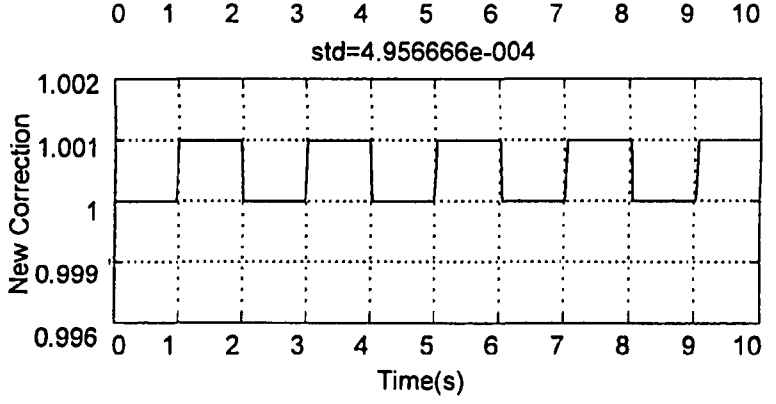


FIG. 21D

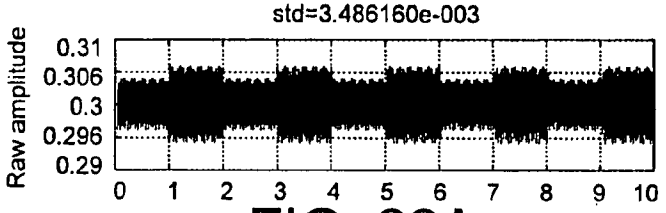


FIG. 22A

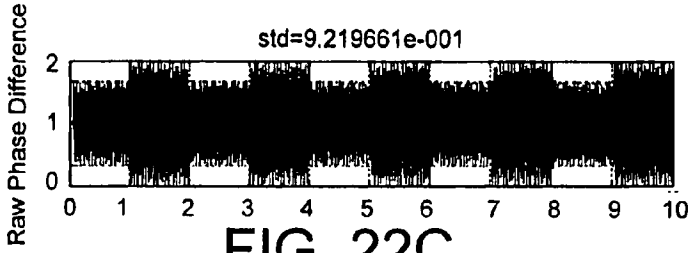


FIG. 22C

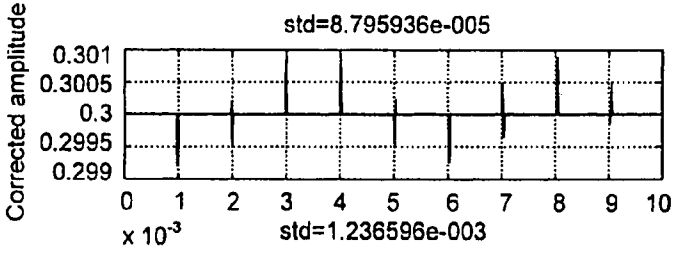


FIG. 22B

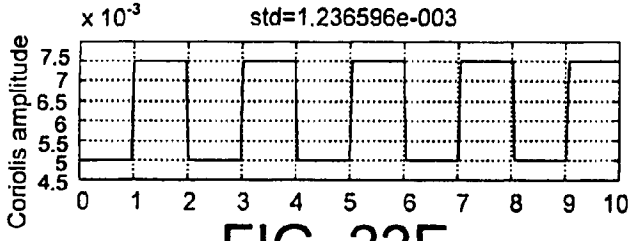


FIG. 22E

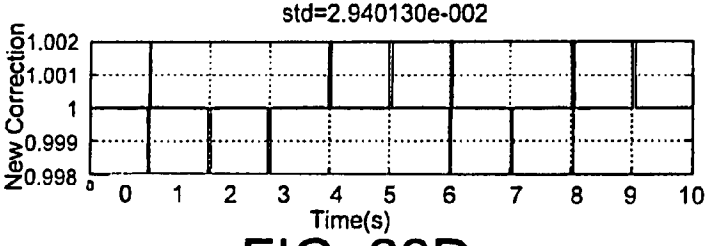


FIG. 22D

CORIOLIS MODE PROCESSING TECHNIQUES

CLAIM OF PRIORITY

This application is a continuation of U.S. patent application Ser. No. 12/761,781, filed Apr. 16, 2010, now U.S. Pat. No. 8,060,320, titled "CORIOLIS MODE PROCESSIONG TECHNIQUES", which is a continuation of U.S. patent application Ser. No. 11/953,773, filed Dec. 10, 2007, now U.S. Pat. No. 7,711,501, and titled "CORIOLIS MODE PROCESSING TECHNIQUES", which is a continuation of U.S. application Ser. No. 11/456,461, filed Jul. 10, 2006, now U.S. Pat. No. 7,313,488 and titled "CORIOLIS MODE PROCESSING TECHNIQUES", which claims the benefit of U.S. Provisional Application No. 60/697,574, filed Jul. 11, 2005, now expired, and titled CORIOLIS MODE PROCESSING FOR FLOWMETERS, all of which are incorporated by reference herein in their entirety.

TECHNICAL FIELD

This description relates to flowmeters.

BACKGROUND

Flowmeters provide information about materials being transferred through a conduit. For example, mass flowmeters provide a measurement of the mass of material being transferred through a conduit. Similarly, density flowmeters, or densitometers, provide a measurement of the density of material flowing through a conduit. Mass flowmeters also may provide a measurement of the density of the material.

For example, Coriolis-type mass flowmeters are based on the Coriolis effect, in which material flowing through a conduit becomes a mass that is affected by a Coriolis force and therefore experiences an acceleration. Many Coriolis-type mass flowmeters induce a Coriolis force by sinusoidally oscillating a conduit about a pivot axis orthogonal to the length of the conduit. In such mass flowmeters, the Coriolis reaction force experienced by the traveling fluid mass is transferred to the conduit itself and is manifested as a deflection or offset of the conduit in the direction of the Coriolis force vector in the plane of rotation.

SUMMARY

According to one general aspect, a method includes receiving a sensor signal from a sensor that is operable to sense a vibration of a flowtube having a fluid flowing therethrough. The sensor signal has a major signal component associated with a drive signal applied to the flowtube and a minor signal component associated with a contaminant of the sensor signal. The method further includes determining major signal parameters of the major signal component based on an analysis of the sensor signal during a time period defined with respect to the minor signal component; and determining a flow parameter of the fluid, based on the major signal parameters.

Implementations may include one or more of the following features. For example, determining the flow parameter may include determining a mass flow rate of the fluid or a density of the fluid. The method may include modifying the drive signal for further application to the flowtube, based on the major signal parameters.

The method may include determining minor signal parameters of the minor signal component based on an analysis of the sensor signal during a time period defined with respect to the minor signal component. The method also may include characterizing an external disturbance of the flowtube, based on the minor signal parameters or modifying the drive signal for further application to the flowtube, based on the minor signal parameters. In addition, the method may further include determining a minor amplitude of the minor signal component; and modifying the drive signal based on the minor amplitude, so as to reduce an influence of the minor signal component on the sensor signal.

The method may include receiving a secondary sensor signal from a secondary sensor; determining secondary major signal parameters of a secondary major signal component of the secondary sensor signal; determining a first timing offset between a first true zero-crossing of the sensor signal and a first observed zero-crossing of the sensor signal; and determining a second timing offset between a second true zero-crossing of the secondary sensor signal and a second observed zero-crossing of the secondary sensor signal. Determining the flow parameter may include determining a difference between the first timing offset and the second timing offset; and determining a mass flow rate of the fluid, based on the difference. The minor signal component associated with the contaminant of the sensor signal may include a Coriolis mode component associated with a Coriolis mode of vibration of the flowtube.

According to another general aspect, a flowmeter control system includes a signal contaminant detection system and a flow parameter determination system. The signal contaminant detection system is operable to receive a first sensor signal from a first sensor that is operable to detect a vibration of a flowtube having a fluid therein and determine first values for first contaminant parameters of a contaminant signal within the sensor signal for a first cycle of the contaminant signal, and being further operable to determine second values for second contaminant parameters of the contaminant signal within the sensor signal for a second cycle of the contaminant signal. The flow parameter determination system is operable to determine a flow parameter of the fluid, based on the sensor signal, the first values of the first contaminant parameters, and the second values of the second contaminant parameters.

Implementations may include one or more of the following features. For example, the first and second values of the first and second contaminant parameters, respectively, may include values for an amplitude and phase of the contaminant signal. The flow parameter determination system may be operable to determine the flow parameter by determining first drive parameters for a first drive mode cycle of a drive mode signal within the sensor signal, and by determining second drive parameters for a second drive mode cycle of the drive mode signal, wherein the drive mode signal corresponds to a drive signal that is applied to the flowtube to maintain oscillation thereof. The flow parameter determination system may be operable to determine the first drive parameters and the second drive parameters, based on the first contaminant parameters and the second contaminant parameters.

The contaminant signal may include a Coriolis mode signal. The first contaminant parameters and the second contaminant parameters may differ from one another due to a change in condition of the flowtube, or of the fluid.

The contaminant determination system may be operable to perform a diagnosis of the condition of the flowtube, or of the fluid, based on the difference between the first contaminant parameters and the second contaminant parameters.

The system may include a drive generator that is operable to output modified drive parameters for use in generating a drive signal to be applied to the flowtube for maintaining

oscillation thereof. The drive generator may be operable to determine the modified drive parameters based on the first contaminant parameters and the second contaminant parameters. The drive generator may be operable to determine the modified drive parameters such that the modified drive parameters include contaminant-canceling parameters that are designed to reduce an effect of the contaminant signal within the sensor signal.

DESCRIPTION OF DRAWINGS

FIG. **1**A is an illustration of a flowmeter using a bent flowtube.

FIG. **1**B is an illustration of a flowmeter using a straight flowtube.

FIG. **2** is a block diagram of a flowmeter using Coriolis mode processing techniques.

FIG. **3** is a first timing diagram of a sensor signal having a drive mode signal component and a Coriolis mode signal component.

FIG. **4** is a flow chart illustrating an operation of flowmeter of FIG. **2**.

FIG. **5** is a flow chart illustrating a first process of the flowmeter of FIG. **2**.

FIG. **6** is a flow chart of a second process of the flowmeter of FIG. **2**.

FIG. **7** is a block diagram of a second implementation of the flowmeter of FIG. **2**.

FIG. **8** is a second timing diagram of a sensor signal having a drive mode signal component and a Coriolis mode signal component.

FIG. **9** is a flow chart illustrating a first operation of the flow meter of FIG. **7**.

FIG. **10** is a flow chart illustrating a second operation of the flow meter of FIG. **7**.

FIG. **11** is a flow chart illustrating a third operation of the flow meter of FIG. **7**.

FIG. **12** is a timing graph illustrating a first type of calculation of the flowmeters of FIGS. **2** and **7**.

FIG. **13** is a timing graph illustrating a second type of calculation of the flowmeters of FIGS. **2** and **7**.

FIG. **14** is a timing graph illustrating a third type of calculation of the flowmeters of FIGS. **2** and **7**.

FIG. **15** is a timing graph illustrating a fourth type of calculation of the flowmeters of FIGS. **2** and **7**.

FIGS. **16**A and **16**B are graphs illustrating a phase difference between two sensor signals.

FIGS. **17**A and **17**B are graphs illustrating an average frequency and a corrected frequency.

FIG. **18** is a graph illustrating an example of a Coriolis frequency estimation.

FIGS. **19**A-**19**D are graphs illustrating raw and corrected values for amplitude and phase of a drive signal.

FIGS. **20**A-**20**D are graphs illustrating amplitude modulation of a drive signal.

FIGS. **21**A-**21**D are graphs illustrating a step change in phase difference of a drive signal.

FIGS. **22**A-**22**E are graphs illustrating variations in the Coriolis amplitude.

DETAILED DESCRIPTION

Types of flowmeters include digital flowmeters. For example, U.S. Pat. No. 6,311,136, which is hereby incorporated by reference, discloses the use of a digital flowmeter and related technology including signal processing and measurement techniques. Such digital flowmeters may be very precise in their measurements, with little or negligible noise, and may be capable of enabling a wide range of positive and negative gains at the driver circuitry for driving the conduit. Such digital flowmeters are thus advantageous in a variety of settings. For example, commonly-assigned U.S. Pat. No. 6,505,519, which is incorporated by reference, discloses the use of a wide gain range, and/or the use of negative gain, to prevent stalling and to more accurately exercise control of the flowtube, even during difficult conditions such as two-phase flow.

Analog flowmeters also exist. Although such analog flowmeters may be prone to typical shortcomings of analog circuitry, e.g., low precision and high noise measurements relative to digital flowmeters, they also may be compatible with the various techniques and implementations discussed herein. Thus, in the following discussion, the term "flowmeter" or "meter" is used to refer to any type of device and/or system in which a flowmeter system, such as, for example, a Coriolis flowmeter system uses various control systems and related elements to measure a mass flow, density, and/or other parameters of a material(s) moving through a flowtube or other conduit.

FIG. **1**A is an illustration of a flowmeter using a bent flowtube **102**. Specifically, the bent flowtube **102** may be used to measure one or more physical characteristics of, for example, a (traveling) fluid, such as, for example, density, as referred to above. In FIG. **1**A, a digital transmitter **104** exchanges sensor and drive signals with the bent flowtube **102**, so as to both sense an oscillation of the bent flowtube **102**, and to drive the oscillation of the bent flowtube **102** accordingly. By quickly and accurately determining the sensor and drive signals, the digital transmitter **104**, as referred to above, provides for fast and accurate operation of the bent flowtube **102**. Examples of the transmitter **104** being used with a bent flowtube are provided in, for example, commonly-assigned U.S. Pat. No. 6,311,136.

FIG. **1**B is an illustration of a flowmeter using a straight flowtube **106**. More specifically, in FIG. **1**B, the straight flowtube **106** interacts with the digital transmitter **104**. Such a straight flowtube operates similarly to the bent flowtube **102** on a conceptual level, and has various advantages/disadvantages relative to the bent flowtube **102**. For example, the straight flowtube **106** may be easier to (completely) fill and empty than the bent flowtube **102**, simply due to the geometry of its construction. In operation, the bent flowtube **102** may operate at a frequency of, for example, 50-110 Hz, while the straight flowtube **106** may operate at a frequency of, for example, 300-1,000 Hz.

FIG. **2** is a block diagram of a flowmeter using Coriolis mode processing techniques. In FIG. **2**, a digital mass flowmeter **200** includes the digital transmitter **104**, one or more motion sensors **205**, one or more drivers **210**, a flowtube **215** (which also may be referred to as a conduit, and which may represent either the bent flowtube **102**, the straight flowtube **106**, or some other type of flowtube), and a pressure sensor **220**. The digital transmitter **104** may be implemented using one or more of, for example, a processor, a Digital Signal Processor (DSP), a field-programmable gate array (FPGA), an ASIC, other programmable logic or gate arrays, or programmable logic with a processor core.

The digital transmitter **104** generates a measurement of, for example, density and/or mass flow of a material flowing through the flowtube **215**, based at least on signals received from the motion sensors **205**. The digital transmitter **104** also controls the drivers **210** to induce motion in the flowtube **215**. This motion is sensed by the motion sensors **205**.

Density measurements of the material flowing through the flowtube are related to, for example, the frequency of the

motion of the flowtube **215** that is induced in the flowtube **215** by a driving force supplied by the drivers **210**, and/or to the temperature of the flowtube **215**. Similarly, mass flow through the flowtube **215** is related to the phase and frequency of the motion of the flowtube **215**, as well as to the temperature of the flowtube **215**. The flowmeter **200** may be configures to measure only density, and thereby to operate as a densitometer.

The temperature in the flowtube **215**, which is measured using the temperature sensor **220**, affects certain properties of the flowtube, such as its stiffness and dimensions. Also in FIG. **2**, a pressure sensor **225** is illustrated that is in communication with the transmitter **104**, and is connected to the flowtube **215** so as to be operable to sense a pressure of a material flowing through the flowtube **215**. More particularly, pressure measurements may relate to an absolute pressure measurement of the fluid within the flowtube **215**, or to a differential pressure drop across a portion of the flowtube.

FIG. **2** also illustrates a liquid fraction probe **230** that is operable to measure an amount of a particular liquid within the flow tube **215** when the flow tube **215** contains a mixed fluid having more than one fluid component, such as, for example, oil and water. Somewhat similarly, a void fraction sensor **235** measures a percentage of gas within a fluid inner flow tube **215** that contains at least one liquid and at least one gas component. Although not specifically illustrated in FIG. **2**, various other components may be used to measure or determine properties of the fluid within the flow tube **215**.

The digital transmitter **104** includes a flow meter output unit **240** that is operable to determine information related to an operation of the flow meter **200**. In particular, the flow meter output unit **240** includes a mass flow rate/density determination system **245** that is operable to determine either a mass flow rate and/or a density of a fluid within the flow tube **215**. The flow meter output unit **240** also includes a drive signal generator **250** that is operable to output drive signal characteristics to the drivers **210**, so as to maintain oscillation of the flow tube **215**.

The flow meter output unit **240** performs the above-described functions based on the sensor signals received from the sensors **205**. For example, the flow meter output unit **240** may analyze sensor signals from the sensors **205** to determine a frequency of the sensor signals, and/or phase differences between the sensor signals from different ones of sensors **205**.

In theory, these sensor signals reflect the form, parameters, and characteristics of the vibration of the flowtube at the drive frequency applied by the drivers **210**, and contain, either within themselves or in relation to one another, information regarding the mass flow rate, density, or other parameters of the fluid flow within the flowtube **215**. For example, if the drive signal is simplified and applied as a pure sinusoidal signal, then the sensor signal detected by the sensors **205** also should be, in theory, essentially a pure sinusoid. In practice, a number of contaminants are present within the sensor signals that may alter the characteristics of the sensor signals in an undesirable way. Thus, measurements output by the flow meter output unit **240** may be less accurate as a result of the presence of these contaminants within the sensor signal.

One example of a contaminant within the sensor signal includes harmonics of the drive frequency that may be within the sensor signals. Such harmonics may be caused by, for example, non-linearities within the sensors **205**, and do not represent actual vibrations within the flow tube **215**. If the drive frequency is designated as the first harmonic, then typical second, third and fourth harmonic amplitudes may be at, for example, 1%, 0.5%, 0.5% and 0.1%, respectively, of the amplitude of the first harmonic. Furthermore, ten or more higher harmonics may be observed within the sensor signal in a given circumstance.

Another source of contaminant of the sensor signal includes other modes of vibration of the flow tube **215** besides the desired driven mode that results from application of the drive signals. For example, external vibrations, sudden changes in flow rate, or various other factors may result in the presence of additional modes of vibration of the flow tubes **215**.

One example of the modes of vibration that may be present within the flow meter **200** is known as the Coriolis mode of vibration. The Coriolis mode is typically the mode nearest to the driven mode, and is referred to as the Coriolis mode because the Coriolis force associated with mass flow measurements of the flow meter **200** operate in this mode of vibration.

Perhaps confusingly, the Coriolis force manifests at the drive frequency, and, therefore, the frequency and/or phase of the drive mode may be analyzed to determine, for example, the mass flow rate of the fluid within the flow tube **215**. That is, as just referenced, the flowtube **215**, as it vibrates, may include at least two modes of vibration, where one mode corresponds to a vibration of the flowtube **215** in the drive or driven mode, and a second mode corresponds to a vibration of the flowtube **215** in the Coriolis mode. These two modes may have different mode shapes corresponding to the movements (e.g., twisting) of the flowtube **215**. A mass flow of fluid within the flowtube **215** causes the Coriolis mode shape to oscillate, but at the drive frequency, while, simultaneously, the Coriolis mode shape has its own natural frequency that is readily excited by external vibration or other factors.

In other words, there are two aspects to the Coriolis mode: its oscillation at the drive frequency (associated with a measurement principle of the flow meter **200**), and the free vibration of the Coriolis mode at its own frequency (i.e., the Coriolis frequency). It is the latter aspect of the Coriolis mode that results from, for example, external vibration and other factors. As explained in more detail below, the flow meter **200** is designed to characterize, identify, and/or minimize the effect of this Coriolis mode.

Referring briefly to FIG. **3** for illustration of the above-described concepts, a signal **302** reflects the above-described drive mode signal, that is, a signal corresponding to a movement (e.g., velocity) of the flowtube **215**, related to a drive signal applied by the driver **210** to the flow tube **215**. The drive signal from the driver **210** and the resulting flowtube movement (velocity) should, ideally, be in phase with one another, but are different quantities, and, in particular, the former is generally represented in mA and the latter in mV. Therefore, it should be understood that in the following description, the signal **302** does not represent the drive signal that is output by the driver **210**, but, rather, represents a drive mode signal that corresponds to a driven mode of vibration of the flowtube **215** that is excited by the action of the drive signal from the driver **210** on the flowtube **215**.

A signal **304** represents a sensor signal that is detected by sensors **205** as a result of the vibration of the flow tube **215**. A Coriolis mode signal **306**, or Coriolis signal **306**, illustrates the Coriolis mode contaminant just referred to. Thus, the sensor signal **304** is composed of at least two modes of vibration: the drive mode signal **302** and the Coriolis mode signal **306**. The drive mode signal **302** and the Coriolis mode signal **306** also may be referred to as the drive frequency signal **302** and the Coriolis frequency signal **306**, or the drive signal component **302** and the Coriolis signal component **306**, or the

drive frequency component **302** and the Coriolis frequency component **306**, all respectively, or by similar terminology.

In the example FIG. **3**, it may be seen that a frequency of the Coriolis mode signal **306** is less than a frequency of the drive mode signal **302** (i.e., the period of the Coriolis mode signal **306** is greater than that of the drive mode signal **302**). In general, however, the Coriolis mode signal **306** may have a frequency that is either less than or greater than that of the drive mode signal **302**. Moreover, there may be multiple Coriolis mode signals **306**, where a first one of the Coriolis mode signal may have a frequency less than that of the drive mode signal **302**, and a second Coriolis mode signal may have a frequency greater than that of the drive mode signal **302**. Generally, the Coriolis mode signal **306** is a mode of vibration that is generally adjacent to a mode of vibration of the drive mode signal **306**. However, the Coriolis mode signal **306** need not be particularly close to the drive mode signal **302** in terms of frequency. For example, in the straight flowtube of FIG. **1**B, when using the lowest mode of vibration as the drive mode, the next (Coriolis) mode of vibration may be two or more times higher, and therefore may be filtered out.

Generally, though, separation (e.g., filtering) or characterization of the Coriolis mode signal **306** with respect to the drive mode signal **302** within the sensor signal **304** may be difficult or impossible. Moreover, a response time of the meter **200** may be improved when the Coriolis mode signal **306** is as close as possible to the drive mode signal in terms of frequency (thus reducing an efficacy or possibility of filtering), since the Coriolis force may then be more easily manifested within the drive mode.

When the drive mode signal **302** corresponds to a lowest mode of vibration of flow tube **215**, the Coriolis mode signal **306** may be the next highest resident mode above the drive mode signal **302**. However, when the drive mode is a relatively high mode of vibration, as just referred to, the Coriolis mode signal **306** may be the next lowest resident mode, so that it may be necessary to consider two adjacent modes (both above and below the drive mode). These may be referred to as the upper and lower Coriolis mode. In the example of FIGS. **2** and **3**, for simplicity's sake, only one Coriolis mode is considered. However, it should be understood that the analysis described herein is valid whether a frequency of the Coriolis mode signal **306** is lower and/or higher than that of the drive mode signal **302**.

Also in FIG. **3**, an area **308** and an area **310** are designated as regions of interest for the following discussion. The area **308** includes a time t=0 at which a zero-crossing of the drive mode signal **302** occurs, as well as a zero-crossing of the sensor signal **304** itself. As shown, a time difference or offset z**1** exists between these two zero-crossings, which is due to, for example, the presence of the Coriolis signal **306** within the sensor signal **304**. As referred to above, detection of zero-crossings may be important, for example, in the operations of the flowmeter output unit **240** in determining a frequency of the sensor signal **304**, so as to thereby deduce a density of the fluid(s) within the flowtube **215**. Thus, the offset z**1** may lead to reduced accuracy or complete failure, or reduced efficiency, of the flowmeter output unit **240**.

The area **310** also includes the offset z**1**. As described in more detail below, an additional offset, referred to below as z**2**, may be present within the sensor signal **304** that is not illustrated for the purposes of discussion of FIGS. **2-6**.

In part by characterizing, accounting for, and/or identifying the offset z**1**, the flowmeter **200** is able to determine characteristics and parameters of the Coriolis mode signal **306**. Put another way, the flowmeter **200** is able to determine characteristics and parameters of the sensor signal **304** that are related to the drive mode signal **302**, and that are not related to the Coriolis mode signal **306**. Thus, the flowmeter **200** accounts for the causes or reasons for the presence of the Coriolis mode signal **306** (e.g., external vibrations, increased flow rate, or a changed percentage of gas within the fluid flow), and outputs mass flow rate and/or density measurements (as well as subsequent drive signals) that are highly accurate, and that are resistant to the causes and effects of the Coriolis mode signal **306**.

Referring back to FIG. **2**, components, operations, and analyses of the flowmeter **200** are illustrated that are used to obtain such accurate and stable operation of the flowmeter **200**. For example, the digital transmitter **104** includes a signal analyzer **255** that is operable to receive the sensor signals from the sensors **205** and output at least two characterizations of the sensor signals.

In particular, the signal analyzer **255** outputs a first characterization of the sensor signal(s) **304** in which an influence of the drive mode signal **302** is maximized or emphasized relative to information within the sensor signal **304** that is related to the Coriolis signal **306**. Further, the signal analyzer **255** outputs a second characterization of the sensor signal(s) **304**, in which an influence of the Coriolis mode signal **306** parameters are maximized relative to a presence of the drive mode signal **302**. In so doing, the first characterization, i.e., the drive-emphasized characterization, may be output to a signal identifier **260** for identification of parameters of the drive mode signal **302**. Similarly, but conversely, the signal analyzer **255** outputs the second characterization, i.e., the Coriolis-emphasized characterization, of the sensor signals to the signal identifier **260** for identification of the Coriolis mode signal **306** parameters.

This general process, as well as various sub-processes, may be iteratively repeated, until a desired level of accuracy is reached with respect to characteristics of the sensor signals **304**. That is, the parameters that are generally of interest to the flow meter output unit **240** are those characteristics of the sensor signal **304** that correspond to vibrations of the flow tube only at the drive frequency, uncontaminated by the presence of the Coriolis mode signal **306** within the sensor signal **304**. These parameters or characteristics of the sensor signal **304** allow the flow meter output unit **240** to determine a mass flow rate and/or density of the fluid within the flow tube **215**, and to generate a drive signal to the driver **210** that accurately maintains a desired oscillation of the flow tube **215**.

In the implementations described herein, then, these parameters of the sensor signal **304** that reflect characteristics of the drive mode signal **302**, and that are referred to herein as drive signal parameters, are referred to as: "A," referring to an amplitude of oscillation of the drive mode signal **302**; "f," a frequency of the drive mode signal **302**; and "θ," a phase of the sensor signal **304** at the drive frequency when time t=0. Analogously, corresponding parameters of the Coriolis mode signal **306** include an amplitude B, a frequency k, and a phase ϕ.

Thus, by determining an accurate representation of the drive parameters A, f, and θ, the signal analyzer **255** and the signal identifier **260** ensure accurate output and operation of the flow meter output unit **240**. Similarly, by determining accurate characterizations of the Coriolis mode signal **306** parameters B, k, and ϕ, the signal analyzer **255** and the signal identifier **260** may assist in the accurate determination of A, f and θ.

Moreover, by determining the Coriolis mode signal **306** parameters B, k, and ϕ, the digital transmitter **104** allows for accurate determination of, for example, characteristics of external vibrations or other factors that lead to a presence in

the Coriolis mode signal **306** in the sensor signal **304**. As a result, such external factors may be extracted from the sensor signal **304**, for, for example, analysis of the external event(s) which lead(s) to the determined value of the Coriolis mode parameters, or otherwise for responding to these factors and/or eliminating an impact of these factors.

The described techniques for determining the drive and Coriolis parameters A, f, θ, B, k, and ϕ may then be performed on a cycle-by-cycle basis (or more or less frequent, as desired). In this way, information from a previous cycle may be used in calculations (e.g., as initial estimates) performed on the next cycle. Moreover, changes in the sensor signal **304** may be detected and characterized within the same or following period of the sensor signal in which the changes occur.

As described in more detail below, the signal analyzer **255** operates by implementing a zero-crossing detector **255** that analyzes the sensor signal **304** to determine a time at which the sensor signal **304** crosses a zero value, e.g., within areas **308** and **310** in FIG. **3**. As is known, such detected zero crossings may be used to calculate a period, and thus a frequency, of the sensor signal **304**.

A frequency calculator **270** may be used to receive an output of the zero-crossing detector **265**, to calculate the frequency f of the sensor signal **304**. Then, a frequency k of the Coriolis mode signal **306** may be determined from the frequency f. For example, it is often the case that an existing relationship between the frequency f and the frequency k is known. For example, the frequency k may be expressed as the frequency f reduced by a factor of √3, or by some other factor.

Once the frequency f and k are known, an integrator **275** may be used to perform two characterizations of the sensor signal **304**. That is, as described above, the integrator **275** may perform a first integration of the signal **304** in which parameters A, f, and θ of the drive mode signal **302** within the sensor signal **304** are maximized or emphasized relative to the Coriolis mode parameters B, k, and ϕ of the Coriolis mode signal **306** that are present within the sensor signal **304**. As a result, the integrator **275** may output a drive-emphasized characterization of the sensor signal **304** to the signal identifier **260**, in which the effect of parameters B, k, and ϕ the Coriolis mode signal **306** is minimized or eliminated.

Similarly, the integrator **275** may perform a second integration in which parameters or characteristics B, k, and ϕ of the Coriolis mode signal **306** within the sensor signal **304** are maximized or emphasized relative to the corresponding drive signal parameters A, f, θ, within the sensor signal **304**. The result is a Coriolis-emphasized characterization being output by the integrator **275** to the signal identifier **260**.

The signal identifier **260** receives the integration results, i.e., the drive-emphasized characterization of the sensor signal **304** and the Coriolis-emphasized characterization of the sensor signal **304**, within integration results **280**. This function of the integrator **275** also may be referred to as mode maximization; i.e., the integrator **275** performs a first integration to maximize an effect of the drive mode signal **302** within the sensor signal **304** (minimizing the effect of the Coriolis mode signal **306**), and performs a second integration to maximize an effect of the Coriolis signal **306** within the sensor signal **304** (minimizing the effect of the drive mode signal **302**).

For example, the integrator **275** may perform the two integrations as numerical integrations of the sensor signal **304**, examples of which are provided in more detail below. Then, the results of these numerical integrations may be stored within the integration results **280**.

A second memory or database **285** stores initial and/or revised estimates of the various signal parameters to be calculated. Accordingly, a parameter calculator **290** inputs the integration results and the initial parameter estimates, and calculates remaining ones of the parameters, as well as improved values for the parameter estimates. The same or similar parameter estimates may be used by the signal analyzer **385**, so that the parameter estimates database **285** is illustrated within the signal analyzer **255**, as well. Of course, both the signal analyzer **255** and the signal identifier **260** may access the same or different parameter estimates database(s) **285**.

An example of an operation of the signal analyzer **255** is provided in more detail below with respect to FIGS. **3** and **4**. In particular, it should first be understood that known techniques for determining the amplitude A and phase data θ on the sensor signal **304** include a Fourier analysis of the signals **304**, as described in detail in, for example, commonly-assigned U.S. Pat. No. 6,311,136, which is incorporated by reference above. Within such analysis, for example, an integration may be performed over a period of the sensor signal **304** that is presumed to equate to a period of the drive mode signal **302**, as illustrated by Eqs. 1, 1a, 2 and 2a, below:

$$I_S(A, f, \theta) := \int_0^{\frac{1}{f}} A \cdot \sin[(2 \cdot \pi \cdot f \cdot t) + \theta] \cdot \sin(2 \cdot \pi \cdot f \cdot t) dt \quad \text{Eq. (1)}$$

$$I_S(A, f, \theta) = \frac{1}{2f} A\cos(\theta) \quad \text{Eq. (1a)}$$

$$I_C(A, f, \theta) := \int_0^{\frac{1}{f}} A \cdot \sin[(2 \cdot \pi \cdot f \cdot t) + \theta] \cdot \cos(2 \cdot \pi \cdot f \cdot t) dt \quad \text{Eq. (2)}$$

$$I_C(A, f, \theta) = \frac{1}{2f} A\sin(\theta) \quad \text{Eq. (2a)}$$

As may be seen, Eqs. (1) and (2) rely on integrations with modulating functions sin(2πft) and cos(2πft), respectively. Eqs. (1) and (2) may be simplified into Eqs. (1a) and (2a), respectively, which may be manipulated to determine analytical expressions for A and θ, as shown in Eqs. (3) and (4):

$$A_est := 2 \cdot f \sqrt{I_S^2 + I_C^2} \quad \text{Eq. (3)}$$

$$\theta_est := a\tan\left(\frac{I_C}{I_S}\right) \quad \text{Eq. (4)}$$

Thus, given values for the functions I_S and I_C, as well as the frequency f, estimates for the values of A and θ may be obtained.

In summary, then, the expressions, for example, Asin (2πt+θ) and Acos(2πt+θ) represent the sensor signal **304**. Higher harmonics of the sensor signal may be present without impacting the results of Eqs. (1)-(4), since the zero-crossings of the harmonics will, by definition, be the same as the zero-crossings of the sensor signal **304** itself, and the Fourier analysis is designed to eliminate the influence of such harmonics. In Eqs. (1) and (2), the sensor signal **304** is multiplied through by a pure sine or cosine modulating function (i.e., sin(2πft) and cos(2πft), respectively) at the drive frequency f, and integrated over one complete drive cycle, as described above.

As a result of these operations, a phase difference between a plurality of the sensor signals **304**, which is approximately proportional to a mass flow rate of fluid within the flow tube **215**, may be determined by determining a difference between

observed phase data on two separate sensor signals (e.g., a difference in θ for two different sensors). Further, since the frequency is known, a density of the material also may be determined. Still further, these factors, along with the determined value for the amplitude A, may be used to generate a drive signal to the driver(s) **210** such that a desired oscillation of the flowtube **215** is maintained. The analysis of Eqs. (1)-(4) does not specifically consider an impact of the Coriolis mode signal **306**, and, therefore, may be sufficient when there are little or no disturbances or other factors that may lead to a presence of the Coriolis mode signal **306** in the sensor signal **304**.

In FIGS. **2** and **3**, however, the presence and impact of the Coriolis mode signal **306** is considered, as referenced above and described in more detail, below. Specifically, for example, the integrator **275** performs a related analysis to that of Eqs. (1)-(4), but performs an integration(s) based on the period of operation of the Coriolis mode signal **306**, as opposed to the period of oscillation of the drive mode **302**.

For example, in the examples that follow, the integration interval is extended symmetrically in both directions away from the zero crossings of the drive mode signal **302**, so as to encompass an entirety of a period of oscillation of the Coriolis mode signal **306**. In other words, rather than integrating over a period from time t=0 to time t=1/f, the period of integration is extended negatively by value of [(½ k)-(½ f)], and is extended in a positive direction from an end of the relevant drive cycle by a corresponding amount [(½ k)-(½ f)], as illustrated in FIG. **3**.

This approach results in alterations to the integral limits of Eqs. (1) and (2), and, in particular, in addition to altering the limits themselves, alters the modulation functions, as described in more detail below. As also described below, further alteration of the modulation functions in this context allows for the mode maximization capabilities of the integrator **255**, as described above. For example, if a first modulation function is used that is twice the Coriolis mode frequency (i.e., 2 k), then the influence of the drive mode will be maximized, while the influence of the Coriolis mode will be reduced or eliminated. If, however, a second modulation function that is equal to the Coriolis frequency (k) is used, then an influence of the Coriolis mode will be maximized. Equations 5-8 provide an example of the first-described modulation function that is twice the Coriolis mode frequency.

Specifically, Eq. (5) illustrates the CS**2**_z**1** integral. That is, using the notation above, Eq. (5) represents a form of Eq. (1) above, but with a number of points of note regarding the form and notation used with respect to Eq. (5). First, Eq. (5) includes a "B" term (i.e., Bsin[2πkt+ϕ]) representing the Coriolis mode signal **306**, in addition to the "A" term of Eq. (1) that represents an effect of the drive mode signal **302**. That is, Eq. (5) takes a general form of "integral value=(A or drive mode term)+(B or Coriolis mode term)" that is seen throughout the following equations and discussion.

Second, Eq. (5) has integral limits extended to encompass a full cycle of the Coriolis mode, which, again, is indicated in Eq. (5) by the "B" term. Third, Eq. (5), like Eq. (1), represents the sine term of the Fourier analysis, as represented by the "S" term. Fourth, Eq. (5) has a modulation function with frequency 2 k, designated by the use of (4πk) in the modulation function and by the "2" term in the expression CS**2**_z**1**. Fifth, as designated by the z**1** term in the CS**2**_z**1** expression, Eq. (5) includes the offset value z**1** in the integral limits, and thereby in the modulation function, in order to take into account an effect of the altered zero-crossing of the sensor signal **304** discussed above with respect to areas **308** and **310** of FIG. **3**.

$$\mathrm{CS2_z1_int}(A, f, B, k, \phi, z1) := \qquad \text{Eq. (5)}$$

$$\int_{-\left(\frac{1}{2k}-\frac{1}{2f}\right)+z1}^{\frac{1}{f}+\left(\frac{1}{2k}-\frac{1}{2f}\right)+z1} [B\cdot\sin[(2\cdot\pi\cdot k\cdot t)+\phi]+A\cdot\sin(2\cdot\pi\cdot f\cdot t)]\cdot \sin\left[4\cdot\pi\cdot k\cdot\left[t-z1+\left(\frac{1}{2k}-\frac{1}{2f}\right)\right]\right]dt$$

Further in the expression of Eq. (5), it should be understood that the integral limits are expressed such that a point of zero phase for the drive mode component (A term) occurs at time t=0 in FIG. **3**, while the zero crossing point of the sensor signal **304** occurs at time t=z**1**, due to the presence of the Coriolis mode component **306** within the sensor signal **304**. This notation may be selected to reflect calculations performed within the integrator **275**, in which integrations are generally performed between zero-crossings, rather than starting at z**1**, since, at the time of integration, a value of z**1** is generally not known.

Having expressed this CS**2**_z**1** integral, an analytical expression for its value may be expressed in terms of its parameters f, k, A, z**1**, B, ϕ, and z**1**. As seen below, and generally speaking, analytical forms for each of the A term and the B term of Eq. (5) may be determined, and, in particular, B terms may turn out to be exactly zero. Thus, for the A term of Eq. 5, analogous to Eq. (1a), may be determined and is expressed in Eq. (6):

$$\mathrm{CS2_z1}(A, f, B, k, \phi, z1) := \qquad \text{Eq. (6)}$$

$$\frac{-2\cdot k\cdot A}{\pi\cdot(f^2-4\cdot k^2)}\cdot\sin\left(\frac{f}{k}\cdot\pi\right)\cdot\cos(2\cdot f\cdot\pi\cdot z1)$$

A corresponding expression for the B term of Eq. (5) may be determined to be zero, which was the first desired result of the integrator (mode maximizer) **275**, as described above. That is, Eq. (6) provides the first term of the first pair of integrals in which the drive mode is emphasized or maximized relative to the Coriolis mode, and, in fact, Eq. (6) obtains the desired result of eliminating the Coriolis mode (B term) entirely, so that Eq. (6) may be considered to be the analytical result of an entire integration of Eq. (6), having the above term for A and with the B term entirely eliminated. As explained, this result is obtained naturally from extending the integral limits and doubling the modulation function frequency, and takes into account the effect of the offset z**1**.

A corresponding analysis may be performed with respect to Eq. (2), i.e., the cosine term of the Fourier analysis. Using the notation above, Eq. (7) represents the CC**2**_z**1** integral. That is, the first "C" again designates the integration over the full Coriolis mode cycle, the second "C" designates the fact that the cosine term is being represented, and the "2" represents doubling of the modulation frequency.

$$\mathrm{CC2_z1_int}(A, f, B, k, \phi, z1) := \qquad \text{Eq. (7)}$$

$$\int_{-\left(\frac{1}{2k}-\frac{1}{2f}\right)+z1}^{\frac{1}{f}+\left(\frac{1}{2k}-\frac{1}{2f}\right)+z1} [B\cdot\sin[(2\cdot\pi\cdot k\cdot t)+\phi]+A\cdot\sin(2\cdot\pi\cdot f\cdot t)]\cdot \cos\left[4\cdot\pi\cdot k\cdot\left[t-z1+\left(\frac{1}{2k}-\frac{1}{2f}\right)\right]\right]dt$$

As with Eq. (6), an analytical expression for Eq. (7) may be obtained, and is shown below as Eq. (8).

$$CC2_z1(A, f, B, k, \phi, z1) := \quad \text{Eq. (8)}$$
$$\frac{-A \cdot f}{\pi \cdot (f^2 - 4 \cdot k^2)} \cdot \sin\left(\frac{f}{k} \cdot \pi\right) \cdot \sin(2 \cdot f \cdot \pi \cdot z1)$$

Again, a similar expression for the B term of Eq. (6) may be shown to be zero, which is the desired result for minimizing the Coriolis mode effect and maximizing the effect of the drive mode signal **302**. In other words, Eq. (8) provides an analytical expression for CC**2**_z**1** having no B term at all, as it has been cancelled out by using twice the Coriolis frequency k (i.e., 2 k) as a modulation function and integrated over the Coriolis period.

Thus, Eq. (8) represents the second term in the first pair of integrals output by the integrator (mode maximizer) **275**, in which the drive mode signal **302** is emphasized relative to the Coriolis mode. That is, in this example, the drive-emphasized characterization of the sensor signal **304** includes the pair of integrals CS**2**_z**1** and CC**2**_z**1** of Eqs. (6) and (8), respectively.

As described below, Eqs. (6) and (8) may be used in a manner analogous to Eqs. (3) and (4) above, in order to obtain solvable expressions for A and z**1**, respectively. An accuracy of these values will be increased with respect to what may be calculated from Eqs. (3) and (4) when applied to a sensor signal contaminated with the Coriolis mode component **306**, however, since the effect of the Coriolis signal **306** is minimized in Eqs. (6) and (8).

Further, these improved values of A and z**1** may be used to more-accurately determine values for corresponding terms B and ϕ of the Coriolis mode signal **306** itself, which may themselves then be used to determine yet-more accurate values for A and z**1**. This process may be iteratively repeated until a desired level of accuracy is reached. Then, the value A may be used to generate appropriate parameters for a new drive signal to be applied to the flowtube **215**, and the value z**1** for a first sensor signal from a first sensor may be used together with a corresponding value for z**1** determined for a second sensor signal from a second sensor, in order to determine a phase difference between the sensor signals (thereby to determine a mass flow rate of the fluid within the flowtube **215**).

Specifically, the corresponding terms B and ϕ may be determined from Eqs. (9)-(14), below. In Eqs. (9)-(14), the two analogous terms CS**1**_z**1** and CC**1**_z**1** are determined, where again the first term "C" represents the use of integral limits corresponding to an entire drive cycle of the Coriolis mode, the second term "S" or "C" represents the sine or cosine term, respectively, and the "1" term designates the use of the frequency k as the modulation frequency.

Accordingly, Eq. (9) represents the CS**1**_z**1** term, in which the only difference between Eq. (9) and Eq. (5) is that the modulation term involves a term of the form sin(2πk(. . .)) instead of sin(4πk(. . .)). Thus, Eq. (9) may be written as:

$$CS1_z1_int(A, f, B, k, \phi, z1) := \quad \text{Eq. (9)}$$
$$\int_{-\left(\frac{1}{2k}-\frac{1}{2f}\right)+z1}^{\frac{1}{f}+\left(\frac{1}{2k}-\frac{1}{2f}\right)+z1} [B \cdot \sin[(2 \cdot \pi \cdot k \cdot t) + \phi] + A \cdot \sin(2 \cdot \pi \cdot f \cdot t)] \cdot \sin\left[2 \cdot \pi \cdot k \cdot \left[t - z1 + \left(\frac{1}{2k} - \frac{1}{2f}\right)\right]\right] dt$$

Eq. (9) has an analytical expression for the A term that is shown in Eq. (10):

$$CS1_Aonly_z1(A, f, B, k, \phi, z1) := \quad \text{Eq. (10)}$$
$$\frac{-k \cdot A}{\pi \cdot (f^2 - k^2)} \cdot \sin\left(\frac{f}{k} \cdot \pi\right) \cdot \cos(2 \cdot f \cdot \pi \cdot z1)$$

Eq. (9) has an analytical expression for the B term that is shown in Eq. (11):

$$CS1_Bonly_z1(A, f, B, k, \phi, z1) := \quad \text{Eq. (11)}$$
$$\frac{-B}{2 \cdot k} \cdot \cos\left[k \cdot \pi \cdot \left(\frac{1}{f} + 2 \cdot z1\right) + \phi\right]$$

As seen below, the B term of Eq. (10) is maximized with respect to the A term of Eq. (11), although the A term does not go to zero.

Similar analysis may be performed for the cosine term of the Coriolis-emphasized (i.e., B term maximized) characterization of the sensor signal **304** that is output by the integrator **275**. This cosine term is expressed as CC**1**_z**1**, as shown in Eq. (12):

$$CC1_z1_int(A, f, B, k, \phi, z1) := \quad \text{Eq. (12)}$$
$$\int_{-\left(\frac{1}{2k}-\frac{1}{2f}\right)+z1}^{\frac{1}{f}+\left(\frac{1}{2k}-\frac{1}{2f}\right)+z1} [B \cdot \sin[(2 \cdot \pi \cdot k \cdot t) + \phi] + A \cdot \sin(2 \cdot \pi \cdot f \cdot t)] \cdot \cos\left[2 \cdot \pi \cdot k \cdot \left[t - z1 + \left(\frac{1}{2k} - \frac{1}{2f}\right)\right]\right] dt$$

Eqs. (13) and (14) represent the analytical expressions for the A term and B term, respectively, of Eq. (12).

$$CC1_Aonly_z1(A, f, B, k, \phi, z1) := \quad \text{Eq. (13)}$$
$$\frac{-f \cdot A}{\pi \cdot (f^2 - k^2)} \cdot \sin\left(\frac{f}{k} \cdot \pi\right) \cdot \sin(2 \cdot f \cdot \pi \cdot z1)$$

$$CC1_Bonly_z1(A, f, B, k, \phi, z1) := \quad \text{Eq. (14)}$$
$$\frac{-B}{2 \cdot k} \cdot \sin\left[k \cdot \pi \cdot \left(\frac{1}{f} + 2 \cdot z1\right) + \phi\right]$$

As with Eqs. (10) and (11), above, and as described in more detail below, the B term of Eq. (13) is maximized with respect to the A term of Eq. (14). As a result, expressions for B and ϕ, analogous to Eqs. (3) and (4), respectively, may be determined, so that B and ϕ may be determined to a relatively high degree of accuracy, particularly since improved-accuracy A and z**1** terms above may be used in the calculations thereof.

Further explanation and examples for the derivation and use of Eqs. (5)-(14) are provided in more detail below, and, in particular, with respect to FIGS. **12-15**, including further explanation for the above described selection of the first and second modulation functions. However, with respect to the described operations of FIGS. **2-11**, and associated examples, it is enough to understand that the integrator **275** is operable to perform a numerical integration of the sensor signal **304**, over a time interval defined by a period of the Coriolis mode signal **306** with respect to a period of the drive mode signal **302**, including the zero-crossing offset z**1** that results from the

presence of the Coriolis mode signal **306**. As a result, the integrator **275**, as described above, outputs a drive-emphasized characterization of the sensor signal **304** as a first pair of integrals CS**2**_z**1** and CC**2**_z**1**, and a Coriolis-emphasized characterization of the sensor signal **304** as a second pair of integrals CS**1**_z**1** and CC**1**_z**1**.

As a result, the signal analyzer **255** and the signal identifier **260** of FIG. **2** may be considered to be a contaminant determination or detection system, that is operable to determine actual values for contaminant signals, such as the Coriolis mode signal **306**, within the sensor signal **304**. Moreover, these values may be determined on a cycle-by-cycle basis, even when the drive mode signal **302** is very close to the contaminant signal, and without requiring filtering of the contaminant signal. A key philosophy is that the motion sensor signal is not filtered prior to the integration process, for example in order to reduce the influence of any specific mode of vibration, thus avoiding any loss of dynamic response. As a result, a dynamic response of the flowmeter **200** is very good, and, in particular, a response of the flowmeter both to changing flow parameters of the fluid within the flowtube **215** (e.g., a change in mass flow rate of the fluid), and to changing contaminant parameters of the contaminant signal (e.g., a change due to an external disturbance of the flowtube, or due to a change in condition of the flowtube, or of the fluid).

Given the above explanation, FIGS. **4-6** provide an overview of the structure, function, and operation of the signal analyzer **255** and the signal identifier **260** of the flowmeter **200** of FIG. **2**.

Specifically, FIG. **4** is a flow chart **400** illustrating an operation of the signal analyzer **255** of FIG. **2**. In FIG. **4**, the signal analyzer **255** receives the sensor signal **304**, which, as explained above, includes portions related to the drive mode signal **302** and other portions related to contaminants, such as the Coriolis mode **306** (**402**).

The zero crossing detector **265** of the signal analyzer **255** analyzes the sensor signal **304** to observe zero crossings of the sensor signal **304** (**404**). From this information, the frequency calculator **270** is operable to determine the drive frequency f and, thereby, the Coriolis frequency k (**406**). For example, as described above, the drive frequency f may simply be determined to be the intervals of the period of time between two consecutive zero crossings, while frequency k may be determined based on a known relationship between f and k, such as, for example, k=(√3)f.

With knowledge of f and k, the integrator **275** may determine integral boundaries as described above with respect to Eqs. (5), (7), (9), and (12) (**408**). That is, the integral boundaries start at the zero crossings, but adjusted for the Coriolis mode period rather than the drive mode period, with the knowledge that the observed zero crossings are offset from the true zero crossings by the time offset z**1**, which is unknown and to be solved for at a later stage for determination of phase difference and mass flow rate.

Accordingly, the integrator **275** may perform a first numerical integration of the sensor signal **304** in which parameters of the drive mode will be maximized (**410**). The result of this calculation is the first pair of integrals CS**2**_z**1** and CC**2**_z**1** of Eqs. (5) and (7), respectively.

Similarly, the integrator **275** may perform a second numerical integration of the sensor signal **304**, in which the parameters of the Coriolis mode signal **306** are maximized (**412**). The result of this calculation is the second pair of integrals CS**1**_z**1** and CC**1**_z**1**, related to Eqs. (9) and (12), respectively.

FIG. **5** is a flow chart **500** illustrating a first process of the signal identifier **260** of FIG. **2**. In FIG. **5**, the signal identifier **260** receives first integration results from the integrator **275**, where the first integration results provide the drive-emphasized characterization of the sensor signal **304** (**502**). That is, as described above, the integration results include the values CS**2**_z**1** and CC**2**_z**1** of Eqs. (5) and (7), respectively.

The parameter calculator **290** receives these integration results **280**, and obtains estimates for the parameters A and z**1** (**504**). Sufficiently rough estimates for values for the parameters A and z**1** may be determined based on, for example, knowledge of these parameters gained from the immediately-previous cycle, on the assumption that the parameters will not have changed by a large amount between close or consecutive cycles. Estimates also may be determined from, for example, the type of flow tube **215** being used, or based on a value of the drive frequency f, or from the use of Eqs. (1)-(4), above, or from other known sources. As mentioned, such parameter estimates may be calculated and stored with respect to the parameter estimates database **285**.

The parameter calculator **290** may determine an improved value for the drive amplitude A, using the integration results CS**2**_1 and CC**2**_z**1**, along with Eq. (15), which, as referenced above, provides an analytical expression for the value A that is analogous to Eq. 3.

$$A_est_CS2(CS2_z1_val, CC2_z1_val, f, k) := \sqrt{\left(\frac{CC2_z1_val}{f}\right)^2 + \left(\frac{CS2_z1_val}{2k}\right)^2} \cdot \left[\frac{\pi \cdot (f^2 - 4k^2)}{\sin\left(\frac{f}{k} \cdot \pi\right)}\right] \quad \text{Eq. (15)}$$

In Eq. 15, it should be understood that the terms CS**2**_z**1**_val and CC**2**_z**1**_val represent numerical values for the CS**2**_z**1** and CC**2**_z**1** integrals, which are determined by the integrator **275** and output to the signal identifier **260**.

Subsequently, the numerical values for the CS**2**_z**1** and CC**2**_z**1** integrals may be used to determine an improved value for the parameter z**1** (**508**), using Eq. (16) (in which atan is the inverse tangent function), which is analogous to Eq. (4), above:

$$z1_est(CS2_z1_val, CC2_z1_val, f, k) := \frac{atan\left(\frac{2k \cdot CC2_z1_val}{f \cdot CS2_z1_val}\right)}{2 \cdot \pi \cdot f} \quad \text{Eq. (16)}$$

If the values of the drive amplitude A and the zero offset z**1** are determined to be accurate (**510**), then the values A and z**1** may be output (**512**). If, however, additional iterations are desired or required, then the determined values of A and z**1** may be used as a starting point for a second iteration of the process **500** (**504**).

In some implementations, the estimation/iteration process described above for A and z**1** may not be necessary or desired. In these cases, the integration results (**502**) may be used to determine A (**506**) and z**1** (**508**) directly, and the obtained values may be sufficiently accurate for a given design or purpose, without the need to use initial estimates and subsequent iterations to convergence(s).

FIG. **6** is a flow chart **600** of a second process implemented by the signal identifier **260** of FIG. **2**. In FIG. **6**, the parameter calculator **290** receives the second integration results with the Coriolis mode parameters maximized therein (**602**). That is, the signal identifier receives from the integrator **275** the

Coriolis-emphasized characterization of the sensor signal **304**, expressed as numerical values calculated for the integrals CS**1**_z**1** and CC**1**_z**1** of Eqs. (9) and (12), respectively, in which the Coriolis frequency k is used with the modulation function(s) of those expressions.

The parameter calculator **290** then obtains the values for the drive amplitude A and the zero crossing offset z**1** that were previously obtained as an output of the process **500** of FIG. **5**, and estimates the Coriolis parameters of amplitude B and phase ϕ (**604**). As referenced above, the initial estimates for parameters B and ϕ may be obtained based on knowledge of these parameters from previous cycles, and/or based on knowledge of the already-determined parameters of, for example, f, k, A, and z1.

Similarly to the process **500** of FIG. **5**, then, the Coriolis amplitude B may be determined based on the integration results CS**1**_z**1** and CC**1**_z**1** (**606**). Specifically, the procedure summarized in Eq. (17) may be used in this calculation, which is analogous to Eqs. (3) and (15), but for the B term:

$$\text{B_est_CS1}(A, f, k, z1, \text{CS1_val}, \text{CC1_val}) := \quad \text{Eq. (17)}$$
$$\left| \begin{array}{l} c \leftarrow \text{CC1_val} - \text{CC1_Aonly_z1}(A, f, 0, k, 0, z1) \\ s \leftarrow \text{CS1_val} - \text{CS1_Aonly_z1}(A, f, 0, k, 0, z1) \\ 2 \cdot k \cdot \sqrt{c^2 + s^2} \end{array} \right.$$

In Eq. (17), the terms "c" and "s" are numerical estimates of the integral values CC**1**_Bonly_z**1** and CS**1**_Bonly_z**1**. They may be obtained by subtracting estimates of the influence of A in these integrals (i.e., CC**1**_Aonly_z**1** and CS**1**_Aonly_z**1**) from the numerical values of CC**1**_z**1** and CS**1**_z**1**, or CC**1**_z**1**_val and CS**1**_z**1**_val, as defined by the analytical results given in Eqs. (13) and (10), above. Then, as shown, the resulting values of c and s are combined in a root-sum-square manner to obtain the estimate for B.

Then, the integration results CS**1**_z**1** and CC**1**_z**1** and determined value of z**1** may be used to determine a value of ϕ (**608**), as shown in Eq. (18) and analogously to Eqs. (4) and (16), above, where the terms c and s are defined for Eq. (17), above:

$$\phi\text{_est_CS1}(A, f, k, z1, \text{CS1_val}, \text{CC1_val}) := \quad \text{Eq. (18)}$$
$$\operatorname{atan}\left(\frac{s}{c}\right) - k \cdot \pi \cdot \left(\frac{1}{f} + 2z1\right)$$

If the determined values of B and ϕ are sufficiently accurate (**610**), then the values B and ϕ may be output (**612**). Otherwise, as in FIG. **5**, additional iterations may be performed to improve the resulting values of B and ϕ.

As a further alternative, and again as explained above for FIG. **5**, it may not be necessary to obtain initial estimates of B and ϕ for performing subsequent iterations. Rather, sufficiently accurate results may be obtained in some implementations by determining B (**606**) and ϕ (**608**) directly from the integration results CS**1**_z**1** and CC**1**_z**1** (**602**).

As described above, the process **400** of the signal analyzer **255** results in integration results which characterize the sensor signal **304** in a manner that encompasses all of the information pertaining to both the Coriolis mode **306** and the drive mode **302**, as well as information related to an offset of the zero crossing of the sensor signal **304** that is caused by the presence of the Coriolis mode **306**. More specifically, the process **400** of the integrator **275** results in a first pair of integration results CS**2**_z**1** and CC**2**_z**1** in which parameters of the drive mode signal **302** are maximized or emphasized relative to the parameters of the Coriolis mode signal **306**. Further, the integrator **275** outputs a second pair of integration results CS**1**_z**1** and CC**1**_z**1** which provide a Coriolis-enhanced characterization of the sensor signal **304**, in which the Coriolis parameters B and ϕ are maximized or emphasized within the integration results relative to the drive parameters A and z1.

Subsequently, process **500** uses the drive emphasized characterization of the sensor signal **304**, i.e., the integration results CS**2**_z**1** and CC**2**_z**1**, in which a modulation function that is twice a frequency of the Coriolis mode is used. These drive-emphasized characterizations may then be used to determine the parameters A and z**1**, related to the drive mode signal **302**. Similarly, the process **600** of the signal identifier **260** uses the Coriolis-enhanced characterization of the sensor signal **304**, i.e., the integration results CS**1**_z**1** and CC**1**_z**1** in which a modulation function having a frequency equal to that of the Coriolis mode signal **306** is used, to obtain the Coriolis mode parameters B and ϕ.

Some or all of the processes **400**-**600** may be performed at each cycle of the drive mode signal **302**, or may be performed twice per cycle of the drive mode signal **302**, or may be performed at some other interval. The processes **400**-**600** may be iterated until acceptable values for the parameters A, B, z**1**, and ϕ are determined. Further, as described in more detail below, these parameters and related information may then be used to determine improved estimates for the frequencies f and k, whereupon the processes **400**-**600** may be performed again, using these improved frequency estimates.

Once acceptable values for f, A, and z**1** are determined (specifically, once values of z**1** for two different sensor **205** are determined relative to one another), the flow meter output unit **240** may use these values to determine and output a mass flow rate and/or density of fluid within the flow tube **215** and may further use the parameters f, A, and z**1** to generate an appropriate new version of the drive mode signal **302** for maintaining oscillation of the flow tube **215**.

Since the flow meter output unit **240** receives very accurate values for the drive signal parameters f, A, and z**1** from the signal identifier **260**, the flow meter output unit **240** is able to output correspondingly accurate values for the mass flow rate, density, and new drive signal parameters, even in the presence of a strong Coriolis mode signal that may be caused by, for example, external vibration to the flow tube **215**, sudden changes in flow rate of the fluid within the flow tube **215**, or some other causes.

Further, such transient effects that appear as large parameter values B and ϕ of the Coriolis mode signal **306** may be isolated and identified for analysis thereof. For example, it may be the case that the flow tube **215** is subject to external vibrations of unknown source, duration, and/or magnitude. In this case, the results of such external vibrations may be analyzed through the above-described analysis of the Coriolis mode signal **306**. In this way, the external vibration and characteristics thereof may be characterized and/or determined.

Moreover, the above-described, cycle-by-cycle, active tracking of the Coriolis mode component **306** permits and facilitates active control of an amplitude B thereof. For example, an excessive Coriolis amplitude B (due to external disturbances, onset of two-phase flow, or other factors) may be suppressed through the inclusion of an inverse Coriolis mode component within the drive signal that is output by the driver(s) **210** and applied to the flowtube **215**. In other words,

a negative drive gain may be applied that reduces or cancels out an effect of the existing Coriolis mode component **306**.

Still further, the Coriolis mode signal component **306** may be used to perform general diagnostics regarding a current state or condition of the flowtube **215**. For example, similar conditions may occur over a period of time, e.g., a given disturbance may occur periodically, or an onset of two-phase flow may occur on a regular or semi-regular basis. However, the Coriolis mode signal **306** may be determined to be different over time in response to these conditions. The varying (e.g., increasing) Coriolis mode parameters may thus be indicative of a changing or changed condition and/or behavior of the flowtube **215**, such as, for example, a reduced reliability, or a lowered response time/characteristic.

Finally, and most generally, the basic flow and density calibrations of the meter may vary with the relative positioning of the frequencies of the drive and Coriolis modes respectively. Some flowtube designs are constrained to ensure that this frequency positioning is kept relatively stable over the range of operating drive frequencies of the meter. Using this form of analysis to directly track the relative positions of the drive and Coriolis frequencies, it may be possible to improve flowtube designs by removing the constraint of relative frequency positioning. Alternatively, this analysis can be used to improve the basic mass flow and density measurement on flowtube designs where it is not possible to control the relative positioning of the two mode frequencies, where mass flow and density corrections can be applied if the actual drive and Coriolis frequencies are tracked in real time.

Having described the above examples of general operations **400**-**600** of the flowmeter **200**, the following provides numerical examples of these operations, with reference back to FIGS. **2**-**6**. Specifically, the following example assumes that the signal analyzer **255** determines a frequency f=100 Hz, where a value of the amplitude A of the drive mode signal **302** is assumed to be 0.3V for the purpose of simulating the numerical integration to be performed by the integrator **275**, and for comparison to a value for A that is determined using the techniques described herein.

In this case, the frequency k for the Coriolis mode signal **306** is determined to be 57.735 Hz, using the assumption that $f=(\sqrt{3})k$. The amplitude B of the Coriolis mode signal **306**, which is typically much smaller than the drive amplitude A, is used in this example as 0.0001V, and the Coriolis phase parameter ϕ may be used as 1.0000 radians. Finally, z**1**, i.e., the time in seconds between a start of a cycle of the drive mode signal **302** at time t=0 and an observed point of zero phase on the sensor signal **304**, may be set as $z1=5\times10^{6}$ s.

For clarity, it is emphasized that the values of A, z**1**, B and ϕ given above are the "true" values which are to be deduced from the numerical values of the integrations performed on the sensor data.

Thus, with reference to FIG. **4**, it may be seen that the signal analyzer **255** receives the sensor signal **304**, determines the frequencies f and k from the observed zero-crossings, and determines integral boundaries for integrating over the Coriolis mode period (**402**, **404**, **406**, and **408**). With this information, the integrator **275** may use the modulation function having twice the frequency of the Coriolis frequency k to perform a first numerical integration on the sensor signal **304** to obtain the drive-emphasized characterization CS**2**_z**1** and CC**2**_z**1**, which, in this example, and using the "true" parameter values for A, B, and z**1**, as well as the frequencies f and k, calculates as values CS**2**_z**1**_val; $=-2.46718958053974\times10^{-3}$ and CC**2**_z**1**_val$=-6.71250242220871\times10^{-6}$ (**410**).

Similarly, the integrator **275** may use the modulation function having the same frequency as the Coriolis frequency k to perform a second numerical integration on the sensor signal **304** to obtain the Coriolis-emphasized characterization CS**1**_z**1**_val and CC**1**_z**1**_val, which, in this example, calculates as CS**1**_z**1**=$\mathbf{6.17617813486415\times10^{-4}}$ and CC**1**_z**1**=$\mathbf{-3.07891796642618\times10^{-6}}$ (**412**).

Dealing with the drive parameters and drive-emphasized characterization first (as shown in FIG. **5**), the parameter calculator **290** of the signal identifier **260** of FIG. **2** may solve for the value of drive amplitude A using Eq. (15), above (**506**). That is, since, by definition, the values CS**2**_z**1**_val and CC**2**_z**1**_val include a minimized or zero value for the Coriolis amplitude B and phase ϕ, then using these values in Eq. (15) provides a more accurate value for the amplitude A, which, in this example, turns out to be A=0.299999999999986. Similarly, the parameter calculator **290** may use this improved value of A, along with Eq. (16) above, to solve for an improved value of z**1** (**508**), which, in this example, is z**1**=$\mathbf{5.00000000000295\times10^{-6}}$ s.

Dealing with the Coriolis parameters and Coriolis-emphasized characterization next (as shown in FIG. **6**), the parameter calculator **290** of the signal identifier **260** of FIG. **2** may solve for the value of Coriolis amplitude B using Eq. (17), above (**606**). That is, since, by definition, the values CS**1**_z**1**_val and CC**1**_z**1**_val include a maximized value for the Coriolis amplitude B and phase ϕ, then using these values in Eq. (17) provides a more accurate value for the amplitude B, which, in this example, turns out to be $B=1.00000000003168\times10^{-4}$. Similarly, the parameter calculator **290** may use this improved value of B, along with Eq. (18) above, to solve for an improved value of ϕ (**608**), which, in this example, is $\phi=1.00000000000807$.

As described above, these calculations may be performed on a cycle-by-cycle basis, such that the values A, B, z**1**, and ϕ may be dynamically updated on a regular basis. As a result, the impact of the Coriolis mode signal **306** may be dynamically compensated, at or near real time. For example, in the presence of an external vibration, the flowmeter **200** may nonetheless determine the drive amplitude A and the phase difference θ (using z**1** values from different sensors **205**), and also may output values for the Coriolis amplitude B and phase ϕ, which will reflect and characterize the presence of the external vibration. As a result, the flowmeter **200** will operate in a continuous fashion, outputting accurate measurements, even in the presence of such disturbances. Moreover, the response time of the flowmeter **200** may be improved with respect to its operation and output during such instances.

In other implementations, the entire processes of FIGS. **4**-**6** may be iterated in their entirety, in order to obtain even more accurate values for A, z**1**, B, and ϕ. Further, improved values for the frequency parameters f and k may be determined (examples techniques are provided below), and these frequency values may be used in subsequent iterations. Still further, the calculations may be performed twice per cycle, rather than once per cycle.

In the latter case, extra calculations may be required which make use of a value z**1**_offset, that may be defined as a dual value, i.e., either 0.5/f for calculations done from a negative zero crossing to a negative zero crossing, or 0.0 (no effect) for calculations done from a positive zero crossing to a positive zero crossing. In this example, then, the calculated value of z**1**, above, may be kept as the described value when an absolute value of z**1**_offset is less than or equal to 0.25/f. Otherwise, the value of z**1** may be expressed as z**1** =z**1** +z**1**_offset.

The description of FIGS. **2**-**6** above acknowledges that the presence of the Coriolis mode component **306** in the sensor

signal **304** will shift the observed zero crossing at the start of the cycle by time z**1** from the "true" zero crossing point of the drive mode component **302** of the sensor signal **304**, as shown in FIG. **3**. Additionally, however, the zero crossing at the end of the same cycle of the sensor signal **304** may be shifted by a different amount, because of the asynchronous interaction between the drive mode signal **302** and the Coriolis mode signal **306**, and their respective frequencies f and k.

As a consequence, if the frequency f is estimated based on the period between zero crossings, then the resulting estimate for f may be erroneous. Further, if the integration interval is based on these zero crossings, then additional error may be introduced, and, most importantly, an erroneous frequency will be used for the modulation function.

Consequently, a parameter z**2** may be incorporated into the analysis above, where z**2** is defined as a time offset between the true period 1/f of the drive mode signal **302** and the observed period between zero crossings that is seen with respect to the sensor signal **304**. Then, as above, analytical results may be derived for the resulting integrals, including the z**2** term.

In the discussion below, the values of z**1** and z**2** may be arbitrary within certain parameters and assumptions, with the assumption, for example, that, in practice, z**2** may often be assumed to be small. The expressions for the integral values that include z**2**, i.e., CS**2**_z**2**, CC**2**_z**2**, CS**1**_z**2**, and CC**1**_z**2**, are analytically exact, and apply to any values of z**1** and z**2**. Hence, although the need for z**1** and z**2** arises from the effect of the Coriolis mode component **306** in shifting the locations of zero crossings in the sensor signal **304**, the resulting and described analysis is valid for any integral limits, whether or not the integral limits actually coincide with the zero crossings of the sensor signal **304**. As described in detail below, this analysis offers many practical benefits, including, for example, significant reductions in the computational effort required.

FIG. **7** is a block diagram of a flow meter **700**. The flow meter **700** of FIG. **7** operates similarly to the flow meter **200** of FIG. **2**, but further includes an additional effect of the Coriolis mode signal **306** on the sensor signal **304**, mentioned above and referred to herein as offset z**2**.

Referring to FIG. **8**, the offset z**2** may be seen to result from the asymmetry of the Coriolis mode signal **306** relative to the drive mode signal **302**, such that the offset z**2** exists independently of the offset z**1** defined above. As shown in FIG. **8**, the offset z**2** may be defined as the difference between the true drive period of the drive mode signal **302** and the actual, observed drive period of the corresponding sensor signal **304**, based on zero crossings.

In the first instance, then, the value z**2** may be incorporated into modified versions of Eqs. (5)-(18). That is, equations may be developed for the two pairs of integrals, i.e., the drive-emphasized integrals CS**2**_z**2** and CC**2**_z**2**, and the Coriolis-emphasized integrals CS**1**_z**2** and CC**1**_z**2**, where the designator _z**2** indicates the inclusion of both offsets z**1** and z**2** (although z**1** is not included in this notation, for brevity's sake). The resulting equations are shown as Eqs. (19)-(30).

Thus, CS**2**_z**2** may be written as Eq. (19):

$$\mathrm{CS2_z2_int}(A, f, B, k, \phi, z1, z2) := \qquad \text{Eq. (19)}$$

$$\int_{-\left(\frac{1}{2k}-\frac{1}{2f}\right)+z1}^{\frac{1}{f}+\left(\frac{1}{2k}-\frac{1}{2f}\right)+z1+z2} [B\cdot\sin[(2\cdot\pi\cdot k\cdot t)+\phi]+A\cdot\sin(2\cdot\pi\cdot f\cdot t)]\cdot \sin\left[4\cdot\pi\cdot\frac{k}{(1+k\cdot z2)}\cdot\left[t-z1+\left(\frac{1}{2k}-\frac{1}{2f}\right)\right]\right]dt$$

It may be observed that the z**2** term occurs twice in Eq. (19). Firstly, z**2** occurs in the upper limit of the integral, so that it may be seen that the integration period deviates from an ideal length of 1/k seconds (i.e., a period of the Coriolis mode signal **306**) by z2 seconds. Secondly, the period of the modulating sine term is also adjusted by z**2** seconds. Overall, therefore, Eq. (19) the numerical integration(s) to be performed on the sensor signal **304** (which are based on the observed zero crossings) inherently include errors caused by the presence of z**2** and reflected in the integration limits and modulation function(s) (frequencies), so that Eq. (19) represents the consequences of applying these 'wrong' integral limits and corresponding 'wrong' modulation frequency.

The A term is given by Eq. (20):

$$\mathrm{CS2_Aonly_z2}(A, f, B, k, \phi, z1, z2) := -2\cdot A\cdot k\cdot \qquad \text{Eq. (20)}$$

$$(1+k\cdot z2)\cdot\frac{\sin\left[\pi\cdot f\cdot\left(\frac{1}{k}+z2\right)\right]\cdot\cos(\pi\cdot f\cdot(2\cdot z1+z2)]}{\pi\cdot(f+f\cdot k\cdot z2+2\cdot k)\cdot(f+f\cdot k\cdot z2-2\cdot k)}$$

In the case where z**2**=0, Eq. (20) simplifies to the corresponding expression for CS**2**_z**1**, given above in Eq. (6).

The B term is not exactly zero as above, as shown in Eq. (21):

$$\mathrm{CS2_Bonly_z2}(A, f, B, k, \phi, z1, z2) := \qquad \text{Eq. (21)}$$

$$\frac{2\cdot B\cdot(1+k\cdot z2)}{\pi\cdot k\cdot(3+k\cdot z2)\cdot(1-k\cdot z2)}\cdot \cos\left[k\cdot\pi\cdot\left(\frac{1}{f}+2\cdot z1+z2\right)+\phi\right]\cdot\sin(\pi\cdot k\cdot z2)$$

However, the B term is very small, being a product of both B itself and sin(z**2**), both of which may be assumed to be small. In the case where z**2** is zero, the B term also goes to zero.

The CC**2**_z**2** integral may be written as in Eq. (22):

$$\mathrm{CC2_z2_int}(A, f, B, k, \phi, z1, z2) := \qquad \text{Eq. (22)}$$

$$\int_{-\left(\frac{1}{2k}-\frac{1}{2f}\right)+z1}^{\frac{1}{f}+\left(\frac{1}{2k}-\frac{1}{2f}\right)+z1+z2} [B\cdot\sin[(2\cdot\pi\cdot k\cdot t)+\phi]+A\cdot\sin(2\cdot\pi\cdot f\cdot t)]\cdot \cos\left[4\cdot\pi\cdot\frac{k}{(1+k\cdot z2)}\cdot\left[t-z1+\left(\frac{1}{2k}-\frac{1}{2f}\right)\right]\right]dt$$

The A term for CC**2**_z**2** of Eq. (22) takes the form of Eq. (23):

$$\mathrm{CC2_Aonly_z2}(A, f, B, k, \phi, z1, z2) := \qquad \text{Eq. (23)}$$

$$-A\cdot f\cdot(1+k\cdot z2)^2\cdot\frac{\sin\left[\pi\cdot f\cdot\left(\frac{1}{k}+z2\right)\right]\cdot\sin(\pi\cdot f\cdot(2\cdot z1+z2)]}{\pi\cdot(f+f\cdot k\cdot z2+k)\cdot(f+f\cdot k\cdot z2-2\cdot k)}$$

while the B term takes the form of Eq. (24):

$$CC2_Bonly_z2(A, f, B, k, \phi, z1, z2) := \frac{-B\cdot(1+k\cdot z2)^2}{\pi\cdot k\cdot(k\cdot z2+3)\cdot(k\cdot z2-1)}\cdot \sin\left[k\cdot\pi\cdot\left(\frac{1}{f}+2\cdot z1+z2\right)+\phi\right]\cdot\sin(\pi\cdot k\cdot z2) \quad \text{Eq. (24)}$$

As in Eq. (21), the B term of Eq. (24), being a product of the two small terms B and sin(z**2**), is small.

Having described the above drive-emphasized characterization, having the first pair of integrals CS**2**_z**2** and CC**2**_z**2**, corresponding equations may be developed for the Coriolis-emphasized characterization, including the second pair of integrals CS**1**_z**2** and CC**1**_z**2**.

Specifically, CS**1**_z**2** may be written as Eq. (25):

$$CS1_z2_int(A, f, B, k, \phi, z1, z2) := \int_{-\left(\frac{1}{2k}-\frac{1}{2f}\right)+z1}^{\frac{1}{f}+\left(\frac{1}{2k}-\frac{1}{2f}\right)+z1+z2} [B\cdot\sin[(2\cdot\pi\cdot k\cdot t)+\phi]+A\cdot\sin(2\cdot\pi\cdot f\cdot t)]\cdot \sin\left[2\cdot\pi\cdot\frac{k}{(1+k\cdot z2)}\cdot\left[t-z1+\left(\frac{1}{2k}-\frac{1}{2f}\right)\right]\right]dt \quad \text{Eq. (25)}$$

Eq. (25) has an analytical expression for the A term given by Eq. (26):

$$CS1_Aonly_z2(A, f, B, k, \phi, z1, z2) := -A\cdot k\cdot(1+k\cdot z2)\cdot\frac{\sin\left[\pi\cdot f\cdot\left(\frac{1}{k}+z2\right)\right]\cdot\cos(\pi\cdot f\cdot(2\cdot z1+z2)]}{\pi\cdot(f+f\cdot k\cdot z2+k)\cdot(f+f\cdot k\cdot z2-k)} \quad \text{Eq. (26)}$$

Eq. (25) has a B term given by Eq. (27):

$$CS1_Bonly_z2(A, f, B, k, \phi, z1, z2) := \frac{-B\cdot(1+k\cdot z2)}{\pi\cdot k^2\cdot z2\cdot(2+k\cdot z2)}\cdot \cos\left[\pi\cdot k\cdot\left(\frac{1}{f}+2\cdot z1+z2\right)+\phi\right]\cdot\sin(\pi\cdot k\cdot z2) \quad \text{Eq. (27)}$$

The presence of z**2** in the denominator of Eq. (27) may suggest that the B term goes to infinity as z**2** tends to zero. However, the presence of the sin(π.k.z**2**) term in the numerator allows for re-arrangement of Eq. (27) in terms of the sinc function sin(π.k.z **2**)/(π.k.z**2**), which may be shown to tend towards CS**1**_Bonly_z**1** of Eq. (11), as z**2** tends to zero.

Finally, CC**1**_z**2** may be written as Eq. (28):

$$CC1_z2_int(A, f, B, k, \phi, z1, z2) := \int_{-\left(\frac{1}{2k}-\frac{1}{2f}\right)+z1}^{\frac{1}{f}+\left(\frac{1}{2k}-\frac{1}{2f}\right)+z1+z2} [B\cdot\sin[(2\cdot\pi\cdot k\cdot t)+\phi]+A\cdot\sin(2\cdot\pi\cdot f\cdot t)]\cdot \cos\left[2\cdot\pi\cdot\frac{k}{(1+k\cdot z2)}\cdot\left[t-z1+\left(\frac{1}{2k}-\frac{1}{2f}\right)\right]\right]dt \quad \text{Eq. (28)}$$

For Eq. (28), the A term may be written as in Eq. (29):

$$CC1_Aonly_z2(A, f, B, k, \phi, z1, z2) := -A\cdot f\cdot(1+k\cdot z2)^2\cdot\frac{\sin\left[\pi\cdot f\cdot\left(\frac{1}{k}+z2\right)\right]\cdot\sin(\pi\cdot f\cdot(2\cdot z1+z2)]}{\pi\cdot(f+f\cdot k\cdot z2+k)\cdot(f+f\cdot k\cdot z2-k)} \quad \text{Eq. (29)}$$

Further for Eq. (28), the B term, where again the sinc function sin(π.k.z**2**)/(π.k.z **2**) is included, may be written as in Eq. (30):

$$CC1_Bonly_z2(A, f, B, k, \phi, z1, z2) := \frac{-B\cdot(1+k\cdot z2)^2}{\pi\cdot k^2\cdot z2\cdot(2+k\cdot z2)}\cdot \sin\left[\pi\cdot k\cdot\left(\frac{1}{f}+2\cdot z1+z2\right)+\phi\right]\cdot\sin(\pi\cdot k\cdot z2) \quad \text{Eq. (30)}$$

A full derivation and development of Eqs. (5)-(30) is provided below with respect to FIGS. **12-15**. Here, Eqs. (19)-(30) are included to explain the operation of the signal analyzer **255** and the signal identifier **260**, in the context of the implementation of the flowmeter **700** of FIG. **7**.

Specifically, the integrator **275** outputs integration results CS**2**_z**2** and CC**2**_z**2** within the drive-emphasized characterization of the sensor signal **304**, taking into account both the offset z**1** and the offset z**2** over a period that is close to, but not necessarily equal to, period of the Coriolis mode signal **306**. Similarly, the integrator **275** also outputs integration results CS**1**_z**2** and CC**1**_z**2**, representing the Coriolis-enhanced characterization of the sensor signal **304**, and also taking into effect the offsets z**1**, and z**2** over the same integration interval.

As described above, and as may be seen in Eqs. (19)-(30), the CS**2**_z**2** and CC**2**_z**2** integration results use a modulation function having a frequency that is approximately twice that of the Coriolis mode signal **306**, while the integration results CS**1**_z**2** and CC**1**_z**2** use a modulation function having a frequency approximately equal to the Coriolis mode frequency. Generally speaking, then, the flowmeter **700** may proceed with corresponding calculations described above with respect to FIGS. **4-6**, but using the integration results CS**2**_z**2**, CC**2**_z**2**, CS**1**_z**2** and CC**1**_z**2**. Further illustration and examples of such calculations are provided below, with respect to FIGS. **9-11**.

Additionally, these calculations may be further modified for computational convenience and improved accuracy. Specifically, in FIG. **8**, samples **802** are illustrated to illustrate a sampling of the sensor signal **304** that may be performed by an analog-to-digital conversion (ADC) implemented in association with operation of the digital transmitter **104** of the flow meter **700**. Although not drawn to scale, FIG. **8** illustrates that the samples **802** will not necessarily coincide directly with any of the zero crossings of the sensor signal **304**, or zero crossings of the drive mode signal **302**, or of the Coriolis signal **306**. As in virtually any digital system that relies on conversion to and/or from analog signals, some loss of accuracy may result from such sampling errors. For example, the signal analyzer **255** may use integral limits between a first sampled value of the sensor signal **304** and a second sampled value, rather than integrating between true zero-crossing values.

A shift in the starting point of the integral to the exact time of an ADC sample implies a corresponding shift in the (initially unknown) value of z**1**. However, as sampling on each of a plurality of sensor signals (i.e., from different sensors **205**) is simultaneous, the same shift applied during the processing

of each sensor signal will apply the same shift to the respective values of z1, hence leaving the resulting phase difference calculation(s) unaffected.

Similarly, shifting the end-point of the integral to the exact time of an ADC sample will adjust the integration period from its ideal value of the Coriolis mode period, and will, in other words, adjust the value of z2. However, given the analytical results in Eqs. (19)-(30), it is possible to compensate the integral values for a non-zero value of z2. It is thus possible to integrate over whole samples, with little or no loss of accuracy.

More specifically, in order to address such sampling errors and issues, in FIGS. **7** and **8**, the values z2 may be modified or chosen such that integral limits each coincide directly with one of the samples **802**. In other words, as shown in FIG. **8**, an adjusted integration period may be effectively selected, such that the value z2 is defined as a difference between the actual integration period used by the integrator **275** and a period of the Coriolis mode signal **306**.

This modification of z2 results in computational convenience and reduced processing requirements, and may be obtained by a corresponding adjustment of the value z1, without effecting a calculation of the drive amplitude A. It should be understood that such an adjustment of the value z1 will not substantially affect determination of phase difference required by the flowmeter output unit **240**, since determination of the mass flow rate relies on a relative difference between the phases of two separate sensor signals, i.e., a difference between two values of z1.

As a result of this ability to compensate for the value of z2, the modulation functions of the integrals described above may be adjusted such that the integral limits and modulation frequencies of the CS2_z2, CC2_z2, CS1_z2, and CC1_z2 integrals correspond to an exact number of samples, as shown by the integration period **804** of FIG. **8**. Such an adjustment results in a simplification of an integration calculation, as well as an improvement in accuracy of these calculations. Further, the modulation frequencies may be stored and reused.

Existing techniques allow for integration over periods that do not start and end on exact sample boundaries, but include various errors and calculations that are included for the purpose of dealing with such integrations. These errors and calculations may be eliminated through the use of z1 and z2, as described herein.

Furthermore, a significant computational effort associated with the type of Fourier integrations described herein and in the prior art is the calculation of the modulation sine and cosine functions. If the exact (or best estimate of) the instantaneous drive or Coriolis frequency is used for these integrations, then the modulation functions may need to be recalculated each time. If, however, through the use of z1 and z2, the integration time is restricted to convenient whole-sample periods, then it is possible to "cache" modulation sine and cosine values, so that recalculation thereof occurs only when there is a shift in the drive frequency f that is determined to be sufficiently large to warrant such a recalculation.

Accordingly, the signal analyzer **255** includes modulation sets **702** which store modulation frequencies and sample-specific drive frequencies. For example, if a true frequency vibration of the flow tube **215** is equal to 82.51 hertz, then this frequency may correspond to, for example, 121.197 samples at a sample rate of 10 kHz. Therefore, modulation sets corresponding to 121 samples and 122 samples may be calculated, for use by the integrator **275** in determining the integration results CS2_z2, CC2_z2, CS1_z2, and CC1_z2. The modulation sets **702** in this example may thus continue to be used by the integrator **275** until the drive period moves below 121 or above 122 samples, at which time other modulation set(s) may be used.

For example, in one implementation, z2 may be set so as to vary by ±0.5 of a sample period, since, for example, whenever z2 would move beyond this value, the next drive frequency (modulation set) may begin to be used. For example, the flowmeter **700** may be measuring parameters of a fluid in the flowtube **215**, and a density of the fluid (or some other parameter) may change such that a Coriolis frequency k (and corresponding period) changes from corresponding to 121.2 samples to corresponding to 121.7 samples, over some window of time. During that window of time, z2 will thus change incrementally on, for example, a cycle-by-cycle basis, while the modulation set with exactly 121 samples will be used for integration calculations, so that z2 gets bigger until the true period of 121.5 is reached. At that time, z2 will be approximately equal to half of the sample period, in seconds, and a new modulation set corresponding to 122 samples will begin to be used. Then, the value of z2 will jump to –0.5* the sample period in seconds, and will increase towards zero until the true period of 121.7 samples is reached, at which point z2 equals –0.3 sample periods.

In this way, z2 may be viewed as varying, on a cycle-by-cycle basis, to accommodate small changes in the drive frequency f, so as to avoid otherwise-necessary recalculations of modulation function values that would be caused by these frequency changes. Thus, z2 may be viewed as representing the time difference between the best estimate of the exact period of the Coriolis mode component **306**, and the integration period **804** that is used for integration (e.g., 121 or 122 samples), as shown in FIG. **8**.

FIG. **9** is a flow chart **900** illustrating an operation of the flow meter **700**. The basic strategy of the technique of FIG. **9**, including z2, is the same as that described above with respect to FIGS. **4-6**, with the following additional considerations. Specifically, as already described, and as shown in more detail below with respect to FIGS. **12-15**, the analytical expressions (Eq. (20)/(21), (23)/(24), (26)/(27), and (29)/(30)) for each of the four integrals including z2, i.e., CS2_z2, CC2_z2, CS1_z2, and CC1_z2 (Eqs. (19), (22), (25), and (28), respectively) simplify to the corresponding analytical expressions (Eq. (6), (8), (10)/(11), and (13)/(14)) for the z1 integrals, i.e., CS2_z1, CC2_z1, CS1_z1, and CC1_z1 (Eq. (5), (7), (9), and (12), respectively), when z2 equals zero.

Thus, a z2_error term may be defined for each of the z2 integrals, and, specifically, may be defined as a difference between each pair of corresponding z1 and z2 analytical expressions (e.g., CS2_z2_err=CS2_z2−CS2_z1; CC2_z2_err=CC2_z2−CC2_z1, CS1_z2_err=CS1_z2−CS1_z1; and CC1_z2_err=CC1_z2−CC1_z1). The z2_error terms may be estimated analytically using the best estimates of each of the parameter values f, k, A, z1, B, ϕ, and z2. The value of the z2_error term may then be subtracted from the numerical value of the z2 integral calculated by the integrator **275**, to give an estimate of what the z1 integral value would be, (i.e., if z2=0).

With the resulting estimates of the z1 integral values, improved estimates of A, z1, B, ϕ may be calculated as described above, which in turn lead to improved estimates of f, k, and hence z2. These improved parameter estimates can be used to provide better values for the z2_error terms, and, hence, the system of equations may be iterated to convergence. As long as z2 has a sufficiently small value (e.g., less than half a sample period), the influence of B on the CS2_z2

and CC2_z2 remains very small. Thus, good first estimates of the parameters A and z1 may be achieved by assuming z2=z2_error=0.

Having described techniques for using z2 in general terms, FIG. **9** illustrates more specific and detailed examples of these techniques. In FIG. **9**, the process begins with determination of values for the drive signal frequency f and the Coriolis mode frequency k, as determined by the zero crossing detector **265**, the frequency calculator **270**, and the modulation sets **702** (**902**). These values may be determined in conjunction with, and/or based on, a selection of an appropriate value for z2, i.e., a value that results in sample-specific integration limits. As noted, this setting of a z2 value may result in an adjustment to a value of z1, that will be reflected in the following calculations and results, but that does not impact actual outputs of the flowmeter **700** (e.g., mass flow rate, density, and/or new drive signal parameters), assuming the same integration interval is used for the relevant sensor sets.

Using the frequency values and modulation set values, the integrator **275** may thus determine appropriate integral values (**904**), i.e., CS2_z2_val, CC2_z2_val, CS1_z2_val, and CC1_z2_val. The signal identifier **260** may then determine initial estimates of the parameters A, z1, B, and ϕ, as described above (**906**).

Then, the parameter calculator **290** may determine improved values for A and z1, using equations that are analogous to Eqs. (3) and (4) (and Eqs. (15) and (16)), above (**908**), that is, for example, using Eqs. (31) and (32), respectively: Based on the current best estimates of z1, z2, f, k, A, B, and ϕ, estimates of the z2_error terms are calculated based on the analytical expressions given above:

$$CS2_z2_err = CS2_z2 - CS2_z1$$

$$CC2_z2_err = CC2_z2 - CC2_z1$$

$$CS1_z2_err = CS1_z2 - CS1_z1$$

$$CC1_z2_err = CC1_z2 - CC1_z1$$

These error terms are best estimates of the small adjustments needed to the numerical values of the integral values to compensate for non-zero values of z2. Accordingly, estimated values of the z1 integral values are calculated by subtracting the z2_error values from the numerical values of the integrals generated by the integrator **275**.

$$CS2_z1_est = CS2_z2_val - CS2_z2_err$$

$$CC2_z1_est = CC2_z2_val - CC2_z2_err$$

$$CS1_z1_est = CS1_z2_val - CS1_z2_err$$

$$CC1_z1_est = CC1_z2_val - CC1_z2_err$$

Based on these estimated numerical values of the z1 integrals, improved estimates of A and z1 are calculated using similar equations to

$$A_est_CS2_z2(CS2_z1_est, CC2_z1_est, f, k) = \sqrt{\left(\frac{CC2_z1_est}{f}\right)^2 + \left(\frac{CS2_z1_est}{2k}\right)^2} \cdot \left[\frac{\pi \cdot (f^2 - 4k^2)}{\sin\left(\frac{f}{k} \cdot \pi\right)}\right] \quad \text{Eq. (31)}$$

$$z1_est(CS2_z1_est, CC2_z1_est, f, k) = \frac{a\tan\left(\frac{2k \cdot CC2_z1_est}{f \cdot CS2_z1_est}\right)}{2 \cdot \pi \cdot f} \quad \text{Eq. (32)}$$

At this point, further iterations may be made to account for errors within the calculations that are due to the presence of z2. Such phase iterations are discussed in more detail below, with respect to FIG. **10**.

Subsequently, the parameter calculator **290** may determine values for B and ϕ, using equations that are analogous to Eqs. (3) and (4) (and Eqs. (17) and (18)), above (**910**), that is, for example, using Eqs. (33) and (34), respectively:

$$c = CC1_z1_est - CC1_Aonly_z1(A, f, 0, k, 0, z1)$$
$$s = CS1_z1_est - CS1_Aonly_z1(A, f, 0, k, 0, z1)$$
$$B_est_CS1_z2 = 2k \cdot \sqrt{c^2 + s^2} \quad \text{Eq. (33)}$$

$$\phi_est_CS1_z2 = a\tan\left(\frac{c}{s}\right) - k \cdot \pi \cdot \left(\frac{1}{f} + 2 \cdot z1\right) \quad \text{Eq. (34)}$$

As with the determination of A and z1, additional iterations may be performed to account for errors introduced by the z2 offset. Such iterations are discussed in more detail with respect to FIG. **11**.

If the values for A, z1, B, and ϕ are not sufficiently accurate (**912**), then the process may iterate through the determinations of those values, using the just-determined values (**906**). Otherwise, the process may re-calculate the original integral values CS2_z2, CC2_z2, CS1_z2, and CC1_z2 (**904**).

Otherwise (**912**), the process may perform additional processing to determine harmonics of the drive signal present within the sensor signal **304** (**914**). For example, referring to FIG. **7**, a harmonics removal system **704** is illustrated that is designed to remove, or account for the effects of, harmonics of the drive mode signal **302**. That is, as mentioned above, various factors may lead to the presence of harmonics or multiples of the drive frequency within the sensor signal **304**. In conventional processing, such as the Fourier analysis of Eqs. (1)-(4), such harmonics do not generally impact the analysis, because the integrations are performed over the drive cycle itself, and, since the harmonics of the drive mode signal **302** will have the same zero-crossings as the drive mode signal **302** itself, the harmonics do not impact the calculations of A and θ.

In contrast, the calculations of Eqs. (5)-(34) include integrations performed over a period of the Coriolis signal **306**, which will not generally have the same zero-crossings as the drive mode signal **302**, as explained above. As a result, the drive harmonics may be considered as part of a separate or additional processing.

One technique for accounting for these drive harmonics is to include a simple low pass filter as the drive harmonics removal system **704**. In this case, the filter may be implemented within the digital transmitter **104**, or outside of the digital transmitter **104**, e.g., in the sensor **205**. Such a filter may be operable to remove some or all of the drive harmonics that are above the Coriolis mode signal **306**.

Additionally, or alternatively, an analysis of the sensor signal **304** may be performed at the harmonics removal system **704** in which estimates of the parameters of the drive harmonics are obtained, perhaps from periodic integrations over a period of the drive signal. Then, by making certain assumptions about the relationships of the parameters to one another, effects of the drive signal harmonics may be removed from the analysis of the sensor signal by the signal analyzer **255**.

In other words, considering drive harmonics, the sensor signal **304** may be expressed in the form of $S(t)=A\sin(2\pi ft+\psi)+B\sin(2\pi k+\phi)$ (for the sine terms), so that the second har-

monic may be written as $A_2 \sin(2\pi ft+\psi_2)+B_2 \sin(2\pi k+\phi_2)$, and the third harmonic may be written in the form $A_3 \sin(2\pi ft+\psi_3)+B_3 \sin(2\pi k+\phi_3)$, and so on. In this formulation, it may be assumed that the signal parameters have certain relationships to one another that may be known or determined. For example, it may be assumed that a ratio of A_2/A is known, as well as A_3/A_2, or that a relationship between ψ and ψ_2 is known. Accordingly, additional corrections can be made to the numerical values of the integrals CS**2** etc based on estimates of the influence of the higher harmonics.

Therefore, for example, once a value for A is known from the above calculations, the value of A_2 may be determined, and thereafter the value of A_3. Similar comments apply to the phase information ψ of the various harmonics. In other words, the above Coriolis-based integrations may be performed to determine estimates of A, z**1**, B, and ϕ compensating for the estimated influence of the higher harmonics of the drive frequency. Then, periodically, the integrator **275** may perform integrations over the drive cycle, rather than the Coriolis cycle, in order to update, for example, information regarding the relationships between the harmonics.

Of course, combinations of the above techniques may be implemented. For example, a filter may be used to remove harmonics having value A_3 and above, so that the above analysis need only be performed for the second harmonic. Determination of how many harmonics to be filtered may be made based on, for example, a relationship between the frequencies f and k, or based on a desired dynamic response of the particular flowmeter (which may be impacted by such filtering).

Further, it may be possible to calculate improved frequencies f and k (**916**). If so, then, the improved frequency values may be used in a further iteration of the entire process **900**.

Examples of such techniques generally contemplate the use of the exact phase observed over each integration period of the calculation(s), and to note the shift in phase over adjacent ones of the integrations periods. Then, the calculated frequency is given by the time taken to generate a phase shift of 2π radians.

For example, it should be understood that the offset value z**1** essentially provided information regarding true zero crossings of the drive signal (as shown, for example, in FIGS. **3** and **8**). That is, a parameter X_n may be defined as a phase offset in degrees between a zero-crossing of the drive mode signal **302** (e.g., at time t=0) and an actual zero-crossing zc_n of the sensor signal **304** (illustrated in FIG. **8**). Then, considering only say zero crossings from negative to positive sensor signal values consecutive phases X_n, X_{n+1}, X_{n+2}, and zero crossing locations zc_n, zc_{n+1}, and zc_{n+2} may be identified.

In this formulation, it may be seen that $(zc_{n+1}-zc_n)$ is the obvious estimate of the drive period. However, at each of these positions we have observed phase offsets from the zero crossing of the drive component of $X_{n+1}-X_n$. If $(zc_{n+1}-zc_n)$ were exactly equal to the true drive period, then it would be found that $(X_{n+1}-X_n)=0$ (even if neither X_{n+1} nor X_n are zero themselves. Hence the difference $X_{n+1}-X_n$ can be used to improve the estimate of frequency.

One approach is to calculate the true instant of zero crossing for the drive phase component by adjusting for the observed phase offset. The true instant of zero phase for associated with cycle n, tz_n may be expressed in Eq. (36):

$$tz_n=zc_n-(X_n/360)f_{est} \quad \text{Eq. (36)}$$

while Eq. (37) defines the equivalent instant of zero phase for the next cycle, n+1.

$$tz_{n+1}=zc_{n+1}-(X_{n+1}/360)f_{est} \quad \text{Eq. (37)}$$

Then, finally, a corrected period (and thereby a revised frequency) may be obtained as a difference of these zero values, i.e., $(1/f_{revised})=tz_{n+1}-tz_n$.

It should be understood that FIG. **9** is intended to show examples of general flows of the process **900**, but that the above-described operations are not restricted to the outline or order of the process **900**. For example, the just-described frequency updating procedure may be performed cycle-by-cycle, intra-cycle, or merely periodically.

A revised frequency k may be determined from the revised value of f. Alternatively, a similar procedure to that just described may be performed for k, using the determined value(s) for the parameter ϕ. For example, if ϕ is calculated once per cycle, then consecutive values of ϕ may be compared to calculate k in the above-described manner.

Determining k from f as described above relies on a particular relationship between these two parameters, and, to the extent that this relationship is not exact, the value of k may generally be less accurate in the first instance than a value of f. As a result, cycle-by-cycle estimates of the Coriolis frequency k may be relatively noisy. Nonetheless, averaged values of k over a given time period (e.g., one minute) will give a relatively stable estimate of the Coriolis frequency k.

Additionally, in some implementations, a ratio of f to k may be determined based on the improved estimates of each parameter. Then, sudden changes in the drive frequency (resulting, e.g., from changes in fluid density in the flowtube **215**, instigation of two-phase flow, or other abrupt changes) will result in corresponding and proportional changes in the Coriolis mode.

If improved frequencies are not calculated (**916**), then the flowmeter output unit **240** may proceed with the calculation of flow parameters (e.g., mass flow rate and/or density), as well as with the outputting of appropriate parameters for generating the next drive signal.

FIG. **10** is a flowchart **1000** illustrating an example of a first operation of FIG. **9**. Specifically, FIG. **10** illustrates the techniques discussed above for FIG. **9** in which the values A and z**1** are calculated, including iterations for phase offsets introduced by the presence of the value z**2** (**908**).

Similarly, FIG. **11** is a flowchart **1100** illustrating an example of a second operation of FIG. **9**. Specifically, FIG. **11** illustrates the techniques discussed above for FIG. **9** in which the values B and ϕ are calculated, including iterations for phase offsets introduced by the presence of the value z**2** (**910**).

In FIGS. **10** and **11**, numerical examples are provided for illustration. These examples assume the same true values for the parameters f, k, A, z**1**, B, and ϕ, above. However, as should be understood from the above description of FIG. **9**, the integrals calculated by the integrator **275** reflect the presence of the value z**2**. In the following examples, it is assumed that the value of z**2** is chosen, as described above, so as to define the relevant integration limits as falling exactly on sampling points of the sensor signal **304**. In this example the value of $z2=1\times10^{-5}$ s.

Referring first to FIG. **10**, then, the process **1000** begins with a determination of the value A, using the numerically calculated integral values for CS**2**_z**2** and CC**2**_z**2**, in which the drive parameters are maximized relative to the Coriolis parameters, i.e., using Eqs. (19)-(30), above. In this example, these values turn out to be $CS2_z2=-2.46414954242338\times10^{-3}$ and $CC2_z2=-1.07153028732249\times10^{-10}$. Using Eq. (31), above (and initially assuming B is zero), the value for A may be determined to be 0.299628865383374 (**1002**).

Next, an error due to the presence of z**2** is calculated and removed (**1004**). Specifically, for example, the term CS**2**_z**2**_err is recalculated using the just-obtained value for

A, and this value is subtracted from the value CS2_z2=−2.46414954242338×10^−3 (**1006**). The remainder is thus an estimate of CS2_z1=−2.46720949500005×10^−3. Analogous calculations may be performed for CC2_z2, recalculating CC2_z2 with the obtained value of A (**1004**), or CC2_z2_err=6.6920402455379×10^−6, which, subtracted from the original value of CC2_z2, provides an estimate for CC2_z1=−6.69214739856663×10^−6 (**1004**, **1006**).

Then, using these values for CS2_z1 and CC2_z1, an improved value for A may be determined using Eq. (31) (**1008**), which, in this example, is A=3.00002412526826×10^−1. Subsequently, using Eq. (32), the values for CS2_z1 and CC2_z1 also may be used to obtain an estimate of z1 (**1010**), or z1=4.98479784037622×10^−6. Techniques for modifying this approach of obtaining z1 for cases where calculations are performed twice per cycle are described above, and may be used here, as well.

If the values of A and z1 are sufficiently accurate (**1012**), then the process **1000** may proceed to analogous calculations for the Coriolis mode signal **306**, i.e., may proceed to FIG. **11** (**1014**). Otherwise, the process **1000** may use the newly-obtained values for A and z1 to find yet-further improved values for CS2_z1 and CC2_z1 (**1004**, **1006**). Then, improved values for A and z1 may be obtained, which, in this case, turn out to be A=0.299999935356127 and z1=5.00009360798378×10^−6.

In FIG. **11**, analogous operations may be performed for the Coriolis-emphasized characterizations (integrals) CS1_z2 and CC1_z2. That is, the previously-determined information of A and z1, along with values from numerical integrations of the integrator **275** of CS1_z2=6.20062871680545×10^−4 and CC1_z2=−2.78579266493641×10^−7, may be used to determine an estimate for B (**1102**), using Eq. (33). In some cases, since B is relatively small, an initial estimate may be considered to be zero.

Then, an error due to the presence of z2 is calculated and removed (**1104**). Specifically, the term CS1_z2 is recalculated using the just-obtained value for B, and this value of (here) 2.44579936376226×10^−6 is subtracted from the value CS1_z2=6.20062871680545×10^−4 (**1106**). The remainder is thus an estimate of CS1_z1=6.17617072316783×10^−4.

Analogous calculations may be performed for CC1_z2, calculating the error in CC1_z2 due to z2 using the obtained value of B (**1104**), giving CC1_z2_err=−3.35625027516248×10^−6, which, subtracted from the original value of CC1_z2, provides an estimate for CC1_z1=3.07767100866884×10^−6 (**1104**, **1106**).

Then, using these values for CS1_z1 and CC1_z1, an improved value for B may be determined using Eq. (33) (**1108**), which, in this example, is B=9.99820189036286×10^−5. Further, using Eq. (34), the values for CS1_z1 and CC1_z1 also may be used to obtain an estimate of ϕ (**1010**), or ϕ=9.98342808946008×10^−1 (**1110**).

If the values of B and ϕ are not sufficiently accurate (**1112**), then the process **1100** may iterate (**1104**). Such an iteration, in the present example, would result in further improved values of B=1.00017250689519×10^−4, and ϕ=9.9997870785885×10^−1.

Otherwise (**1112**), the process **1100** may return to FIG. **9** (**912**). That is, all calculations may be refined in light of the just-determined values for A, z1, B, and ϕ, so that the processes **900**, **1000**, and **1100** are repeated. Alternatively, or additionally, the process **1100** may return directly to FIG. **10** (**1004**), and re-calculate the parameters of that process. Such iterations may be performed until a desired level of accuracy is reached, or may be truncated based on some other criteria, such as a time and/or computing resource limitation.

The descriptions of FIGS. **2-11**, above, provide explanation and examples for implementation and uses of the flowmeters **200** and **700**, and other variations thereof. The description provided below in conjunction with FIGS. **12-15** provides derivation, proof, and further explanation of the techniques implemented above for FIGS. **2-11**, as well as alternative techniques.

As noted above, Eqs. (1)-(4) provide the basis for a Fourier analysis of the sensor signal **304**, integrating over the drive signal period, and ignoring the impact of the Coriolis mode. In order to initially include an impact of the Coriolis mode, a first approximation of the effect of the Coriolis mode on the Fourier calculation may be made such that it is assumed that the correct integral limits and modulation frequency are used, and the only influence of the Coriolis mode is the contamination of the drive integral of Eqs. 1 and 2. The sine integral of Eq. 1 is thus defined as shown in Eq. (38) (assuming no phase offset on the drive frequency):

$$S1_int(A, f, B, k, \phi) := \qquad \text{Eq. (38)}$$

$$\int_0^{\frac{1}{f}} [B \cdot \sin[(2 \cdot \pi \cdot k \cdot t) + \phi] + A \cdot \sin(2 \cdot \pi \cdot f \cdot t)] \cdot \sin(2 \cdot \pi \cdot f \cdot t) dt$$

The drive mode or A term is simply A/2f, and the modulation function remains sin(2πft). The analytical expression for the influence of the B term (Coriolis mode) is given by Eq. (39):

$$S1_Bonly(A, f, B, k, \phi) := \qquad \text{Eq. (39)}$$

$$-B \cdot f \cdot \sin\left(\frac{1}{f} \cdot \pi \cdot k\right) \cdot \frac{\cos\left(\frac{1}{f} \cdot \pi \cdot k + \phi\right)}{\pi \cdot (f^2 - k^2)}$$

Similarly, the cosine integral of Eq. 2 is shown in Eq. (40)

$$C1_int(A, f, B, k, \phi) := \qquad \text{Eq. (40)}$$

$$\int_0^{\frac{1}{f}} [B \cdot \sin[(2 \cdot \pi \cdot k \cdot t) + \phi] + A \cdot \sin(2 \cdot \pi \cdot f \cdot t)] \cdot \cos(2 \cdot \pi \cdot f \cdot t) dt$$

with modulation function cos(2πft). Here the A term is exactly zero, while the B term is given by Eq. (41):

$$C1(A1, f, B, k, \phi) := \qquad \text{Eq. (41)}$$

$$\frac{-B \cdot k}{\pi \cdot (f^2 - k^2)} \cdot \sin\left(\frac{1}{f} \cdot \pi \cdot k\right) \cdot \sin\left(\frac{1}{f} \cdot \pi \cdot k + \phi\right)$$

For both integrals, the effect of the B term modulates with ϕ, resulting in a Coriolis mode beating effect that may be observed in both amplitude and phase (see, e.g., FIGS. **19**A-**19**D).

As described, the Coriolis mode shifts the positions of the zero crossings of the sensor signal **304**, so that the zero-crossings no longer occur at the exact points of zero (or π) phase for the drive frequency, as shown in FIGS. **3** and **8**. This effect is reflected in the z1 parameter, reflecting this shift from the point of zero phase on the drive signal. In this case the sine integral of the Fourier analysis may be shown as in Eq. (42):

$$S1_z1_int(A, f, B, k, \phi, z1) := \quad \text{Eq. (42)}$$

$$\int_{z1}^{\frac{1}{f}+z1} [B \cdot \sin[(2 \cdot \pi \cdot k \cdot t) + \phi] + A \cdot \sin(2 \cdot \pi \cdot f \cdot t)] \cdot \sin[2 \cdot \pi \cdot f \cdot (t - z1)] dt$$

In Eq. (42), the modified modulating sine function sin[2πf(t−z**1**)] is zero at the start and end of the integral while the A term is slightly offset. As a consequence the A term contribution to the integral may be shown as in Eq. (43):

$$S1_Aonly_z1(A, f, B, k, \phi, z1) := \frac{A}{2f} \cdot \cos(2f \cdot \pi \cdot z1) \quad \text{Eq. (43)}$$

while the B term is shown as in Eq. (44):

$$S1_Bonly_z1(A, f, B, k, \phi, z1) := \quad \text{Eq. (44)}$$

$$\frac{-B \cdot f}{\pi \cdot (f^2 - k^2)} \cdot \sin\left(\frac{1}{f} \cdot \pi \cdot k\right) \cdot \cos\left(\frac{1}{f} \cdot \pi \cdot k + \phi + 2 \cdot \pi \cdot k \cdot z1\right)$$

Similarly, the cosine integral may be shown as in Eq. (45):

$$C1_z1_int(A, f, B, k, \phi, z1) := \quad \text{Eq. (45)}$$

$$\int_{z1}^{\frac{1}{f}+z1} [B \cdot \sin[(2 \cdot \pi \cdot k \cdot t) + \phi] + A \cdot \sin(2 \cdot \pi \cdot f \cdot t)] \cdot \cos[2 \cdot \pi \cdot f \cdot (t - z1)] dt$$

Here, the modified modulation function is seen to be cos[2πf(t−z**1**)]. The A term for Eq. (45) is shown in Eq. (46):

$$C1_Aonly_z1(A, f, B, k, \phi, z1) := \frac{1}{2 \cdot f} \cdot A \cdot \sin(2 \cdot \pi \cdot z1 \cdot f) \quad \text{Eq. (46)}$$

and B term shown in Eq. (47):

$$C1_Bonly_z1(A, f, B, k, \phi, z1) := \quad \text{Eq. (47)}$$

$$\frac{-B \cdot f}{\pi \cdot (f^2 - k^2)} \cdot \sin\left(\frac{1}{f} \cdot \pi \cdot k\right) \cdot \sin\left(\frac{1}{f} \cdot \pi \cdot k + \phi + 2 \cdot \pi \cdot k \cdot z1\right)$$

Beyond this, and as described above, because the Coriolis mode is asynchronous, there is a different timing offset for the zero crossings at the beginning and the end of the integral. The analytical convenience is described above of denoting the time offset (from the point of true zero phase on the drive mode) at the beginning of the integral as z**1**, while adding the additional time offset z**2** to the end of the integral period. Of course, it also may be possible to express the combined time offset as a single parameter. A further effect of the offset zero crossings is that as the zero crossings are not exactly 1/f seconds apart, the wrong modulation frequency is applied; instead of using frequency f, as above, the modulation frequency within the now-modified modulation function(s) is given by f/(1+f*z**2**). The size of the expressions involved suggest separating A and B terms. Thus the A integral is defined in Eq. (48) as:

$$S1_Aonly_z2_int(A, f, B, k, \phi, z1, z2) := \quad \text{Eq. (48)}$$

$$\int_{z1}^{\frac{1}{f}+z1+z2} A \cdot \sin(2 \cdot \pi \cdot f \cdot t) \cdot \sin\left[2 \cdot \pi \cdot \frac{f}{(1 + f \cdot z2)} \cdot (t - z1)\right] dt$$

The analytical value of Eq. (48) is given by Eq. (49);

$$S1_Aonly_z2(A, f, B, k, \phi, z1, z2) := \quad \text{Eq. (49)}$$

$$A \cdot \sin(\pi \cdot f \cdot z2) \cdot \cos[\pi \cdot f \cdot (2 \cdot z1 + z2)] \cdot \frac{1 + f \cdot z2}{f^2 \cdot \pi \cdot (2 + f \cdot z2) \cdot z2}$$

As in the previous analysis, Eq. (49) contains a sinc function, only in terms of f rather than k: sin(π.f.z**2**)/(π.f.z**2**) which is well behaved as z**2**->0; it can be shown analytically that this expression tends to the function S**1**_Aonly_z**1** defined above in Eq. (43) for small z**2**.

The B integral is defined in Eq. (50) as:

$$S1_Bonly_z2_int(A, f, B, k, \phi, z1, z2) := \quad \text{Eq. (50)}$$

$$\int_{z1}^{\frac{1}{f}+z1+z2} [B \cdot \sin[(2 \cdot \pi \cdot k \cdot t) + \phi]] \cdot \sin\left[2 \cdot \pi \cdot \frac{f}{(1 + f \cdot z2)} \cdot (t - z1)\right] dt$$

An analytical expression for a value of Eq. (50) is given by Eq. (51):

$$S1_Bonly_z2(A, f, B, k, \phi, z1, z2) := \quad \text{Eq. (51)}$$

$$B \cdot f \cdot \frac{1 + f \cdot z2}{2\pi \cdot (k + f \cdot k \cdot z2 + f) \cdot (k + f \cdot k \cdot z2 - f)} \cdot \left[\sin\left[2 \cdot \pi \cdot k \cdot \left(\frac{1}{f} + z1 + z2\right) + \phi\right] - \sin(2 \cdot \pi \cdot z1 \cdot k + \phi)\right]$$

The total integral value is given by the sum of the A and B terms of Eq. (49) and Eq. (51), respectively.

The corresponding cosine integral is shown in Eq. (52):

$$C1_z2_int(A, f, B, k, \phi, z1, z2) := \quad \text{Eq. (52)}$$

$$\int_{z1}^{\frac{1}{f}+z1+z2} [B \cdot \sin[(2 \cdot \pi \cdot k \cdot t) + \phi] + A \cdot \sin(2 \cdot \pi \cdot f \cdot t)] \cdot \cos\left[2 \cdot \pi \cdot \frac{f}{(1 + f \cdot z2)} \cdot (t - z1)\right] dt$$

where the A term is analytically equal to Eq. (53);

$$C1_Aonly_z2(A, f, B, k, \phi, z1, z2) := \quad \text{Eq. (53)}$$

$$\frac{A \cdot (1 + f \cdot z2)^2}{f^2 \cdot \pi \cdot z2 \cdot (2 + f \cdot z2)} \cdot \sin(\pi \cdot f \cdot z2) \cdot [\sin[\pi \cdot f \cdot (2 \cdot z1 + z2)]]$$

Then, the B term is shown in Eq. (54):

$$C1_Aonly_z2(A, f, B, k, \phi, z1, z2) := \frac{A\cdot(1+f\cdot z2)^2}{f^2\cdot\pi\cdot z2\cdot(2+f\cdot z2)}\cdot\sin(\pi\cdot f\cdot z2)\cdot[\sin[\pi\cdot f\cdot(2\cdot z1+z2)]] \quad \text{Eq. (53)}$$

Eqs. (48)-(54) define the influence of the Coriolis mode on the integral values that are calculated, assuming the start and end points of the integral are shifted from the points of zero phase in the drive mode by z**1** and z**1** +z**2** seconds, respectively, as described. In other words, Eqs. (48)-(54) show what is calculated during an integration between zero crossings related to the drive mode signal **302**. Eqs. (48)-(54) above are analytically exact for any values of z**1** and z**2** (and for any of the other described parameters). Thus, Eqs. (48)-(54) illustrate an alternative solution approach for determining drive parameters and Coriolis signal parameters. That is, given the observed zero crossings (as detected, for example, by the zero-crossing detector **265**) and the numerical values of the S**1**_int_z**2** and C**1**_int_z**2** integrals of Eqs. (48)/(50) and (52), respectively, the values of A, f, B, k, ϕ, z**1**, and z**2**, may be deduced. In particular, it may be possible to make certain assumptions regarding relationships between the parameters A, f, B, k, ϕ, z**1**, and z**2**, such as the relationship between f and k for a specific flowtube, as referred to above. Other assumptions may be made about how parameter values vary from drive cycle to cycle during operation of the flowmeters **200** or **700**.

However, the approaches described above with respect to FIGS. **2-11** take the basic analysis of Eqs. (48)-(54), and modify both the integration limits and the modulation functions to encapsulate required information regarding the drive parameters and the Coriolis parameters within the sensor signal, in a form that is amenable to solution for each.

Thus, the approaches of FIGS. **2-11** describe analysis of a sensor signal having a relatively large term (e.g., the amplitude of A is typically 300 mV) and a relatively small term (e.g., the amplitude of B is typically less than or equal to 3 mV, and may be 0.1 mV or less in many cases), where both are to be calculated to very high precision. The various solution techniques operate by first selecting the integral limits and the modulation function such that the smaller influence (Coriolis mode) is reduced or eliminated entirely, so that a very accurate estimate of the larger influence (drive mode) may be obtained. Then, use this very accurate estimate of the larger influence to deduce the residual effect of the smaller influence.

Specifically, as described above, integrating over the period of the Coriolis mode instead of the period of the drive mode allows for effective separation of the drive (A) and Coriolis (B) terms. Further, if the sensor signal **304** is integrated over the period of the Coriolis mode, and a modulation function is used which is twice the Coriolis mode frequency (i.e. 2 k), then the influence of the Coriolis mode (B) term will be largely or entirely eliminated. If, however, a modulation function which is equal to the Coriolis frequency (i.e., k) is used, then this will maximize the influence of the Coriolis (B) term.

It is for this reason that the techniques of FIGS. **2-11** effectively generate four integral values instead of the two integral forms of, for example, Eqs. (48)/(50) and (52). These four integral values include two sets of sine and cosine terms, having modulating frequency 2 k and k, respectively, and are referred to above as CS**2**, CC**2**, CS**1**, and CC**1**. From these integrals, as described above, the various drive parameters and Coriolis parameters may be determined.

FIGS. **12-15** and the corresponding discussion, below, illustrate a development of these techniques of FIGS. **2-11**, based on an extension of the analysis of Eqs. (1)-(4) and Eqs. (38)-(54). Thus, various ones of the Eqs. (5)-(38) are repeated below, as part of this development, and are therefore designated by the same numerical identifiers as above.

FIG. **12** is a timing graph illustrating a development of the CS**2** integrals. In FIG. **12**, the sensor signal **304** is illustrated as having integral limits extended symmetrically from the beginning and end of the drive period to make up one complete Coriolis period, as shown, and as just described. A modulation function **1202** is shown as being multiplied by the sensor signal **304**, to obtain a product signal **1204**. As should be understood from the above, the modulation signal **1202** has a frequency that is equal to twice that of the Coriolis frequency k, and the product signal **1204** thus includes little or no influence of the Coriolis signal **306**.

Hence the CS**2** integral, here ignoring the influence of z**1** and z**2**, can be written as Eq. (55):

$$CS2_int(A, f, B, k, \phi) := \int_{-\left(\frac{1}{2k}-\frac{1}{2f}\right)}^{\frac{1}{f}+\left(\frac{1}{2k}-\frac{1}{2f}\right)} [B\cdot\sin[(2\cdot\pi\cdot k\cdot t)+\phi]+A\cdot\sin(2\cdot\pi\cdot f\cdot t)]\cdot \sin\left[4\cdot\pi\cdot k\cdot\left[t+\left(\frac{1}{2k}-\frac{1}{2f}\right)\right]\right]dt \quad \text{Eq. (55)}$$

Thus, it may be seen from Eq. (55) that the modulating function sin[4πk[t+((½k)−(½f))]] has frequency 4πk, corresponding to twice the Coriolis mode frequency.

The form of the integral limits and the modulation function are explained as follows. The previous assumption that the drive mode phase is close to zero at time t=0 is maintained, so the integral is extended beyond 0 . . . 1/f symmetrically, by the period ½k−½f. If the Coriolis mode frequency k is lower than that of the drive frequency f, this operation results in an expansion of the integration region. If, however, the Coriolis mode frequency is higher than the drive frequency, then the integration region would be reduced. The relevant equations are valid, and may be appropriately expressed, either way.

The analytical value of the CS**2** integral is given by Eq. (56):

$$CS2(A, f, B, k, \phi) := \frac{-2\cdot k\cdot A}{\pi\cdot(f^2-4\cdot k^2)}\cdot\sin\left(\frac{f}{k}\cdot\pi\right) \quad \text{Eq. (59)}$$

In Eq. (56), the B term has been eliminated entirely, as a result of the fact that the B term is a function of sin(2πkt), and Eq. (56) uses the modulation function of sin(4πt).

If a non-zero value of initial time offset, z**1**, is included, then the CS**2** integral, or CS**2**_z**1**, may be written as above in Eq. (5):

$$CS2_z1_int(A, f, B, k, \phi, z1) := \int_{-\left(\frac{1}{2k}-\frac{1}{2f}\right)+z1}^{\frac{1}{f}+\left(\frac{1}{2k}-\frac{1}{2f}\right)+z1} [B\cdot\sin[(2\cdot\pi\cdot k\cdot t)+\phi]+A\cdot\sin(2\cdot\pi\cdot f\cdot t)]\cdot \sin\left[4\cdot\pi\cdot k\cdot\left[t-z1+\left(\frac{1}{2k}-\frac{1}{2f}\right)\right]\right]dt \quad \text{Eq. (5)}$$

with an analytical expression shown in Eq. (6):

$$CS2_z1(A, f, B, k, \phi, z1) := \quad \text{Eq. (6)}$$

$$\frac{-2 \cdot k \cdot A}{\pi \cdot (f^2 - 4 \cdot k^2)} \cdot \sin\left(\frac{f}{k} \cdot \pi\right) \cdot \cos(2 \cdot f \cdot \pi \cdot z1)$$

Again, the influence of B has been eliminated.

Finally, if a non-zero value of z**2** and corresponding modulation frequency are used, then the CS**2** integral, or CS**2**_z**2**, may be written as above in Eq. (19):

$$CS2_z2_int(A, f, B, k, \phi, z1, z2) := \quad \text{Eq. (19)}$$

$$\int_{-\left(\frac{1}{2k} - \frac{1}{2f}\right) + z1}^{\frac{1}{f} + \left(\frac{1}{2k} - \frac{1}{2f}\right) + z1 + z2} [B \cdot \sin[(2 \cdot \pi \cdot k \cdot t) + \phi] + A \cdot \sin(2 \cdot \pi \cdot f \cdot t)] \cdot \sin\left[4 \cdot \pi \cdot \frac{k}{(1 + k \cdot z2)} \cdot \left[t - z1 + \left(\frac{1}{2k} - \frac{1}{2f}\right)\right]\right] dt$$

The A term is given by Eq. (20):

$$CS2_Aonly_z2(A, f, B, k, \phi, z1, z2) := -2 \cdot A \cdot k \cdot \quad \text{Eq. (20)}$$

$$(1 + k \cdot z2) \cdot \frac{\sin\left[\pi \cdot f \cdot \left(\frac{1}{k} + z2\right)\right] \cdot \cos(\pi \cdot f \cdot (2 \cdot z1 + z2))}{\pi \cdot (f + f \cdot k \cdot z2 + 2 \cdot k) \cdot (f + f \cdot k \cdot z2 - 2 \cdot k)}$$

The B term is no longer exactly zero, as shown in Eq. (21):

$$CS2_Bonly_z2(A, f, B, k, \phi, z1, z2) := \quad \text{Eq. (21)}$$

$$\frac{2 \cdot B \cdot (1 + k \cdot z2)}{\pi \cdot k \cdot (3 + k \cdot z2) \cdot (1 - k \cdot z2)} \cdot \cos\left[k \cdot \pi \cdot \left(\frac{1}{f} + 2 \cdot z1 + z2\right) + \phi\right] \cdot \sin(\pi \cdot k \cdot z2)$$

However, it is very small, being a product of both B itself and sin(z**2**), both of which may be assumed to be small.

FIG. **13** is a timing graph illustrating a development of the CC**2** integrals. The major change from CS**2** in FIG. **12** and the above discussion, is that a modulation function **1304** is a cosine rather than a sine function, leading to a different product function **1306** than seen in FIG. **12**.

Thus, first assuming both z**1** and z**2** are zero, the CC**2** integral takes the form of Eq. (57):

$$CC2_int(A, f, B, k, \phi) := \quad \text{Eq. (57)}$$

$$\int_{-\left(\frac{1}{2k} - \frac{1}{2f}\right)}^{\frac{1}{f} + \left(\frac{1}{2k} - \frac{1}{2f}\right)} [B \cdot \sin[(2 \cdot \pi \cdot k \cdot t) + \phi] + A \cdot \sin(2 \cdot \pi \cdot f \cdot t)] \cdot \cos\left[4 \cdot \pi \cdot k \cdot \left[t + \left(\frac{1}{2k} - \frac{1}{2f}\right)\right]\right] dt$$

Eq. (57) has a value of exactly zero, as both the A term and B term disappear.

Next allowing for a non-zero value of z**1**, the value CC**2**_z**1** may be expressed as above in Eq. (7):

$$CC2_z1_int(A, f, B, k, \phi, z1) := \quad \text{Eq. (7)}$$

$$\int_{-\left(\frac{1}{2k} - \frac{1}{2f}\right) + z1}^{\frac{1}{f} + \left(\frac{1}{2k} - \frac{1}{2f}\right) + z1} [B \cdot \sin[(2 \cdot \pi \cdot k \cdot t) + \phi] + A \cdot \sin(2 \cdot \pi \cdot f \cdot t)] \cdot \cos\left[4 \cdot \pi \cdot k \cdot \left[t - z1 + \left(\frac{1}{2k} - \frac{1}{2f}\right)\right]\right] dt$$

which has analytical form, in which again the B term is exactly zero, as shown in Eq. (8):

$$CC2_z1(A, f, B, k, \phi, z1) := \quad \text{Eq. (8)}$$

$$\frac{-A \cdot f}{\pi \cdot (f^2 - 4 \cdot k^2)} \cdot \sin\left(\frac{f}{k} \cdot \pi\right) \cdot \sin(2 \cdot f \cdot \pi \cdot z1)$$

Finally, and most generally, allowing non-zero z**1** and z**2**, and the resulting error in the modulation frequency, the CC**2**_z**2** integral may be written as in Eq. (22):

$$CC2_z2_int(A, f, B, k, \phi, z1, z2) := \quad \text{Eq. (22)}$$

$$\int_{-\left(\frac{1}{2k} - \frac{1}{2f}\right) + z1}^{\frac{1}{f} + \left(\frac{1}{2k} - \frac{1}{2f}\right) + z1 + z2} [B \cdot \sin[(2 \cdot \pi \cdot k \cdot t) + \phi] + A \cdot \sin(2 \cdot \pi \cdot f \cdot t)] \cdot \cos\left[4 \cdot \pi \cdot \frac{k}{(1 + k \cdot z2)} \cdot \left[t - z1 + \left(\frac{1}{2k} - \frac{1}{2f}\right)\right]\right] dt$$

Thus, the A term for CC**2**_z**2** of Eq. (22) takes the form of Eq. (23):

$$CC2_Aonly_z2(A, f, B, k, \phi, z1, z2) := -A \cdot f \cdot \quad \text{Eq. (23)}$$

$$(1 + k \cdot z2)^2 \cdot \frac{\sin\left[\pi \cdot f \cdot \left(\frac{1}{k} + z2\right)\right] \cdot \sin[\pi \cdot f \cdot (2 \cdot z1 + z2)]}{\pi \cdot (f + f \cdot k \cdot z2 + 2 \cdot k) \cdot (f + f \cdot k \cdot z2 - 2 \cdot k)}$$

while the B term takes the form of Eq. (24):

$$CC2_Bonly_z2(A, f, B, k, \phi, z1, z2) := \quad \text{Eq. (24)}$$

$$\frac{-B \cdot (1 + k \cdot z2)^2}{\pi \cdot k \cdot (k \cdot z2 + 3) \cdot (k \cdot z2 - 1)} \cdot \sin\left[k \cdot \pi \cdot \left(\frac{1}{f} + 2 \cdot z1 + z2\right) + \phi\right] \cdot \sin(\pi \cdot k \cdot z2)$$

which again, being a product of B and sin(z**2**), is small.

FIG. **14** is a timing graph illustrating a development of the CS**1** integrals. In FIG. **14**, as shown, a modulating function **1402** completes a single cycle over the integration period, having the Coriolis frequency k, thus resulting in a product function **1404**.

Proceeding through to the development of the CS**1** integrals, the first CS**1** integral, i.e., assuming z**1** and z**2** are both zero, is defined as in Eq. (58):

$$\mathrm{CS1_int}(A, f, B, k, \phi) := \int_{-\left(\frac{1}{2k}-\frac{1}{2f}\right)}^{\frac{1}{f}+\left(\frac{1}{2k}-\frac{1}{2f}\right)} [B\cdot\sin[(2\cdot\pi\cdot k\cdot t)+\phi]+A\cdot\sin(2\cdot\pi\cdot f\cdot t)]\cdot \sin\left[2\cdot\pi\cdot k\cdot\left[t+\left(\frac{1}{2k}-\frac{1}{2f}\right)\right]\right]dt \quad \text{Eq. (58)}$$

The analytic value of Eq. (58) is given by Eq. (59);

$$CS1(A, f, B, k, \phi) := \frac{-k\cdot A}{\pi\cdot(f^2-k^2)}\cdot\left(\frac{f}{k}\cdot\pi\right)-\frac{b}{2k}\cdot\cos\left(\frac{k}{f}\cdot\pi+\phi\right) \quad \text{Eq. (59)}$$

Assuming next a non-zero value of z**1**, the CS**1**_z**1** integral is shown in Eq. (9) as:

$$\mathrm{CS1_z1_int}(A, f, B, k, \phi, z1) := \int_{-\left(\frac{1}{2k}-\frac{1}{2f}\right)+z1}^{\frac{1}{f}+\left(\frac{1}{2k}-\frac{1}{2f}\right)+z1} [B\cdot\sin[(2\cdot\pi\cdot k\cdot t)+\phi]+A\cdot\sin(2\cdot\pi\cdot f\cdot t)]\cdot \sin\left[2\cdot\pi\cdot k\cdot\left[t-z1+\left(\frac{1}{2k}-\frac{1}{2f}\right)\right]\right]dt \quad \text{Eq. (9)}$$

Eq. (9) has an A term given by Eq. (10):

$$\mathrm{CS1_Aonly_z1}(A, f, B, k, \phi, z1) := \frac{-k\cdot A}{\pi\cdot(f^2-k^2)}\cdot\sin\left(\frac{f}{k}\cdot\pi\right)\cdot\cos(2\cdot f\cdot\pi\cdot z1) \quad \text{Eq. (10)}$$

Eq. (10) has a B term given by Eq. (11):

$$\mathrm{CS1_Bonly_z1}(A, f, B, k, \phi, z1) := \frac{-B}{2\cdot k}\cdot\cos\left[k\cdot\pi\cdot\left(\frac{1}{f}+2\cdot z1\right)+\phi\right] \quad \text{Eq. (11)}$$

Finally, with a non-zero z**2** term, the CS**1**_z**2** integral may be written as in Eq. (25):

$$\mathrm{CS1_z2_int}(A, f, B, k, \phi, z1, z2) := \int_{-\left(\frac{1}{2k}-\frac{1}{2f}\right)+z1}^{\frac{1}{f}+\left(\frac{1}{2k}-\frac{1}{2f}\right)+z1+z2} [B\cdot\sin[(2\cdot\pi\cdot k\cdot t)+\phi]+A\cdot\sin(2\cdot\pi\cdot f\cdot t)]\cdot \sin\left[2\cdot\pi\cdot\frac{k}{(1+k\cdot z2)}\cdot\left[t-z1+\left(\frac{1}{2k}-\frac{1}{2f}\right)\right]\right]dt \quad \text{Eq. (25)}$$

Eq. (25) has an analytical expression for the A term given by Eq. (26):

$$\mathrm{CS1_Aonly_z2}(A, f, B, k, \phi, z1, z2) := -A\cdot k\cdot(1+k\cdot z2)\cdot\frac{\sin\left[\pi\cdot f\cdot\left(\frac{1}{k}+z2\right)\right]\cdot\cos(\pi\cdot f\cdot(2\cdot z1+z2)]}{\pi\cdot(f+f\cdot k\cdot z2+k)\cdot(f+f\cdot k\cdot z2-k)} \quad \text{Eq. (26)}$$

Eq. (26) has a B term given by Eq. (27):

$$\mathrm{CS1_Bonly_z2}(A, f, B, k, \phi, z1, z2) := \frac{-B\cdot(1+k\cdot z2)}{\pi\cdot k^2\cdot z2\cdot(2+k\cdot z2)}\cdot \cos\left[\pi\cdot k\cdot\left(\frac{1}{f}+2\cdot z1+z2\right)+\phi\right]\cdot\sin(\pi\cdot k\cdot z2) \quad \text{Eq. (27)}$$

The B term of Eq. (27) includes the sinc function sin (π.k.z**2**)/(π.k.z**2**), and may be shown to tend towards CS**1**_Bonly_z**1** of Eq. (11), as z**2** tends to zero.

FIG. **15** is a timing graph illustrating a development of the CC**1** integrals. In FIG. **15**, as shown, a modulating (cosine) function **1502** completes a single cycle over the integration period, having the Coriolis frequency k, and results in a product function **1504**.

Proceeding in an analogous fashion to the above, and starting with z**1** and z**2** both assumed to be zero, the CC**1** integral takes the form of Eq. (60):

$$\mathrm{CC1_int}(A, f, B, k, \phi) := \int_{-\left(\frac{1}{2k}-\frac{1}{2f}\right)}^{\frac{1}{f}+\left(\frac{1}{2k}-\frac{1}{2f}\right)} [B\cdot\sin[(2\cdot\pi\cdot k\cdot t)+\phi]+A\cdot\sin(2\cdot\pi\cdot f\cdot t)]\cdot \cos\left[2\cdot\pi\cdot k\cdot\left[t+\left(\frac{1}{2k}-\frac{1}{2f}\right)\right]\right]dt \quad \text{Eq. (60)}$$

The A term disappears, leaving only the following B term of Eq. (61):

$$CC1(A, f, B, k, \phi) := \frac{-B}{2\cdot k}\cdot\sin\left(\frac{k}{f}\cdot\pi+\phi\right) \quad \text{Eq. (61)}$$

With a non-zero value of z**1**, the CC**1**_z**1** integral may be shown as above in Eq. (12):

$$\mathrm{CC1_z1_int}(A, f, B, k, \phi, z1) := \int_{-\left(\frac{1}{2k}-\frac{1}{2f}\right)+z1}^{\frac{1}{f}+\left(\frac{1}{2k}-\frac{1}{2f}\right)+z1} [B\cdot\sin[(2\cdot\pi\cdot k\cdot t)+\phi]+A\cdot\sin(2\cdot\pi\cdot f\cdot t)]\cdot \cos\left[2\cdot\pi\cdot k\cdot\left[t-z1+\left(\frac{1}{2k}-\frac{1}{2f}\right)\right]\right]dt \quad \text{Eq. (12)}$$

Eq. (12) results in an A term of Eq. (13):

$$\mathrm{CC1_Aonly_z1}(A, f, B, k, \phi, z1) := \frac{-f\cdot A}{\pi\cdot(f^2-k^2)}\cdot\sin\left(\frac{f}{k}\cdot\pi\right)\cdot\sin(2\cdot f\cdot\pi\cdot z1) \quad \text{Eq. (13)}$$

Eq. (13) results in a B term of Eq. (14):

$$\mathrm{CC1_Bonly_z1}(A, f, B, k, \phi, z1) := \frac{-B}{2\cdot k}\cdot\sin\left[k\cdot\pi\cdot\left(\frac{1}{f}+2\cdot z1\right)+\phi\right] \quad \text{Eq. (14)}$$

Finally, with non-zero z2, the CC1_z2 integral is represented in Eq. (28) as:

$$CC1_z2_int(A, f, B, k, \phi, z1, z2) := \quad \text{Eq. (28)}$$
$$\int_{-\left(\frac{1}{2k}-\frac{1}{2f}\right)+z1}^{\frac{1}{f}+\left(\frac{1}{2k}-\frac{1}{2f}\right)+z1+z2} [B\cdot\sin[(2\cdot\pi\cdot k\cdot t)+\phi]+A\cdot\sin(2\cdot\pi\cdot f\cdot t)]\cdot \cos\left[2\cdot\pi\cdot\frac{k}{(1+k\cdot z2)}\cdot\left[t-z1+\left(\frac{1}{2k}-\frac{1}{2f}\right)\right]\right]dt$$

For Eq. (28), the A term may be written as in Eq. (29):

$$CC1_Aonly_z2(A, f, B, k, \phi, z1, z2) := \quad \text{Eq. (29)}$$
$$-A\cdot f\cdot(1+k\cdot z2)^2\cdot\frac{\sin\left[\pi\cdot f\cdot\left(\frac{1}{k}+z2\right)\right]\cdot\sin(\pi\cdot f\cdot(2\cdot z1+z2))}{\pi\cdot(f+f\cdot k\cdot z2+k)\cdot(f+f\cdot k\cdot z2-k)}$$

Further for Eq. (29), the B term, where again the sinc function sin(π.k.z2)/(π.k.z2) in included, may be written as in Eq. (30):

$$CC1_Bonly_z2(A, f, B, k, \phi, z1, z2) := \frac{-B\cdot(1+k\cdot z2)^2}{\pi\cdot k^2\cdot z2\cdot(2+k\cdot z2)}\cdot \quad \text{Eq. (30)}$$
$$\sin\left[\pi\cdot k\cdot\left(\frac{1}{f}+2\cdot z1+z2\right)+\phi\right]\cdot\sin(\pi\cdot k\cdot z2)$$

Thus, the above discussion of FIGS. **12-15** illustrates a development of all of the CS2_z1, CC2_z1, CS1_z1, CC1_z1, CS2_z2, CC2_z2, CS1_z2, and CC1_z2 integrals, the development being based on extensions of existing techniques for performing Fourier analysis of the sensor signal **304**.

FIGS. **16-22** illustrate examples of results of implementations of the techniques of FIGS. **2-11**, above. In FIGS. **16-22**, unless mentioned otherwise, data is illustrated in which parameter values are A=0.3, f=100 Hz, k=f/√3, and B=0.005. Of course, these parameters are merely for example's sake.

FIGS. **16**A and **16**B are graphs illustrating a phase difference between two sensor signals **304**, e.g., between two offsets z1 of two signals from two sensors **205**. FIG. **16**A illustrates a raw phase difference, before the corrections discussed above, and FIG. **16**B illustrates a phase difference after the corrections.

FIGS. **17**A and **17**B are graphs illustrating an average frequency f (in FIG. **17**A) and a corrected frequency $f_{revised}$ (in FIG. **17**B). As illustrated, significant improvements in frequency values, and reductions in errors, may be obtained by using the techniques described above with respect to FIG. **9** (**916**). For example, a standard deduction reduction of 10-1000 may be obtained, depending, for example, on the level of Coriolis noise.

FIG. **18** is a graph illustrating an example of a Coriolis frequency estimation along the lines described above with respect to FIG. **9** (**916**). That is, FIG. **18** illustrates the calculations of an average Coriolis frequency over a given time period. As described above, a ratio or other relationship between $f_{revised}$ of FIGS. **17**B and k of FIG. **18** may be determined.

FIGS. **19**A-**19**D are graphs illustrating raw and corrected values for amplitude and phase of a drive signal. Specifically, FIGS. **19**A and **19**B illustrate a raw and corrected amplitude of a drive signal, while FIGS. **19**C and **19**D illustrate a raw and corrected phase difference z1. As shown, significant reductions in standard deviation may be obtained. Moreover, the beating pattern that typically occurs at the difference between the drive frequency and the Coriolis frequency, referred to above, may be eliminated.

FIGS. **20**A-**20**D are graphs illustrating amplitude modulation of a drive signal. In FIGS. **20**A and **20**B, a raw and corrected amplitude respectively, are illustrated. In FIGS. **20**C and **20**D, a raw and corrected phase difference, respectively, are illustrated.

FIGS. **21**A-**21**D are graphs illustrating a step change in phase difference of a drive signal. In FIGS. **21**A and **21**B, a raw and corrected amplitude respectively, are illustrated. In FIGS. **21**C and **21**D, a raw and corrected phase difference, respectively, are illustrated. As may be seen, the step changes in phase difference are obscured by noise in FIG. **21**C, but are clearly visible in FIG. **21**D.

Finally, FIGS. **22**A-**22**E are graphs illustrating variations in the Coriolis amplitude B. In FIG. **22**A, a raw amplitude of a sensor signal is illustrated, while a corrected amplitude is illustrated in FIG. **22**B. A raw phase difference is shown in FIG. **22**C, while a corrected phase difference is shown in FIG. **22**D.

Finally, FIG. **22**E illustrates a change in Coriolis amplitude that results from any of the various effects referenced above, e.g., external vibrations of the flowtube **215**. In FIG. **22**E, the Coriolis amplitude, as shown, varies between 0.005V and 0.0075V. As shown, the Coriolis amplitude B may be determined to a high level of accuracy, so that the originating causes of the changes in B may be identified, characterized, and/or determined.

Techniques are described above in which a sensor signal having a major (drive) signal component and a minor (e.g., Coriolis) component may be analyzed so as to characterize the signal components, and, ultimately, to identify parameters of the signal components with a high degree of accuracy. As a result, highly accurate, stable, and responsive measurements may be made of a fluid within a vibratable flowtube, and a new drive signal may be generated that maintains a desired oscillation of the flowtube.

In these and related techniques, it should be understood that the signal analyzer **255** and the signal identifier **260** of FIGS. **2** and **7** may be implemented at separate locations. For example, the signal analyzer **255** may be implemented within a specialized processor, such as a FPGA, as referred to above, for high-speed calculation of the integration values. Then, the FPGA may send the results of these integrations to the signal identifier **260** on a separate processor, so that the actions of the signal identifier **260** in extracting the various signal parameters from the integral results may be performed with a minimum of computational load.

A number of implementations have been described. Nevertheless, it will be understood that various modifications may be made. Accordingly, other implementations are within the scope of the following claims.

What is claimed is:

1. A Coriolis flowmeter comprising:

a flowtube having a fluid flowing therethrough, the flowtube being subject to a vibration, the vibration of the flowtube comprising at least a drive mode of vibration and a contaminant mode of vibration;

a sensor for outputting an observed signal representative of the vibration of the flowtube, the observed signal including a drive mode signal corresponding to the drive mode of vibration and a contaminant mode signal corresponding to the contaminant mode of vibration; and,

a transmitter for receiving the observed signal and determining a parameter of the fluid, the transmitter comprising:

a zero-crossing detector for detecting a plurality of observed zero-crossings of the observed sensor signal;

a frequency calculator operable to determine an observed signal frequency and an initial estimate of frequency of the contaminant mode signal, the observed signal frequency and the contaminant mode signal frequency being used to determine a parameter of fluid passing through the flowmeter.

2. The Coriolis flowmeter as set forth in claim **1** further comprising a mode maximizer operable to generate at least a first characterization of the observed sensor signal, the first characterization maximizing the drive mode signal.

3. The Coriolis flowmeter as set forth in claim **2** further comprising a determination system operable to determine the parameter of the fluid using at least the first characterization.

4. The Coriolis flowmeter of claim **3**, wherein the initial estimate of contaminant mode signal frequency is a predetermined function of the observed signal frequency.

5. The Coriolis flowmeter of claim **1**, wherein the mode maximizer is operable to generate a second characterization of the observed sensor signal, the second characterization of the observed sensor signal maximizing the drive mode signal.

6. The Coriolis flowmeter of claim **5**, wherein the determination system calculates the parameter of the fluid using the second characterization.

7. The Coriolis flowmeter of claim **6**, wherein a parameter calculator uses the second characterization to determine an estimate of an amplitude of oscillation of the contaminant mode signal and an estimate of a phase angle of the contaminant mode signal.

8. The Coriolis flowmeter of claim **7**, wherein the parameter calculator uses the first characterization to determine an estimate of an amplitude of oscillation of the drive mode signal and an estimate of an offset between a zero-crossing of the observed signal and a zero-crossing of the drive mode signal.

9. The Coriolis flowmeter of claim **8**, wherein the determination system calculates the parameter of the fluid using the estimate of the amplitude of oscillation of the drive mode signal and the estimate of the offset between the zero-crossing of the observed signal and the zero-crossing of the drive mode signal.

10. The Coriolis flowmeter of claim **7**, wherein the parameter calculator uses the estimate of an amplitude of oscillation of the drive mode signal and the estimate of an offset between a zero-crossing of the observed signal and a zero-crossing of the drive mode signal to calculate the estimate of an amplitude of oscillation of the contaminant mode signal and an estimate of a phase angle of the contaminant mode signal.

11. The Coriolis flowmeter of claim **10**, wherein the parameter calculator uses the estimate of the amplitude of oscillation of the contaminant mode signal and the estimate of the phase angle of the contaminant mode signal to calculate an improved estimate of the amplitude of oscillation of the drive mode signal and an improved estimate of the offset between the zero-crossing of the observed signal and the zero-crossing of the drive mode signal.

12. The Coriolis flowmeter of claim **11**, wherein the determination system calculates the parameter of the fluid using the improved estimate of the amplitude of oscillation of the drive mode signal and the improved estimate of the offset between the zero-crossing of the observed signal and the zero-crossing of the drive mode signal.

13. The Coriolis flowmeter of claim **11**, wherein the parameter calculator uses the improved estimate of the amplitude of oscillation of the drive mode signal and the improved estimate of the offset between the zero-crossing of the observed signal and the zero-crossing of the drive mode signal to calculate an improved estimate of the amplitude of oscillation of the contaminant mode signal and an improved estimate of the phase angle of the contaminant mode signal.

14. The Coriolis flowmeter of claim **1**, wherein the observed signal is not filtered before reaching the frequency calculator to minimize the effect of the contaminant mode signal.

* * * * *